MINNESOTA GEOLOGICAL SURVEY
D.L. SOUTHWICK, *Interim Director*

SHORT CONTRIBUTIONS TO THE GEOLOGY OF MINNESOTA, 1994

D.L. Southwick, Editor

Report of Investigations 43
ISSN 0076-9177

Saint Paul — 1994

SHORT CONTRIBUTIONS TO THE GEOLOGY OF MINNESOTA, 1994

SHORT CONTRIBUTIONS TO

THE GEOLOGY OF MINNESOTA, 1994

EDITOR'S INTRODUCTION

In the course of their normal mapping and research activities, the staff of the Minnesota Geological Survey frequently make significant topical observations or interpretations that for one reason or another are not appropriate for publication in national geological journals. Reasons for this may include (1) dependence on maps or other illustrative materials that are prohibitively expensive or unwieldy for journal publication; (2) subject matter that is not national news, but nevertheless is of local significance to the understanding of Minnesota's geology; or (3) conclusions that, because of the limited outcrop and subsurface databases with which we are routinely forced to contend, are necessarily somewhat speculative. The present document is intended as a venue for short contributions to Minnesota's geology that for these reasons or others might not otherwise see the light of day.

These volumes will be divided into three subject-matter sections, which are (1) contributions to Precambrian geology; (2) contributions to Paleozoic and Mesozoic geology; and (3) contributions to Quaternary geology and hydrogeology. These correspond to the main subject-area divisions of the Minnesota Geological Survey and the first-order divisions of the geology of the state. This particular volume contains papers dealing with the first two topics. If this first compendium is well received, others will follow on an "occasional" basis.

D.L. Southwick, Interim Director
Minnesota Geological Survey
2642 University Avenue
St. Paul, MN 55114-1057

CONTENTS

ASSORTED GEOCHRONOLOGIC STUDIES OF PRECAMBRIAN TERRANES IN MINNESOTA: A POTPOURRI OF TIMELY INFORMATION

By

D. L. Southwick

With data contributed by Z. E. Peterman(1), L. W. Snee(1), and W. R. Van Schmus(2)

ABSTRACT

U-Pb, Rb-Sr, $^{40}Ar/^{39}Ar$, and Nd-Sm isotopic techniques have been applied to seven samples of Precambrian rock from Minnesota. The analytical work was done at various times in the past 12 years in support of regional mapping projects; many of the samples were acquired from drilling done in areas of limited Precambrian exposure and limited knowledge of the temporal relationships among rock units. Samples studied were Archean rocks of tonalitic composition in the southern Superior Province, Proterozoic intrusive rocks associated with the Penokean orogen, and clastic pebbles of rhyolite within a conglomeratic facies of the Early Proterozoic Sioux Quartzite.

A gneissose tonalite from the Giants Range batholith near Embarrass, in the Vermilion district (Wawa subprovince of the Superior Province) is dated by U-Pb at 2,718 ± 67 Ma; U-Pb data combined from two gneissose tonalite samples from different localities in the "quiet zone" (Wawa subprovince) yield an apparent age of 2,688 ± 72 Ma; and a gneissose tonalite from the Jeffers block of the Minnesota River Valley subprovince is dated by U-Pb at 2,624 ± 57 Ma. A quartz monzonite pluton from the subsurface of Jackson County, southwestern Minnesota, is dated by U-Pb at 1,792 ± 31 Ma; a hornblende ferrodiorite pluton near Philbrook, central Minnesota, gives an apparent age of 1,854 ± 4 Ma from the $^{40}Ar/^{39}Ar$ method as applied to hornblende; and rhyolite pebbles from the Sioux Quartzite in Pipestone County, southwestern Minnesota, are dated by U-Pb at 1,902 ± 55 Ma. The implications of these ages and other isotopic and geochemical data from the dated samples are interpreted in the context of the regional tectonic framework.

INTRODUCTION

In the period between 1980 and 1991, geochronologic studies were undertaken on seven samples of Precambrian igneous rocks from various parts of Minnesota (Fig.1) in support of several different mapping projects and subsurface investigations. Some of the results of this work have been cited as personal communications in published articles, and some others have been mentioned in abstracts and unpublished theses. However the existing literature does not present the full isotopic analyses or the details of sample location, field context, composition, and geologic significance of the dated rocks. Consequently the geochronologic data have not had the impact or recognition that they deserve. The purpose here is to present these data in a complete, accessible, and citable form and interpret them in the context of Minnesota's Precambrian geology.

This work represents collaborative science at its simplest. The Minnesota Geological Survey (MGS) has no in-house capability for conducting geochronologic studies, yet it has a continuing need for high-quality geochronology to support its work in Precambrian mapping and derivative topical studies. Through informal arrangements with Zell Peterman, Larry Snee, and Randy Van Schmus, who shared with MGS geologists a common interest in the Precambrian geology of the Lake Superior region,

(1) U. S. Geological Survey
Branch of Isotope Geology
Federal Center, Box 25046, M. S. 963
Denver, CO 80225

(2) Department of Geology
University of Kansas
Lawrence, KS 66045

fundamental geochronologic data were obtained without cumbersome contracts and bureaucratic red tape. It is a pleasure to thank the Isotope Geology Branch of the U.S. Geological Survey and the Department of Geology at the University of Kansas for their cooperation.

Because of administrative reassignments, changes in research interests, and the length of time that has passed since some of the geochronologic data were obtained, Mssrs Peterman, Snee, and Van Schmus have opted to be acknowledged as contributors to this report rather than coauthors. Each age determination reported here is attributed to one of the contributors. To assure proper credit, the contributor who determined an age should be cited by name, along with the phrase "as reported in Southwick (1994)."

PRINCIPAL FACTS AND SAMPLE DESCRIPTIONS

The approximate localities from which the dated samples were collected and the Precambrian terranes of Minnesota in which they occur are shown in Figure 1. This section presents descriptions of the compositions, field settings, and detailed locations for the sample set. Details of the isotopic analyses are presented in the next section, together with interpretations of the results. The last section contains a regional summary and tectonic synthesis.

Sample EM-8. Gneissose tonalite (Tables 1 and 2) within the intrusive complex that constitutes the Giants Range batholith (Late Archean) in the Wawa subprovince of the Superior Province, northeastern Minnesota. The rock is a coarse-grained, strongly foliated phase within the unit mapped as Embarrass tonalite by Southwick (1991). Geologic field relations indicate that this gneissose tonalite is among the oldest intrusive components of the batholith. Modally it consists of essential quartz, plagioclase, and biotite, minor quantities of microcline and epidote, accessory sphene, apatite, and zircon, and variable small amounts of secondary muscovite and chlorite. At the sample site and throughout most of its mapped extent the tonalite contains many slab-shaped inclusions of amphibolite and biotite-quartz-plagioclase schist that are oriented parallel with its grain-scale foliation, and it is cut by abundant dikes and irregular masses of trondhjemite.

Location: SW1/4SE1/4SW1/4SW1/4 sec. 9, T. 60 N., R. 14 W. St. Louis County (Embarrass quadrangle). The sample site is a prominent roadcut on the north side of County Highway 22.

Sample ST-1. Gneissose tonalite (Tables 1 and 2) located within the weakly magnetic "quiet zone" at the south margin of the Wawa subprovince in central Minnesota, just outboard of the eroded tectonic front of the Early Proterozoic Penokean orogen (Fig.1). The rock is medium- to coarse-grained and foliated; the foliation, though pervasive, is variably developed and generally somewhat indistinct. Small, ovoid inclusions of mafic composition form a small fraction of the total tonalite mass. Plagioclase, quartz, hornblende, and biotite are the essential minerals of the tonalite; epidote and other secondary phases account for 5 percent or more of the rock by volume. The tonalite is wallrock to a sharply discordant, northwest-striking, vertical dike of diabase that is inferred to be of Early Proterozoic age and a member of the Kenora-Kabetogama dike swarm (Southwick and Day, 1983; Southwick and Chandler, 1989). Prominent brittle shear veins filled with epidote trend northwest, parallel to the dike. The dated sample was collected about 10 m from the dike margin in an area free of epidote veins.

Location: SE1/4SE1/4SE1/4NE1/4NE1/4 sec. 28, T. 134 N., R. 32 W. Cass County (Motley NW quadrangle). The outcrop is an isolated bedrock knob surrounded by sandy glacial outwash.

Sample BRV-1. Gneissose tonalite (Tables 1 and 2) located in the magnetically featureless "quiet zone" at the southern margin of the Wawa subprovince in central Minnesota. The rock type and its regional geologic setting are very similar to those for dated sample ST-1, described above. The rock is a medium-grained, weakly deformed hornblende tonalite composed of essential quartz, plagioclase, and hornblende, and contains 5 percent or more well-crystallized epidote of possible deuteric origin. Accessory sphene, zircon, and allanite are relatively abundant in unusually large and robust grains. Small, ovoid mafic inclusions of indeterminant origin are scattered throughout. The most prominent element of the structural fabric is a weak to moderate hornblende lineation that plunges at a shallow angle to the northwest.

Location: SE1/4NW1/4SE1/4NE1/4 sec. 15, T. 131 N., R. 33 W. Todd County (Browerville NE quadrangle). The outcrop is a natural, glaciated knob that rises about 10 feet above the surface of the Long Prairie River floodplain.

Sample SQ-8. Gneissic tonalite (Table 2), weakly foliated, medium-grained, from the subsurface Jeffers block of the Minnesota River Valley gneiss subprovince in southwestern Minnesota (Fig. 1). Although the rock has clearly been deformed, its original igneous texture is quite well preserved. The primary minerals include plagioclase, quartz, hornblende, and biotite; accessory apatite, epidote, opaque phases, zircon, and sphene aggregate to as much as 3 percent of the rock by volume. Foliation is carried by modal layers about 10-15 cm thick that differ slightly from one another in abundance of mafic minerals, and by a weak preferred orientation of biotite. The layering, biotite fabric, and preferred orientation of small, discoid mafic schlieren are all essentially coplanar.

Location: SW1/4SW1/4SW1/4NW1/4 sec. 11, T. 107 N., R. 31 W. Watonwan County (La Salle quadrangle). The sample is a diamond drill core from depth interval 448 to 455 feet in a vertical hole drilled in 1980 by the mining division of Pan Ocean Oil, Ltd. Splits of the core are retained in the core library of the Minerals Division of the Minnesota Department of Natural Resources in Hibbing, Minnesota.

Sample SQ-5. Mesocratic quartz monzonite to granodiorite (Tables 1 and 2), medium-grained, that is situated in the south-trending subsurface extension of the plutonic belt of the Penokean orogen in southern Minnesota (Fig. 1). The dated rock contains essential plagioclase, K-feldspar, quartz, hornblende, clinopyroxene, and biotite, and accessory sphene and zircon in prominent, robust crystals. Small, rounded, amphibolitic inclusions of obscure origin and significance are dispersed throughout.

Location: SE1/4SE1/4SE1/4SE1/4 sec. 11, T. 102 N., R. 36 W. Jackson County (Lakeville NE quadrangle). The sample is a diamond drill core from depth interval 967 to 987 feet in a vertical hole drilled in 1979 by the mining division of Pan Ocean Oil, Ltd. Splits of the core are retained in the core library operated by the Minerals Division of the Minnesota Department of Natural Resources in Hibbing, Minnesota.

Sample PBI-27. Melanocratic hornblende ferrodiorite and hornblende pyroxenite (Tables 1 and 2), massive, medium-grained. These rock types are interlayered and intergrade modally; together they form one of several consanguineous intrusive phases in the diorite-ferrodiorite-oxide gabbro-nelsonite-anorthosite range of compositions that collectively make up a small pluton near Philbrook, Minnesota (Boerboom, 1987). The pluton intrudes heterolithic conglomerate and pelitic to psammitic slate within the Long Prairie basin, a probable foredeep accumulation of Early Proterozoic age that is analogous to and possibly correlative with the fill in the Animikie basin a short distance to the east (Southwick and others, 1988; Southwick and Morey, 1991). Both the ferrodiorite and hornblende pyroxenite contain essential olive-green to brown hornblende that is at least in part pseudomorphous after clinopyroxene, and a secondary, acicular, blue-green actinolitic hornblende that is interpreted to be of deuteric origin. The other major rock-forming minerals are clinopyroxene, plagioclase, and Fe-Ti oxides. Apatite is an abundant accessory. The material used for dating by the $^{40}Ar/^{39}Ar$ method is olive-green to brown hornblende inferred to be of primary igneous origin that was separated from the rocks by hand-picking.

Location: SE1/4NW1/4NW1/4NW1/4 sec. 3, T. 132 N., R. 32 W. Todd County (Motley quadrangle). Hornblende was separated from pyroxenite and ferrodiorite intersected by Adams Estate drill cores 1 and 6, depths 74 to 80 feet and 50 to 53 feet, respectively. Both cores were drilled in 1910 and are stored at the Minnesota Geological Survey in St. Paul. Small outcrops of similar ferrodiorite occur near the drill sites.

Sample SX-60PEB. Composite sample of rhyolite pebbles from a conglomeratic facies of the Sioux Quartzite (Fig. 1). The rhyolite pebbles range in size from 1 to 10 cm (most are in range 3-5 cm), are aphanitic with prominent millimeter-size quartz phenocrysts, and are brick-red in color. Some display very well preserved ghosts of former glass shards and clear remnants of perlitic cracking, both indicative of derivation from an ash-flow tuff source. Rhyolite pebbles constitute about 5-10 percent of a mature pebble population that includes in addition pebbles of vein quartz, chert, jaspery iron-formation, pink quartzite, and dark reddish-purple siliceous mudstone. The sampled outcrop consists of conglomerate beds 1 to 3.5 feet thick that alternate with coarse quartzarenite beds of similar thickness. Master bedding strikes slightly east of north and dips about 14 degrees to the southeast at the sample site. Channeling and festoon cross-bedding are well developed, and the flatter clasts in the conglomerate beds tend to be imbricated. The sample material used for geochronology was collected by blasting a low stream-cut exposure of conglomerate with explosives and then hand-cobbing the rubble for clean fragments of rhyolite pebbles.

Location: SE1/4SW1/4SW1/4SW1/4 sec. 36, T. 106 N., R. 47 W. Pipestone County (Jasper NW quadrangle). The sampled outcrop is a low set of cuts and riffles along a small stream about 300 yards east of the Salem Church.

GEOCHRONOLOGIC DATA AND INTERPRETATION

Sample EM-8. Tonalite gneiss from the eastern part of the Giants Range batholith, near Embarrass, Minnesota. Geochronology by Z.E. Peterman.

The zircon separated from this rock is very fine grained; most is finer than 200 mesh (0.074 mm) and somewhat less falls in the range -150, +200 mesh (0.104 to 0.074 mm). Initially, two of the extreme size fractions were analyzed for Pb and U isotopic composition—a fraction in the range -150, +200 mesh (0.104 to 0.074 mm) and a fraction in the range -325, +400 mesh (0.044 to 0.037 mm). The spread in isotopic composition for these two fractions was small, in terms of the ratios $^{206}Pb/^{238}U$ and $^{207}Pb/^{235}U$ (Fig. 2), and, in an effort to increase the spread, a least-magnetic fraction of the -325, +400 mesh size range was obtained and analyzed. The resulting three

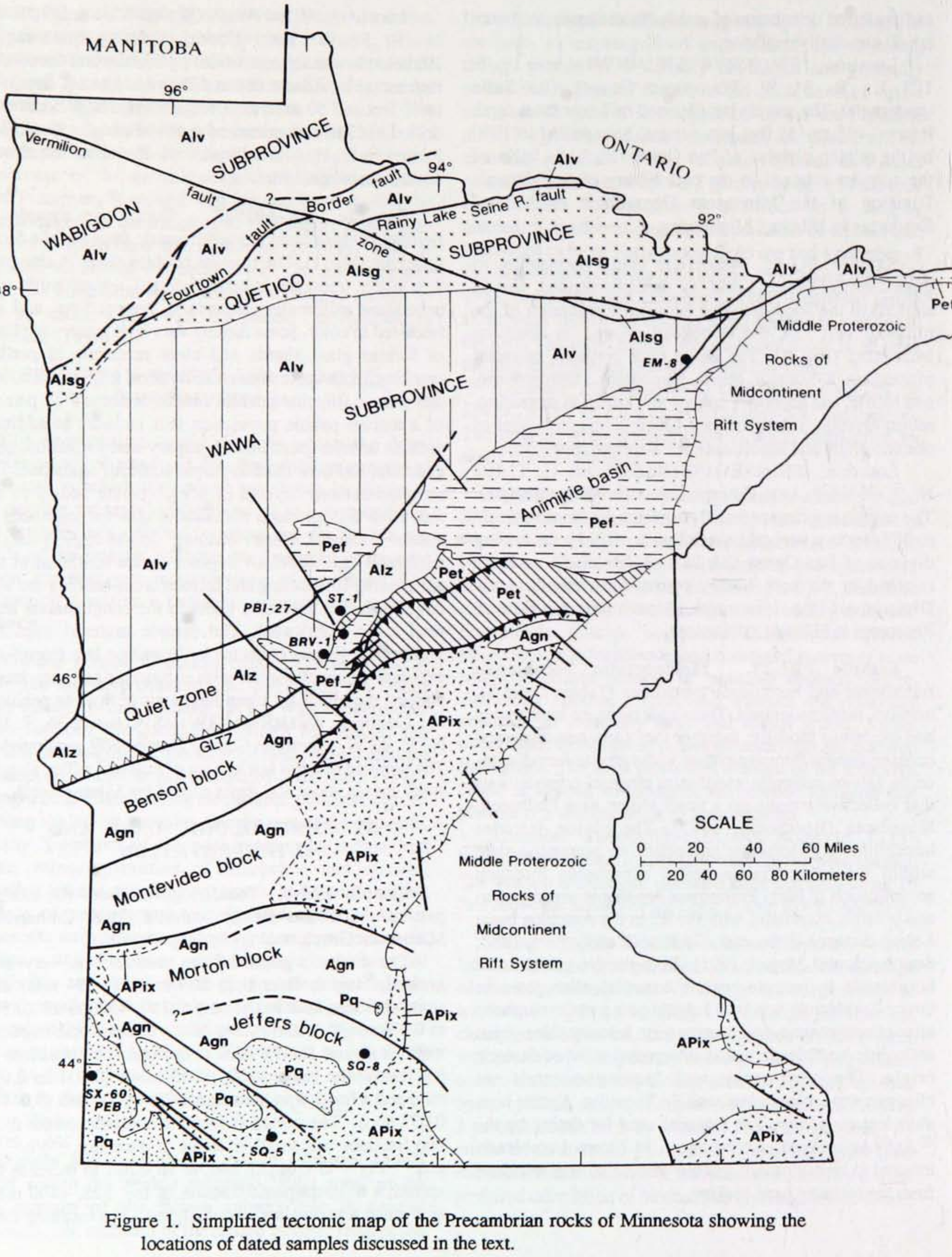

Figure 1. Simplified tectonic map of the Precambrian rocks of Minnesota showing the locations of dated samples discussed in the text.

EXPLANATION (FIGURE 1)

EARLY PROTEROZOIC AND ARCHEAN TERRANES OF MINNESOTA

TECTONIC ELEMENT		PRINCIPAL ROCK TYPES	AGE
Sioux Quartzite basins	Pq	Fluvial, sand-dominated redbed sequence	1,760 to 1,630 Ma (inferred)
Penokean orogen			
foredeeps	Pef	Turbiditic graywacke-shale sequences	
fold-and-thrust belt	Pet	Passive-margin volcanic and sedimentary rocks, tectonically imbricated	2,200 to 1,760 Ma
intrusion-dominated magmatic terrane	APix	Syn- to post-kinematic granitoid rock sand their host rocks	
Superior Province (craton with respect to Penokean events)			
Wabigoon subprovince	Alv	Arc-like volcanoplutonic sequences	Approximately 2,750-2,650 Ma
Quetico subprovince	Alsg	Turbiditic metasedimentary rocks (accretionary complex?), granitoid intrusions	
Wawa subprovince "quiet zone"	Alv Alz	Arc-like volcanoplutonic sequences; rocks of quiet zone (Alz) are regionally retrograded	
Minnesota River Valley subprovince Benson block Montevideo block Morton block Jeffers block	Agn	Complex and variable gneisses; abundant granitoid intrusions	Approximately 3,600-2,600 Ma

Table 1. Chemical data for coarse-grained intrusive rocks discussed in the text

	Giants Range	"Quiet zone"			Southern Minnesota	Philbrook intrusion	
	1	2	3	4	5	6	7
	EM-8	BRV-1	ST-1	ST-G9	SQ-5	PB-1	PB-3-1-74
SiO_2 (wt%)	71.4	61.41	58.2	57.12	60.8	42.1	32.3
TiO_2	0.27	0.40	0.51	0.42	0.56	4.32	5.60
Al_2O_3	15.4	17.60	18.0	18.74	14.9	12.9	2.94
Fe_2O_3	0.68	1.65	2.20	2.62	2.30	2.8	20.0*
FeO	1.0	2.24	2.5	2.42	3.0	14.2	17.2
MnO	0.02	0.05	0.08	0.06	0.09	0.26	0.53
MgO	0.78	2.63	5.06	4.28	4.12	6.24	6.79
CaO	2.39	5.96	4.12	7.06	5.14	11.4	9.28
Na_2O	5.73	5.49	4.58	3.37	4.26	2.60	0.40
K_2O	1.23	0.77	1.99	1.53	2.62	0.61	0.12
P_2O_5	0.06	0.19	0.21	0.45	0.24	2.1	1.34
H_2O	0.60	1.29	2.10	1.20	1.30	n.d.	n.d.
CO_2	0.10	0.09	<0.10	0.34	0.21	n.d.	n.d.
Total	99.66	99.77	99.55	99.61	99.54	99.53	96.50
Rb	48	24	39	–	58	7	1
Sr	798	733	729	–	943	400	45
Ba	565	–	712	–	837	520	35
Nb	15	–	<10	–	11	–	–
Zr	67	–	114	–	151	520	122
Y	<10	–	<10	–	20	45	37
Cr	23	–	150	–	102	3.9	18.3
Ni	–	–	-	–	–	8	39
Cu	–	–	-	–	–	53	97
Zn	–	–	-	–	–	150	215
V	–	–	-	–	390	673	–

Analysts:

Columns 1, 3, 5: X-Ray Assay Laboratories, Don Mills, Ontario, 1991. Major and trace elements by XRF; FeO, CO_2, H_2O, by wet chemistry.

Column 2: K. Ramlal, University of Manitoba 1982. Major elements by XRF; FeO, CO_2, H_2O by wet chemistry. Rb, Sr by XRF at U.S. Geological Survey.

Column 4: F.F. Grout, University of Minnesota; reported in Grout (1908). Sample from same outcrop as ST-1. Major elements by wet chemistry.

Columns 6, 7: R. Knoche, University of Minnesota, 1984-1986. Major and trace elements by DCAP/OES; FeO by wet chemistry for PB-1. *NOTE: Total iron reported as 39.1% of Fe_2O_3 in sample PB-3-1-74; this was recomputed to Fe_2O_3 and FeO as tabulated to account approximately for the modal amount of magnetite present in the rock.

Table 2. Modal compositions of radiometrically dated samples discussed in the text

	1 EM-8	2 BRV-1	3 ST-1	4 SQ8	5 SQ-5	6 PB-1	7 PB-3-1-74
Quartz (vol.%)	25	17	16	23	11	–	–
K-feldspar	2	tr	tr	2.5	17	–	–
Plagioclase	65	62.5*	54*	66	45	29	–
Biotite	6	–	2	1	6	4	–
Hornblende	–	8†	12†	3†	14	19	18
Clinopyroxene	–	–	–	–	4	–	39
Opaques	tr	ttr	ttr	tr	1.3	10	26
Apatite	tr	tr	tr	tr	tr	5	tr
Sphene (+leucoxene)	tr	tr	tr	1	tr	–	–
Zircon	ttr	ttr	ttr	ttr	ttr	–	–
Rutile	ttr	ttr	ttr	ttr	ttr	–	–
Allanite	–	ttr	ttr	ttr	ttr	–	–
Secondary amphibole	–	x	x	x	tr	32	49
Chlorite	0.5	3	6	0.5	0.5	tr	tr
Epidote (+ clinozoicite)	0.5	8	8	1.5	1	tr	tr
Carbonate	–	tr	tr	ttr	–	–	tr
Adularia	–	–	ttr	–	tr	–	–
Prehnite	–	–	ttr	–	ttr	–	–
Muscovite	0.5	12	1.5	0.5	–	–	–
Total	99.5	99.5	99.5	99	99.8	99	99

NOTES:

Analyses based on 1,000-1,500 points each.
tr = present in amounts between 0.1 and 0.5 volume percent.
ttr = present in amounts less than 0.1 volume percent.
x = present in substantial amounts; counted with primary hornblende.
--- = not detected.

* Plagioclase heavily sericitized, saussuritized.
† Entry includes primary and secondary hornblende.

Data in columns 6, 7 are from Boerboom (1987).

points, although moderately discordant (Fig. 2), are colinear, defining intercepts with concordia of 2,718 and 1,159 Ma. The associated uncertainties, based on standard regression techniques (York, 1969), are ± 67 and ± 140 Ma, respectively, for the upper and lower intercepts.

Assuming that the U-Pb isotopic systems are reflecting a simple two-event scenario, the primary age of 2,718 ± 67 Ma is within the range of U-Pb zircon estimates for the Late Archean crystallization age of the Giants Range batholith (summary in Prince and Hanson, 1972). The lower intercept age of 1,159 ± 140 Ma is close to the well-established age of about 1,100 Ma for magmatic and tectonic events in the Midcontinent rift system (Silver and Green, 1963; Davis and Sutcliffe, 1985; Palmer and Davis, 1987; Davis and Paces, 1990), and raises the possibility that U-Pb isotopic systematics in 2,700-Ma zircons were affected by Middle Proterozoic thermal events associated with rifting. This possibility is further indicated by 1,100-Ma lower intercepts in U-Pb data for sphene and zircon in other rocks from the eastern part of the Giants Range batholith studied by Catanzaro and Hanson (1971).

To test the possibility of 1,100-Ma disturbance, biotite from sample EM-8 was dated by the K-Ar method on the supposition that K-Ar systematics in biotite are generally more susceptible to thermal resetting than the U-Pb systematics in zircon, and that a K-Ar "age" on biotite should affirm a Keweenawan thermal event if one did indeed affect the rock. The resulting K-Ar age for the biotite is 2,570 Ma, not significantly different from the biotite ages reported throughout the Superior Province terranes of northern Minnesota (Goldich and others, 1961). Hence, if the lower intercept of the discordia for zircons in Archean tonalite gneiss in EM-8 is recording a Keweenawan thermal event, the intensity was not sufficient to reset the K-Ar system in biotite.

Samples ST-1 and BRV-1. Gneissic tonalite from the Staples-Browerville area of central Minnesota, in the magnetically subdued "quiet zone." These are discussed together because of their petrographic similarity, regional proximity, and similar tectonic setting. Geochronology by Z.E. Peterman.

The zircons in these rocks range in size from -100, +150 mesh to less than 325 mesh (0.149 to less than 0.044 mm). The least magnetic splits of two size fractions for each rock sample were analyzed for Pb and U isotopic composition; the size fractions used and the isotopic results obtained, in terms of the ratios $^{206}Pb/^{238}U$ and $^{207}Pb/^{235}U$, are shown on Figure 3. The data points for the two samples can be interpreted to lie on separate, parallel chords (Fig. 3). For sample ST-1, the upper intercept, presumably representing a primary age, is at 2,640 ± 11 Ma, and for sample BRV-1 the upper intercept is at 2,666 ± 8 Ma. These results suggest that the two tonalites may differ in age by about 26 m.y. However, because each chord is determined by only two data points, the age difference between the two samples and the small uncertainties associated with each age may both be

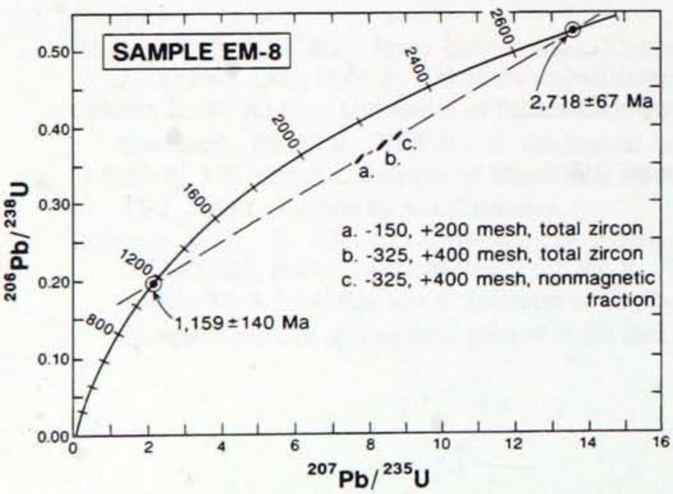

Figure 2. Concordia plot of U-Pb isotopic data from zircons in sample EM-8, a gneissic tonalite in the eastern part of the Giants Range batholith. Data acquired by Z.E. Peterman, U.S. Geological Survey, 1980.

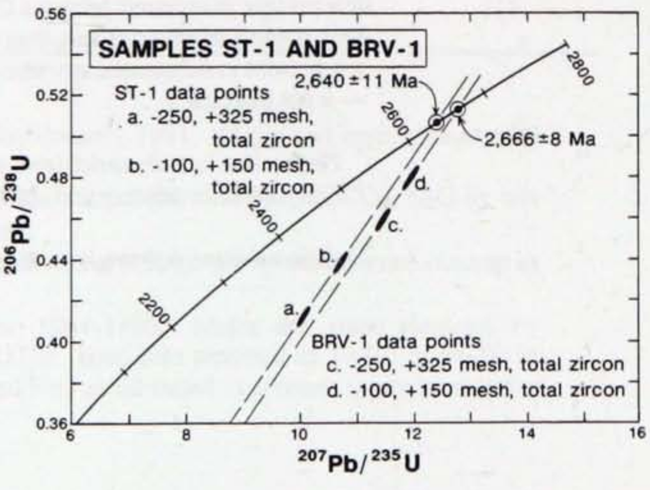

Figure 3. Concordia plot (upper part only) of U-Pb isotopic data from zircons in ST-1 and BRV-1 samples. Both samples are gneissic tonalite within the "quiet zone" at the southern margin of the Wawa subprovince. A chord regressed through both data sets yields an upper intercept age of 2,688 ± 72 Ma. Data acquired by Z.E. Peterman, U. S. Geological Survey, 1983.

illusory. A chord through all four data points is only slightly outside of analytical error and produces an upper intercept at 2,688 ± 72 Ma. This somewhat greater age, and greater uncertainty, may more closely approximate the true age of these gneissic tonalites. Although further work is needed to resolve their precise age, it is clear that the rocks formed in the Late Archean and therefore are unambiguously part of the Superior Province.

The results of whole-rock Rb-Sr analyses for these samples are summarized in Table 3. Both tonalites are high in Sr and low in Rb, as is the case with many Late Archean tonalites elsewhere in the Superior Province (e.g., Peterman, 1979; Feng and Kerrich, 1992), and the Sr is relatively nonradiogenic. The initial $^{87}Sr/^{86}Sr$ ratios (IR of Table 3) were calculated from the observed ratios, assuming the U-Pb zircon ages of 2,640 and 2,666 Ma for samples ST-1 and BRV-1, respectively. The calculated initial ratios are virtually identical to the average IR value of 0.70065 for northern Minnesota Late Archean igneous rocks, further strengthening the association of the "quiet zone" tonalites with tonalites in "normal" parts of the Wawa subprovince to the north. Moreover, the relatively primitive initial ratios in these tonalites argue against the involvement of older continental rocks in the petrogenesis of "quiet-zone" tonalitic magmas.

Sample SQ-8. Gneissic tonalite in the Jeffers block of the Minnesota River Valley subprovince, Watonwan County, southern Minnesota. Geochronology by W.R. Van Schmus.

Four size fractions of unabraided zircon separated from this rock yield a discordant U-Pb age of 2,624 ± 57 Ma. Although the isotopic systematics of the sample are somewhat disturbed, the analytical age is interpreted to be a reasonable approximation of the crystallization age of the tonalite. The tonalite clearly is of Archean age and is not part of the Early Proterozoic suite of plutons associated with tectonic convergence during the Penokean orogeny.

The rock also yields a Sm-Nd model age (Tdm) of 2,700 Ma, based on the depleted mantle model of DePaolo (1981). Such model ages are commonly referred to as mantle separation or crustal residence ages and generally record the time at which a crustal volume first separated from the mantle. If a body of igneous rock was re-activated from older crustal material (by partial melting, for example), or incorporated large quantities of older material (by assimilation of wall rock), the Sm-Nd model age for that body of rock will be older than the emplacement age. Therefore, the gneissic tonalite from Watonwan County either ascended more or less directly from a mantle source in Late Archean time, or it formed from a crustal source that itself had separated from the mantle in the Late Archean. There is no evidence in the present isotopic data that the tonalite interacted with 3,600-Ma continental crust. Therefore, either the sample site lies south of the volume of Middle Archean gneissic crust that constitutes the Minnesota River Valley subprovince (terminology of Card and Ciesielski, 1986; Card, 1990), or the tonalite passed through the older crust without interacting with it. At the present time there is no concrete evidence of Middle or Early Archean rocks south of the geophysically defined north boundary of the Jeffers block (Schaap,1989; also Fig. 1).

Sample SQ-5. Quartz monzonite and granodiorite; drill core from the Precambrian subsurface of Jackson County, southern Minnesota. Geochronology by Z.E. Peterman.

The zircons separated from this rock range in size from -100, +150 mesh to less than 325 mesh (0.149 to less than 0.044 mm). The least magnetic splits of two size fractions were analyzed for Pb and U isotopic compositions; the size fractions used and the isotopic results obtained, in terms of the ratios $^{206}Pb/^{238}U$ and $^{207}Pb/^{235}U$, are shown on Figure 4. These two analyses are rather closely spaced and somewhat discordant; therefore they define intercepts with concordia that have statistically large uncertainties. Nevertheless, the upper intercept value of 1,792 ± 31 Ma unequivocally establishes the rock to be of Early Proterozoic rather than Late Archean in age. This first-order question and its resolution are significant because the sample site is near the inferred tectonic front of the Penokean orogen against Archean cratonic foreland (Chandler and Southwick, 1990; Southwick and others,

Table 3. Whole-rock Rb-Sr data for Late Archean tonalite in the "quiet zone," central Minnesota (BRV-1 and ST-1)

Sample	Rb, ppm	Sr, ppm	$^{87}Rb/^{86}Sr$	$^{87}Sr/^{86}Sr$	IR
BRV-1	24.05	733.4	0.0949	0.70422	0.70056 (at 2,666 Ma)
ST-1	32.88	788.8	0.1207	0.70557	0.70094 (at 2,640 Ma)

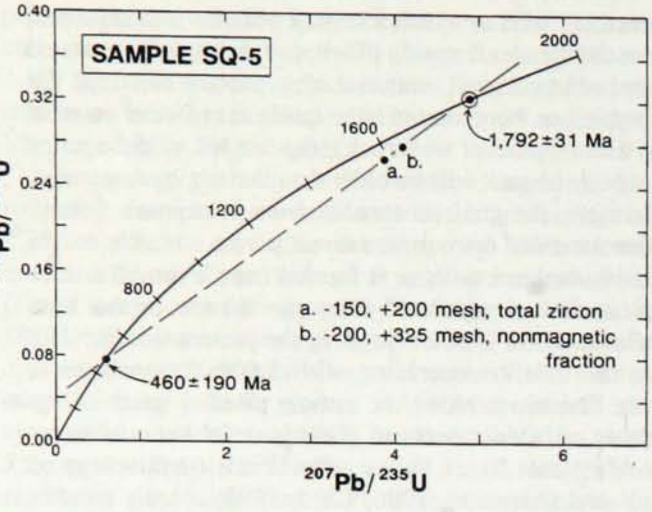

Figure 4. Concordia plot of U-Pb isotopic data from zircons in sample SQ-5, a mesocratic quartz monzodiorite from southern Minnesota. Data acquired by Z.E. Peterman, U.S. Geological Survey, 1986.

1988, 1990). It is now clear that rocks assignable to Penokean magmatic events occur in south-central Minnesota along a north-northeast to south-southwest trend from the St. Cloud area that is characterized geophysically by a markedly nodal pattern of aeromagnetic anomalies (Chandler, 1987, 1989) and a moderate to strong regional gravity high (Ervin and others, 1980; Ervin, 1980).

Whole-rock Rb-Sr results for this sample are summarized in Table 4. These data show that the rock is high in Sr and low in Rb, and that the Sr is relatively nonradiogenic. Therefore its initial $^{87}Sr/^{86}Sr$ ratio of 0.70298 ± 11 (IR in Table 4) is rather precisely defined by the measured Rb-Sr data and the zircon crystallization age of 1,792 Ma. The essentially unenriched IR value suggests that older continental crust did not participate in the petrogenesis of sample SQ-5, despite the fact that well-documented cratonic crust of Middle to Late Archean age (Goldich and Wooden, 1980) crops out within 60 miles of the sample site, and is inferred on geophysical grounds to come within 12 miles of it in the subsurface (Fig. 1; Schaap, 1989).

Sample PBI-27. Hornblende ferrodiorite and pyroxenite, Philbrook intrusion, Morrison County. Geochronology by L. W. Snee.

Hornblende from these rocks that is interpreted on petrographic grounds to be of magmatic and deuteric origin was dated by the $^{40}Ar/^{39}Ar$ technique. It yields a plateau age of $1,854 \pm 4$ Ma (Table 5 and Fig. 5A), which dates the time at which the Philbrook pluton cooled below the blocking temperature for argon release from hornblende. That temperature would have been reached an unknown time interval after the pluton was emplaced, the difference between emplacement age and cooling age depending on the unquantifiable details of the pluton's thermal history. Thus the age determined by the $^{40}Ar/^{39}Ar$ method is a minimum age for the pluton.

The ^{39}Ar age spectrum for hornblende from the Philbrook pyroxenite and ferrodiorite is relatively simple except for the first few and the last few temperature steps (Fig. 5A). Some insight into the cause of this pattern is presented by Figure 5B, which is a plot of the $^{39}Ar/^{37}Ar$ isotopic ratio as a function of the percentage of ^{39}Ar released at each temperature step. Because ^{37}Ar is derived from the radioactive decay of Ca and ^{39}Ar is derived from the radioactive decay of K, the low values of the isotopic ratio $^{39}Ar/^{37}Ar$ observed at the low and high temperature steps indicate that the mineral phase (or phases) being degassed in those increments is lower in K/Ca ratio than the most abundant hornblende in the sample. It is known from petrographic study that primary "igneous" hornblende is epitaxially overgrown by a blue-green "deuteric" amphibole throughout the ferrodiorite and pyroxenite, and that microscopic inclusions of plagioclase, epidote, sphene, and apatite are common within amphibole crystals. The erratically low yields of ^{39}Ar at the low and high temperature ends of the age spectrum therefore may be due to secondary, low-K amphibole overgrowths on igneous hornblende, together with included high-Ca, low-K minerals. The intermediate temperature steps yield relatively constant isotopic compositions of evolved argon; that argon is interpreted to have come from igneous hornblende.

Microprobe analyses of amphiboles of different textural and paragenetic types in the samples support the isotopic argument. The red-brown cores of amphibole grains interpreted to be of primary igneous origin are significantly richer in K (Table 6, cols. 1 and 2) than the outermost colorless zones that surround these cores (col. 3) or the fibrous blue-green amphibole of probable deuteric origin that fringes the primary amphibole and replaces

Table 4. Whole-rock Rb-Sr data for Early Proterozoic quartz monzonite, southern Minnesota (SQ-5)

Sample	Rb, ppm	Sr, ppm	$^{87}Rb/^{86}Sr$	$^{87}Sr/^{86}Sr$	IR
SQ-5	51.99	946.1	0.1582	0.70708	0.70298 (at 1,792 Ma)

Table 5. Argon isotope data for hornblende sample PBI-27

Heating step	Temp.	Radiogenic ^{40}Ar	K-derived ^{39}Ar	F value	Radiogenic yield	$\%^{39}Ar$ total	Apparent age (Ma at 1 sigma)
1	600	.61050	.00289	211.593	23.6	0.3	1800.37 ± 34.93
2	650	.09433	.00136	69.166	28.6	0.2	1800.37 ± 45.54
3	700	.11103	.00185	59.866	38.6	0.2	1640.34 ± 53.4
4	750	.21974	.00314	69.929	66.8	0.4	1812.90 ± 27.4
5	800	2.17693	.02990	72.812	91.8	3.6	1859.45 ± 5.37
6	850	11.60870	.16026	72.426	98.3	19.3	1853.28 ± 25
7	900	5.66522	.08102	72.394	97.8	9.8	1852.77 ± 3.83
8	950	3.29910	.04546	72.570	97.0	5.5	1855.57 ± 4.09
9	1000	4.50189	.06165	73.028	96.9	7.4	1862.88 ± 3.84
10	1050	15.63871	.21567	72.512	99.0	26.0	1854.65 ± 3.43
11	1100	6.26833	.08766	73.509	98.4	10.6	1838.55 ± 4.19
12	1150	.64567	.00980	65.892	87.3	1.2	1745.64 ± 1214
13	1200	.59136	.01057	55.932	84.6	1.3	1567.11 ± 26.01
14	1400	1.19765	.02980	40.189	82.3	3.6	1246.14 ± 5.17
Total gas				71.371			1836.33 ± 4.33

Table 6. Microprobe analyses of amphibole, Philbrook intrusion
[Data from Boerboom (1987)]

	1 HB13-74	2 HB14-74	3 HB16-74	4 ACT1-74	5 ACT2-74
SiO_2 (wt%)	36.91	37.34	46.82	50.95	51.25
Al_2O_3	12.39	12.69	1.63	1.82	1.16
FeO	21.77	22.85	21.38	20.25	20.08
MgO	6.18	5.85	9.92	10.61	10.83
CaO	11.21	11.38	11.61	11.97	11.78
Na_2O	2.45	2.21	0.43	0.38	0.34
K_2O	1.46	1.23	0.23	0.20	0.15
TiO_2	2.54	1.99	.011	0.06	0.0
MnO	0.25	0.23	0.40	0.32	0.44
Total	95.16	95.76	92.52	96.55	96.02
Number of ions per 23 oxygen					
Si	5.958	5.996	7.587	7.733	7.812
Al	2.358	2.402	0.310	0.325	0.208
Fe	2.938	3.068	2.881	2.570	2.560
Mg	1.488	1.397	2.385	2.400	2.461
Ca	1.939	1.958	2.005	1.947	1.923
Na	0.766	0.688	0.134	0.113	0.100
K	0.300	0.252	0.046	0.039	0.030
Ti	0.308	0.241	0.013	0.006	0.000
Mn	0.034	0.031	0.054	0.041	0.056

1, 2: Ferropargasitic hornblende, red-brown; cores of grains interpreted to be primary igneous amphibole.

3: Ferroactinolitic hornblende, colorless; outer zone around red-brown ferropargasitic cores.

4, 5: Actinolite, fibrous, pale blue-green; invades and replaces primary amphibole.

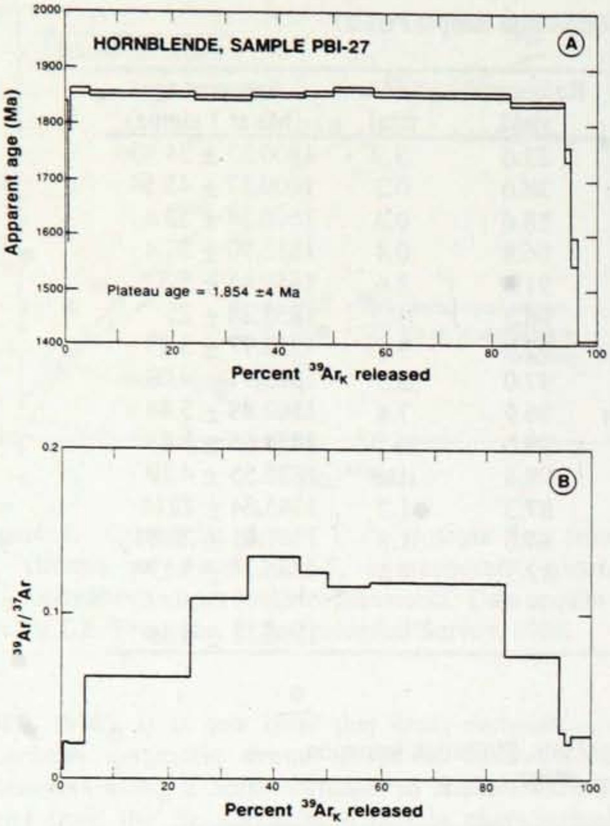

Figure 5. (**A**) ^{39}Ar age spectrum for hornblende sample PBI-27. Hornblende was separated from consanguineous ferrodiorite and pryoxenite phases of the Philbrook pluton. Plateau on heating steps 5 to 11 contains 82.3 percent of the gas. (**B**) Plot of $^{39}Ar/^{37}Ar$ vs percent ^{39}Ar released, same hornblende sample. Data acquired by L.W. Snee, U.S. Geological Survey, 1991.

primary clinopyroxene (cols. 4 and 5). The ferropargasitic core hornblende was the predominant species in the hand-picked amphibole concentrate used for argon analysis, and most probably was the mineral responsible for the flat central plateau of the ^{39}Ar age spectrum.

Sample SX-60PEB. Rhyolite pebbles and cobbles in the Sioux Quartzite, Pipestone County, southwestern Minnesota. Geochronology by E.T. Wallin and W.R. Van Schmus.

The rhyolite pebbles in the Sioux Quartzite give a very discordant and highly uncertain U-Pb zircon age of 1,902 ± 55 Ma (Van Schmus, unpublished circular, 1988; Wallin and Van Schmus, 1988). Given the broad analytical uncertainty of this age determination, rhyolite volcanism in the source region that supplied detritus to the Sioux Quartzite could have overlapped in time with the major period of syntectonic magmatism in the Penokean orogeny (ca 1,860-1,870 Ma), or it could have been much earlier. The depositional age of the Sioux cannot be greater than the age of the rhyolite pebbles, but these new data do not significantly refine the time limits for Sioux deposition beyond the level of precision already extant (Dott , 1983; Southwick and others, 1986; Chandler and Morey, 1992).

The fine-scale petrographic textures of the dated rhyolite pebbles are remarkably preserved and indicate that the pebbles were derived from a sequence of flows and ignimbrites that originally were glassy. Figure 6 shows unmistakable perlitic cracking of a formerly glassy rock that has devitrified to a fine-grained crystalline aggregate of quartz, hematite, and other phases. Figure 7 shows the preservation of delicate bubble-wall shards in a devitrified welded tuff. The principal phenocrysts in the glassy rhyolite are bipyramidal quartz; these typically show evidence of arrested resorption (Fig. 7) and are virtually unstrained. The very low level of strain recorded by the quartz phenocrysts, the excellent preservation of delicate groundmass textures, and the absence of secondary fabrics all point to an anorogenic history for the rhyolite sequence from which these pebbles were derived. Therefore it is unlikely that the rhyolite magmatism had any direct connection with the syntectonic magmatism of the Penokean orogeny (Van Schmus, 1980).

Although the pebbles under discussion have been classified as rhyolite on the basis of their preserved textures and siliceous composition, it is clear from chemical data that they are strongly altered rocks. Direct comparison of their composition (Table 7, cols. 1 and 2) with compositions of unaltered high-silica rhyolites (Table 7, cols. 3 and 4) shows that the pebbles have been modified by large-scale addition of silica and removal of alkalies. These changes are reflected in a norm that is very high in quartz, very low in the feldspars, and greatly elevated in corundum. The metasomatic alteration apparently was an isovolumetric replacement process, as judged from the exquisite preservation of textural details.

The secondary reconstitution of the rhyolite also is reflected in its modal mineralogy. The devitrified glassy groundmass consists of quartz, very fine grained white mica, dusty hematite, and traces of pale greenish-blue chlorite. There is no alkali feldspar in the groundmass. Original phenocrysts of alkali feldspar are totally replaced by fine-grained aggregates of white mica plus quartz or white mica alone. Very sparse mafic phenocrysts, inferred to have been biotite, now consist of finely crystalline quartz, diaspore, hematite, and sphene. Because the bulk composition of the rock is so depleted in alkalies, it is inferred that pyrophyllite may constitute a significant part of the material classed as white mica.

The question naturally arises as to whether the rhyolite pebbles were incorporated in the Sioux Quartzite as altered rocks, or altered in situ by diagenetic processes. Although

Table 7. Chemical data for altered rhyolite pebble in the Sioux Quartzite and for unaltered high-silica rhyolites from Missouri and California

	Analytical data			
	1	2	3	4
SiO_2 (wt%)	83.6	82.06	75.65	74.7
TiO_2	0.22	0.23	0.17	0.07
Al_2O_3	11.5	12.85	11.63	12.29
Fe_2O_3	1.35*	1.34*	2.06*	0.47
FeO	---	---	---	0.55
MnO	0.01	0.01	0.03	0.02
MgO	0.05	0.06	0.05	0.01
CaO	0.17	0.19	0.30	0.51
Na_2O	0.23	0.04	2.95	4.38
K_2O	0.20	0.05	5.68	4.25
P_2O_5	0.09	0.09	n.a.	<0.01
H_2O	2.54	2.98	1.77	2.92
CO_2	---	---	---	---
Total	99.84	99.81	100.28	100.17
Rb (ppm)	10	---	196	305
Sr	240	---	236	7
Ba	240	---	236	7
Nb	20	---	---	80
Zr	320	---	---	100
Y	100	---	---	74
Cr	20	---	---	---
Ni	4	---	---	---
Cu	6	---	---	---
Zn	7	---	---	59
V	10	---	---	---
La	26.6	---	46.9	17
Ce	52	---	84.1	39
Nd	20	---	n.d.	27
Sm	4.02	---	8.8	7.0
Eu	0.90	---	0.86	7.0
Tb	1.1	---	1.95	1.67
Yb	8.38	---	8.2	7.7
Lu	1.29	---	1.30	0.99

	CIPW norms		
	1	3	4
Q	82.88	35.19	32.76
or	1.22	34.15	25.83
ab	2.00	25.69	38.11
an	0.26	1.51	1.36
c	11.12	0.08	—
di	—	—	1.10
en	0.13	0.13	—
fs	1.74	3.23	—
mt	—	—	0.70
il	0.43	0.33	0.14
ap	0.22	---	---

1. Rhyolite pebble in Sioux Quartzite, Salem Church locality, Pipestone County, Minnesota.
2. Approximate major-element composition of rhyolite groundmass, calculated from analysis 1 by subtraction of phenocryst compositions in the proportions of modal phenocryst abundances.
3. Average composition of devitrified glassy rhyolite of Middle Proterozoic age, St. Francois Mountains, Missouri. Based on data from Bickford and others (1981, table 3) and Cullers and others (1981, table A-1).
4. Hydrated glassy rhyolite (Pleistocene), Coso volcanic field, California. Data from Bacon and others (1981, table 1a, analysis 12/3).

*Total Fe reported as Fe_2O_3.

data are insufficient to resolve this matter definitively, diagenetic alteration is suggested by the fact that the Sioux as a whole has undergone diagenesis in which both silica and the alkalies were mobile (Vander Horck, 1984; Morey, 1983, 1984; Southwick and others, 1986). The diagenetic reactions involved dissolution and virtually complete removal of detrital feldspar (Southwick and others, 1986) and the secondary deposition of quartz, kaolinite, sericite, pyrophyllite, and diaspore as cement and authigenic matrix. The alteration of the rhyolite pebbles involved extensive silicification, the loss of feldspar components, and the crystallization of sericite, diaspore, and pyrophyllite. These modifications are entirely compatible with the diagenetic history of the quartz arenite sequence in which the pebbles occur.

Because hematite was produced by diagenetic reactions in the Sioux Quartzite and the rhyolite pebbles it contains, the diagenetic fluids must have been relatively oxidizing. Furthermore, because silica clearly was soluble in the diagenetic fluids, they probably were somewhat alkaline (Garrels and Christ, 1965). Uranium is readily mobilized in oxidizing alkaline solutions (Langmuir, 1978). Therefore

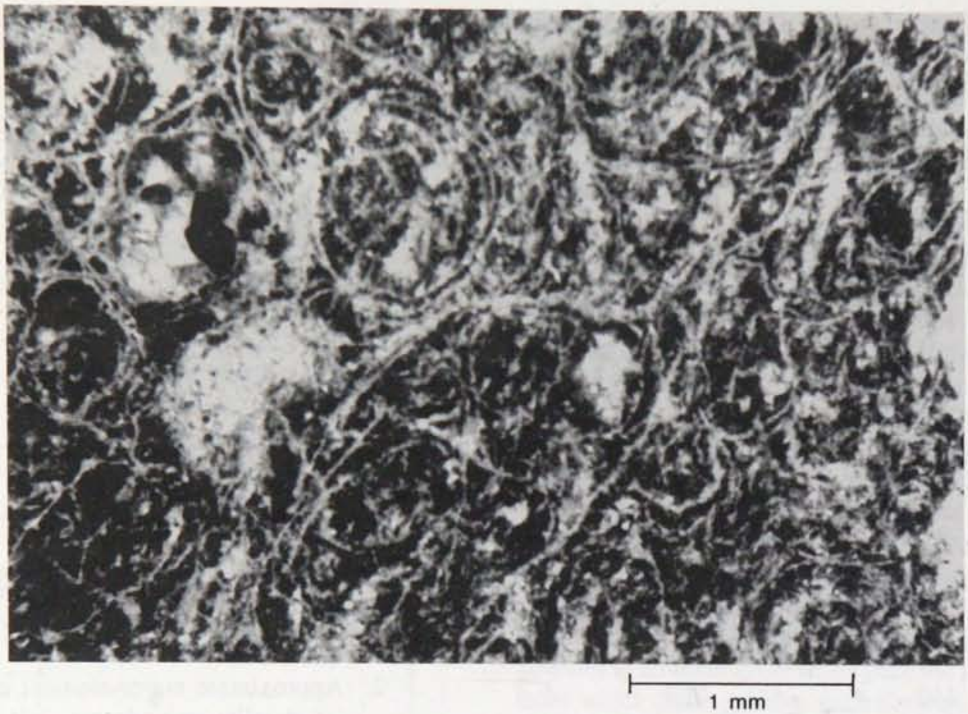

Figure 6. Photomicrograph (plane light) of a rhyolite pebble in the Sioux Quartzite showing perlitic crack pattern. Crack traces are healed by secondary quartz.

Figure 7. Photomicrograph (plane light) of a rhyolite pebble in the Sioux Quartzite showing textural evidence of bubble-wall shards in the groundmass. The shards are made visible by the unequal distribution of dusty hematite between the shards and the intervening quartz-rich matrix material.

uranium-bearing zircons would be vulnerable to selective uranium loss in diagenetic fluids such as those inferred to have affected the Sioux Quartzite, and the potential for uranium loss would be enhanced in zircons that were cracked or otherwise flawed. These factors may account in part for the large analytical uncertainty in the reported U-Pb zircon age for the rhyolite pebbles in the Sioux. Diagenetic uranium loss also would tend to drive the zircon "age" toward a fictitiously old value.

The effects of diagenesis on the systematics of radiogenic isotopic systems must be carefully evaluated when dealing with the constituents of permeable sedimentary rocks. Awwiller and Mack (1991) have recently shown that the Sm-Nd isotopic system is susceptible to diagenetic disturbance in sandstones and shales, and they advise caution in interpreting Sm-Nd data for sedimentary sequences that may have undergone burial diagenesis. Similar caution in interpreting U-Pb zircon data from such rocks may be appropriate.

DISCUSSION AND CONCLUSIONS

Regional interpretation of Archean age data

Although the Late Archean intrusive history of the Superior Province varies regionally and is complicated in detail (Card, 1990), it is generally true that within any volcanoplutonic subprovince there are two major intrusive suites. Plutons of the older suite carry the deformational fabric associated with the main tectonic event that affected the area in question (D_2 in the Wawa subprovince in Minnesota), and therefore they were emplaced before or during major tectonic activity. Most of these plutons fall within the tonalite-trondhjemite-granodiorite composition range; somewhat fewer fall within the monzonite-monzodiorite clan. Plutons of the younger suite lack deformational fabric or carry only a weak, locally developed one. They were emplaced in the waning stages of tectonic activity, and, as a first approximation, their emplacement marked the effective end of regional compression. Most of the large plutons in the late- to post-tectonic suite (areas larger than about 4 mi^2) are granite and monzogranite in composition. Small plutons in this group (areas less than about 4 mi^2) tend to be strongly heterolithic and typically fall into the syenite-monzodiorite-diorite composition range. In the western part of the Wawa subprovince, most of the U-Pb ages of the older plutonic suite are older than about 2,685 Ma and most of the ages of the younger suite are younger than about 2,680 Ma (Corfu and Stott, 1986; Zartman and others, unpub. data). Therefore tectonism appears to have ended, or nearly ended, between 2,685 and 2,680 Ma.

The Minnesota River Valley high-grade gneiss subprovince differs fundamentally from the volcanoplutonic subprovinces to the north in that it contains much older rock suites that have undergone more than one fabric-forming event (Goldich and Wooden, 1980). Therefore the division of intrusive rocks into those that are broadly syntectonic and those that are broadly post-tectonic is a misleading oversimplication. This point is illustrated by the fact that two suites of granite occur in the Minnesota River Valley that clearly differ in age and tectonic imprint, yet are very similar in their mineralogical and geochemical attributes. The older granite, termed adamellite-1 by Goldich and Wooden (1980), yields U-Pb minimum ages in the 3,050 to 3,100 Ma range and contains a strong deformational fabric. Two foliations are discernable locally. The younger granite suite, termed adamellite-2 by Goldich and Wooden (1980), generally lacks tectonic fabric. The most prominent unit of adamellite-2 is the Sacred Heart Granite, which forms a broadly sheetlike, elongate pluton of batholithic dimensions in the northern part of the Morton block (Fig.1).

The Sacred Heart Granite is late- or post-tectonic with respect to the second high-grade metamorphic event that affected the polygenetic gneisses of the Minnesota River Valley. It yields a whole-rock Pb-Pb age of 2,605 ± 6 Ma (Doe and Deleveaux, 1980), which is significantly younger than the ages for tectonically and compositionally similar granite bodies in volcanoplutonic subprovinces to the north.

It appears that sample SQ-8 from a covered part of the Minnesota River Valley subprovince is a relatively uncomplicated intrusive tonalite that underwent mild deformation and recrystallization; there is nothing in its petrography or geochemistry to suggest any genetic connection to the complex high-grade gneisses that typify the subprovince as a whole. Its U-Pb age of 2,626 ± 57 Ma overlaps that of the Sacred Heart Granite, although the statistically preferred age for the tonalite is older than that for the granite. Petrogenetically simple tonalites of Late Archean age have not been reported from the outcrop area along the Minnesota River, and therefore we have no direct knowledge of the time relations between this type of tonalite and the Sacred Heart Granite. Nevertheless, the "best" isotopic age, the composition, and the structural condition of tonalite SQ-8 relative to the same attributes of the Sacred Heart suggest that the tonalite and granite may bracket the end of the latest Archean tectonic event in the Minnesota River Valley subprovince. In other words, they may be analogous to the tonalite-granite pairs that bracket the end of the "Kenoran" event in the Wawa subprovince.

It is now widely accepted that the emplacement age of undeformed Late Archean granite plutons in any of the subprovinces of the Superior Craton marks the effective end of subduction-related tectonism within that subprovince, and also marks the time at which the subprovince became fully docked against a convergent margin of the growing craton (Card, 1990; Thurston and Chivers, 1990). If this interpretation is correct, and if tonalite SQ-8 and the Sacred Heart Granite are correctly dated as to emplacement age, as much as 60 m.y. may have elapsed between the tectonic amalgamation of the Wawa subprovince to the Superior Craton and the amalgamation of the Minnesota River Valley subprovince. The addition of the Minnesota River Valley subprovince to the growing craton appears to have been a late and perhaps final tectonic event.

The age data for gneissic tonalite samples EM-8, BRV-1, and ST-1 add to the knowledge of pre- and syntectonic magmatism in the Wawa subprovince. Field relations clearly indicate that the Embarrass tonalite gneiss of sample EM-8 is among the oldest intrusive units in the Giants Range batholith, and its apparent emplacement age of 2,718 ± 67 Ma (Fig. 2) is consistent with the field relations. Geologically younger components of the batholith yield significantly younger U-Pb ages; post-tectonic intrusions of granite are dated in the range 2,675-2,680 Ma (Zartman and others, unpub. data).

The gneissic tonalites from the "quiet zone" (Fig.1) are somewhat more enigmatic because of the lack of observable geologic context—the sampled outcrops are isolated at some distance from other Precambrian exposures. Nevertheless, it is fairly safe to infer from their well-developed foliations and lineations that tonalites BRV-1 and ST-1 were pre- or syntectonic with respect to the principal fabric-forming event (presumably D_2). The apparent emplacement age of 2,688 ± 72 Ma for these rocks, deduced from data from both samples (Fig. 3), is consistent with emplacement ages for precisely dated, pre- to syntectonic tonalites in the Shebandowan district in Canada (Corfu and Stott, 1986).

Regional interpretation of Early Proterozoic age data

The most significant Early Proterozoic age to emerge from these investigations is the one for sample SQ-5 from extreme southern Minnesota (Fig. 1). The dated rock is petrographically indistinguishable from the Reformatory Granite (Morey, 1978), a major Penokean intrusion that is late- or post-tectonic with respect to fabric-forming events in the St. Cloud region of east-central Minnesota. Several drill holes between St. Cloud and the Iowa border have encountered granitoid rocks that possess petrographic attributes similar to those of known Penokean rocks (Southwick and others, 1990). Moreover, the pattern of geophysical anomalies along a diffuse north-south belt that extends southward from St. Cloud distinctly resembles the pattern observed over known Penokean terrane. Therefore the U-Pb age of 1,792 ± 31 Ma on sample SQ-5 (Fig. 4) confirms the trend of the Penokean orogen through east-central and southern Minnesota, as sketched tentatively on Figure 1. Further drilling and geochronologic work are needed to sharpen this picture, but the broad outlines of it are now reasonably well established.

It is fairly clear from previous work that the peak of tonalitic to granodioritic magmatism in the axial deformed zone of the Penokean orogen was in the interval between 1,860 and 1,870 Ma (Van Schmus, 1980; Goldich and Fischer, 1986). The $^{40}Ar/^{39}Ar$ age of the Philbrook ferrodiorite falls just outside that age bracket on the young side. The Philbrook pluton therefore may be a late-stage manifestation of the intrusive activity that marked the approximate culmination of subduction-related compressional events in the Penokean orogen. Its lack of pervasive deformational fabric and its highly evolved petrochemistry are further indications of late-stage, essentially post-collisional emplacement (Boerboom, 1987).

The Philbrook pluton intrudes sedimentary rocks in the Long Prairie basin that are interpreted to be a foredeep sequence deposited on the cratonic side of the Penokean subduction zone (Southwick and others, 1988; Southwick and Morey, 1991). The depositional age of the sedimentary fill in the Long Prairie basin is bracketed by the age of 2,125 ± 45 Ma for the Kenora-Kabetogama dikes, which unconformably underlie the basin fill (Southwick and Day, 1983; Southwick and others, 1988; Beck, 1988), and the minimum age of 1,854 Ma for the Philbrook pluton reported here. It does not follow necessarily that the age of the Philbrook ferrodiorite is the minimum age for deposition of sedimentary rocks in the main bowl of the Animikie basin. Sedimentation in the main bowl may well have outlasted that in the Long Prairie basin.

Taken uncritically, the geochronological and petrologic data presented here for rhyolite pebbles in the Sioux Quartzite could be considered evidence for anorogenic rhyolite volcanism in the northern Midcontinent at about 1,900 Ma. This is the first indication that such a suite of anorogenic rocks might exist, and the possibility cannot be dismissed out of hand. However, because the reported age of the rhyolite pebbles may have been driven toward an erroneously old value by disturbance of U-Pb systematics during diagenesis, alternative interpretations are permitted. It is reasonable from the geologic point of view to interpret the rhyolite pebbles in the Sioux as having been derived from flows that were the extrusive equivalent of 1,770-Ma anorogenic granites (Spencer and Hanson, 1984). Granite plutons of this type and age crop out widely in east-central Minnesota (Morey, 1978), and are interpreted on various geological, geophysical, and geochronological grounds to occur in reduced numbers throughout the Archean gneiss terrane to the west (Lund, 1956; Goldich and others, 1961; Hanson, 1968). Verification of this or any other interpretation of the Sioux rhyolite pebbles must await more definitive geochronological and geochemical data.

REFERENCES CITED

Awwiller, D.N., and Mack, L.E., 1991, Diagenetic modification of Sm-Nd model ages in Tertiary sandstones and shales, Texas Gulf Coast: Geology, v. 19, p. 311-314.

Bacon, C.R., Macdonald, R., Smith, R.L., and Baedecker, P.A., 1981, Pleistocene high-silica rhyolites of the Coso volcanic field, Inyo County, California: Journal of Geophysical Research, v. 86, p. 10223-10241.

Beck, J.W., 1988, Implications for Early Proterozoic tectonics and the origin of continental flood basalts, based on the combined trace element and neodymium/strontium isotopic studies of mafic igneous rocks of the Penokean Lake Superior belt, Minnesota, Wisconsin and Michigan: Unpublished Ph.D. dissertation, Minneapolis, University of Minnesota, 262 p.

Bickford, M.E., Sides, J.R., and Cullers, R.L., 1981, Chemical evolution of magmas in the Proterozoic terrane of the St. Francois Mountains, southeastern Missouri. 1. Field, petrographic, and major element data: Journal of Geophysical Research, v. 86, p. 10365-10386.

Boerboom, T.J., 1987, Tourmalinites, nelsonites, and related rocks (Early Proterozoic) near Philbrook, Todd County, Minnesota: Unpublished M.S. thesis, University of Minnesota, Duluth, 212 p.

Card, K.D., 1990, A review of the Superior Province of the Canadian Shield, a product of Archean accretion: Precambrian Research, v. 48, p. 99-156.

Card, K.D., and Ciesielski, A., 1986, DNAG #1. Subdivisions of the Superior Province of the Canadian Shield: Geoscience Canada, v. 13, p. 5-13.

Catanzaro, E.J., and Hanson, G.N., 1971, U-Pb ages for sphene in northeastern Minnesota-northwestern Ontario: Canadian Journal of Earth Sciences, v. 8, p. 1319-1324.

Chandler, V.W., 1987, Aeromagnetic map of Minnesota, west-central region: Minnesota Geological Survey Aeromagnetic Map Series A-6, scale 1:250,000.

_____1989, Aeromagnetic map of Minnesota, southwestern region: Minnesota Geological Survey Aeromagnetic Map Series A-8, scale 1:250,000.

Chandler, V.W., and Morey, G.B., 1992, Paleomagnetism of the Early Proterozoic Sioux Quartzite, southwestern Minnesota—Implications for correlating quartzites of the Baraboo interval: U.S. Geological Survey Bulletin 1904-N, 14 p.

Chandler, V.W., and Southwick, D.L., 1990, Aeromagnetic Minnesota: EOS, v. 71, p. 329-331.

Corfu, F., and Stott, G.M., 1986, U-Pb ages for late magmatism and regional deformation in the Shebandowan belt, Superior Province, Canada: Canadian Journal of Earth Sciences, v. 23, p. 1075-1082.

Cullers. R.L., Koch, R.J., and Bickford, M.E., 1981, Chemical evolution of magmas in the Proterozoic terrane of the St. Francois Mountains, southeastern Missouri. 2. Trace element data: Journal of Geophysical Research, v. 86, p. 10388-10401.

Davis, D.W., and Paces, J.B., 1990, Time resolution of geologic events on the Keewenawan Peninsula and implications for development of the Midcontinent Rift system: Earth and Planetary Science Letters, v. 97, p. 54-64.

Davis, D.W., and Sutcliffe, R.H., 1985, U-Pb ages from the Nipigon plate and northern Lake Superior: Geological Society of America Bulletin, v. 96, p. 1572-1579.

DePaolo, D.J., 1981, Neodymium isotopes in the Colorado Front Range and crust-mantle evolution in the Proterozoic: Nature, v. 291, p. 193-196.

Doe, B.R., and Delevaux, M.H., 1980, Lead-isotope investigations in the Minnesota River Valley—Late-tectonic and posttectonic granites, *in* Morey, G.B., and Hanson, G.N., eds., Selected studies of Archean gneisses and lower Proterozoic rocks in the southern Canadian Shield: Geological Society of America Special Paper 182, p. 105-112.

Dott, R.H., Jr., 1983, The Proterozoic red quartzite enigma in the north-central United States: Resolved by plate collision?, *in* Medaris, L.G., Jr., ed., Early Proterozoic geology of the Great Lakes region: Geological Society of America Memoir 160, p. 129-141.

Ervin, C.P., 1980, Simple Bouguer gravity map of Minnesota, St. Cloud sheet: Minnesota Geological Survey Miscellaneous Map Series M-44, scale 1:250,000.

Ervin, C.P., Ikola, R.J., and McGinnis, L.D., 1980, Simple Bouguer gravity map of Minnesota, New Ulm sheet: Minnesota Geological Survey Miscellaneous Map Series M-43, Scale 1:250,000.

Feng, R., and Kerrich, R., 1992, Geodynamic evolution of the southern Abitibi and Pontiac terranes: Evidence from geochemistry of granitoid magma series (2700-2630 Ma): Canadian Journal of Earth Sciences, v. 29, p. 2266-2286.

Garrels, R.M., and Christ, C.L., 1965, Solutions, Minerals and Equilibria: New York, Harper and Row, 450 p.

Goldich, S.S., and Fischer, L.B., 1986, Air-abrasion experiments in the U-Pb dating of zircon: Chemical geology, v. 58, p. 195-215.

Goldich, S.S., Nier, A.O., Baadsgaard, H., Hoffman, J.H., and Krueger, H.W., 1961, The Precambrian geology and geochronology of Minnesota: Minnesota Geological Survey Bulletin 41, 193 p.

Goldich, S.S., and Wooden, J.L., 1980, Origin of the Morton Gneiss, southwestern Minnesota: Part 3. Geochronology, *in* Morey, G.B., and Hanson, G.N., eds., Selected studies of Archean gneisses and lower Proterozoic rocks, southern Canadian Shield: Geological Society of America Special Paper 182, p. 77-94.

Grout, F.F., 1908, The granites and associated quartz basalts of Stearns County, Minnesota: Unpublished M.S. thesis, University of Minnesota, Minneapolis, 47 p.

Hanson, G.N., 1968, K-Ar ages for hornblende from granites and gneisses and for basaltic intrusives in Minnesota: Minnesota Geological Survey Report of Investigations 8, 20 p.

Langmuir, D., 1978, Uranium solution-mineral equilibria at low temperature with applications of sedimentary ore deposits: Geochimica et Cosmochimica Acta, v. 42, p. 547-569.

Lund, E.H., 1956, Igneous and metamorphic rocks of the Minnesota River Valley: Geological Society of America Bulletin, v. 67, p. 1475-1490.

Morey, G.B., 1978, Lower and Middle Precambrian stratigraphic nomenclature for east-central Minnesota: Minnesota Geological Survey Report of Investigations 21, 52 p.

_____1983, Evaluation of catlinite resources, Pipestone National Monument, Minnesota: U.S. National Park Service, Research/Resources Management Report MWR-4, 48 p.

_____1984, Sedimentology of the Sioux Quartzite in the Fulda basin, Pipestone County, southwestern Minnesota: Minnesota Geological Survey Report of Investigations 32, p. 59-74.

Palmer, H.C., and Davis, D.W., 1987, Paleomagnetism and U-Pb geochronology of volcanic rocks from Michipicoten Island, Lake Superior, Canada: Precise calibration of the Keweenawan polar wander track: Precambrian Research, v. 37, p. 151-171.

Peterman, Z.E., 1979, Strontium isotope geochemistry of Late Archean to Late Cretaceous tonalites and trondhjemites, *in* Barker, F., ed., Trondhjemites, dacites, and related rocks: Amsterdam, Elsevier, p. 133-147.

Prince, L.A., and Hanson, G.N., 1972, Rb-Sr isochron ages for the Giants Range granite, northeastern Minnesota, *in* Doe, B.R., and Smith, D.K., eds, Studies in mineralogy and Precambrian geology: Geological Society of America Memoir 135, p. 217-224.

Schaap, B.D., 1989, The geology and crustal structure of southwestern Minnesota using gravity and magnetic data: Unpublished M.S. thesis, University of Minnesota, Minneapolis, 75 p.

Silver, L.T., and Green, J.C., 1963, Zircon ages for Middle Keweenawan rocks of the Lake Superior region [abs.]: American Geophysical Union Transactions, v. 44, p. 107.

Southwick, D.L., 1991, Preliminary geologic map of Archean bedrock, Soudan-Bigfork area, northern Minnesota: Minnesota Geological Survey Open-File Report 91-3, 10 p. & 2 map sheets, scale 1:100,000.

Southwick, D.L., and Chandler, V.W., 1989, Proterozoic dyke swarms in Minnesota—A record of intraplate extension and magmatism between 2150 and 1100 Ma [abs.]: International Association of Volcanology and Chemistry of the Earth's Interior, General Assembly, Santa Fe, New Mexico, June 25 - July 1, 1989: New Mexico Bureau of Mines and Mineral Resources Bulletin 131, p. 251.

Southwick, D.L., and Day, W.C., 1983, Geology and petrology of Proterozoic mafic dikes, north-central Minnesota and western Ontario: Canadian Journal of Earth Sciences, v. 20, p. 622-638.

Southwick, D.L., and Morey, G.B., 1991, Tectonic imbrication and foredeep development in the Penokean orogen, east-central Minnesota—an interpretation based on regional geophysics and the results of test-drilling, *in* Sims, P.K., and Carter, L.M.H., eds., Contributions to Precambrian geology of the Lake Superior region: U.S. Geological Survey Bulletin 1904-C, p. C1-C17.

Southwick, D.L., Morey, G.B., and McSwiggen, P.L., 1988, Geologic map (scale 1:250,000) of the Penokean orogen, central and eastern Minnesota, and accompanying text: Minnesota Geological Survey Report of Investigations 37, 26 p.

Southwick, D.L., Morey, G.B., and Mossler, J.H., 1986, Fluvial origin of the lower Proterozoic Sioux Quartzite, southwestern Minnesota: Geological Society of America Bulletin, v. 97, p. 1432-1441.

Southwick, D.L., Setterholm, D.R., and Boerboom, T.J., 1990, Scientific test drilling in west-central Minnesota: Summary of lithologic and stratigraphic results, 1987-1988, and some preliminary geological conclusions: Minnesota Geological Survey Information Circular 31, 97 p.

Spencer, K.J., and Hanson, G.N., 1984, Pb, Nd isotope and REE constraints on east-central Minnesota Proterozoic granites: Evidence for newly derived crustal components [abs.]: EOS (American Geophysical Union Transactions), no. 16, v. 65, p. 292.

Thurston, P.C. and Chivers, K.M., 1990, Secular variation in greenstone belt development, emphasizing the Superior Province, Canada: Precambrian Research, v. 46, p. 21-58.

Vander Horck, M.P., 1984, Diagenesis in the Sioux Quartzite: Unpublished M.S. thesis, University of Minnesota, Minneapolis, 101 p.

Van Schmus, W.R., 1980, Chronology of igneous rocks associated with the Penokean orogeny in Wisconsin, *in* Morey, G.B., and Hanson, G.N., eds., Selected studies of Archean gneisses and lower Proterozoic rocks, southern Canadian Shield: Geological Society of America Special Paper 182, p. 159-168.

Wallin, E.T., and Van Schmus, W.R., 1988, Geochronological studies of the Archean-Proterozoic transition, north-central United States: Geological Society of America, Abstracts and Programs, v. 20, p. 131.

York, D., 1969, Least-squares fitting of a straight line with correlated errors: Earth and Planetary Science Letters, v. 5, p. 320-324.

ALKALIC PLUTONS OF NORTHEASTERN MINNESOTA

By

Terrence J. Boerboom

ABSTRACT

A series of alkalic plutons in northeastern Minnesota intrude metamorphosed sedimentary and volcanic rocks in the Wawa and Quetico subprovinces of the Archean Superior Province. The plutons generally fall into one of three categories—a syenitic clan, a monzodioritic clan, and a granitic clan. The main rock phases of the syenitic and monzodioritic clans are strongly porphyritic, coarse-grained, green and pink, quartz-poor syenite and diorite. Na-rich pyroxene is the predominant mafic mineral in these intrusions, and sphene is prominent in hand sample. Some of the syenitic intrusions contain melanite garnet, and at least one contains the feldspathoids nepheline and cancrinite. The granitic intrusions consist of variably porphyritic, coarse-grained, pink granite and monzonite, with hornblende as the dominant mafic mineral. Whereas these granitic plutons tend to be uniform in texture and composition, the syenite and monzodiorite plutons are characterized by abrupt internal variations in rock type ranging from dark-colored pyroxenite to light-pink leucocratic granite, syenite, and trondhjemite.

The alkalic plutons range in size from 1.5 to 60 mi^2, are oval to amoeboid in shape and elongate to the northeast, and are eroded to middle and upper levels. All of the alkalic plutons produce positive aeromagnetic anomalies; outcrops, although limited, confirm that these anomalies reflect the shapes of the plutons. Several unexposed plutons, whose shapes are inferred from aeromagnetic data, have been verified by test drilling. Field relationships show that these plutons are post-tectonic.

Although chemical data are not available for all of the plutons, those with analyses plot as alkalic in terms of $Na_2O + K_2O$ vs SiO_2, but as mainly calc-alkalic on an AFM diagram. The syenitic and monzodioritic clans are generally nepheline-normative to neither quartz- nor nepheline-normative, with the exception of minor leucocratic phases. All are characterized by steep REE patterns and exceptionally high concentrations of Ba and Sr.

INTRODUCTION

Recent mapping in northern and northeastern Minnesota, including the Koochiching-Itasca-Beltrami County area (Jirsa and Boerboom, 1990) and western St. Louis County (Jirsa and others, 1991), has delineated several previously unrecognized subalkalic to alkalic plutons. This report summarizes the lithological and intrusive relationships of several of these alkalic intrusions and briefly summarizes their geochemical characteristics. Some plutons in this group, such as the Snowbank and Kekekabic stocks and the Daisy Bay and Dead River plutons, have been previously described (Geldon, 1972; Sims and Mudrey, 1972) and are not included in this report. Others (Coon Lake, Linden, Lost Lake plutons) have been briefly described in the literature (Sims and others, 1970, 1972; Sims and Mudrey, 1972), but are detailed here, as are others which have no published information or were unknown (Fig. 1A). Alkalic rock complexes similar to these are well known in Ontario (for example Sage, 1988a, 1988b, 1988c), but few have been described from Minnesota. Several other small alkalic plutons are inferred from aeromagnetic data, but are not exposed or have not been drilled (Jirsa and others, 1991).

Characteristics of the Alkalic Rock Suite

The alkalic intrusions fall into three general categories—a syenitic group comprising the Coon Lake, Linden, Gheen, and Baudette plutons; a monzodioritic group including the Side Lake, Morcom, Idington, and Cook plutons; and a granitoid group containing the Bello Lake, Stingy Lake, and Rice River plutons (Fig. 1). Although most classify into one of the three clans, the many phases in each pluton (Table 1) produce considerable overlap. The syenitic and monzodioritic intrusions consist mainly of medium- to coarse-grained, porphyritic, pink and green syenite and monzodiorite, whereas the granitoid intrusions are typically medium-grained, variably porphyritic, pink quartz monzonite or granodiorite. The syenite and especially the monzodiorite plutons contain multiple erratic melanocratic to felsic phases with aegerine-augite as the predominant mafic mineral, whereas the granitoid plutons generally lack multiple phases, are more uniform in texture, and contain mainly hornblende as the mafic phase.

Most of the alkalic plutons intrude metamorphosed volcanic and sedimentary rocks in the western Wawa subprovince, but some are within the Quetico subprovince

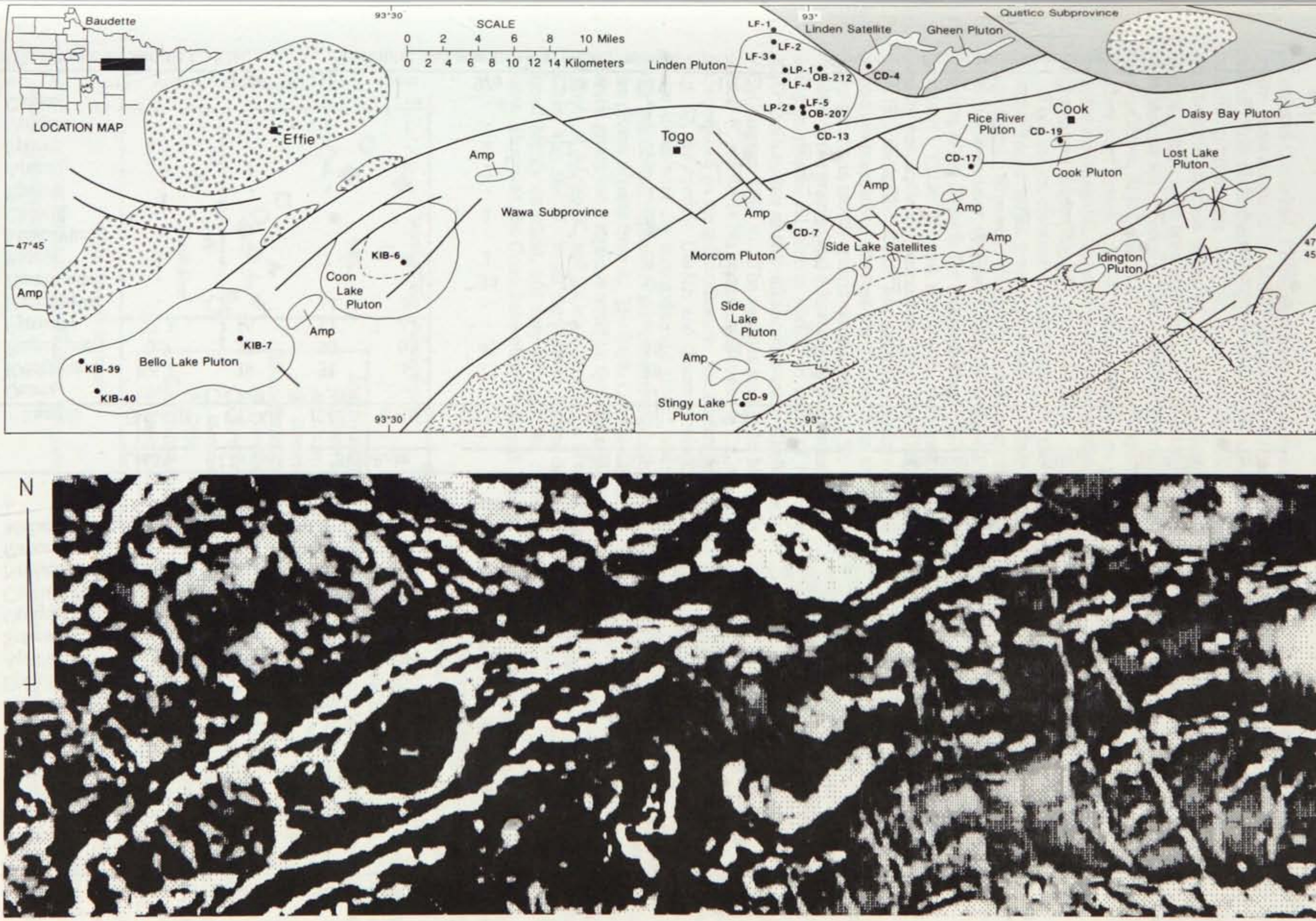

Figure 1. Geologic and aeromagnetic maps. (**A**) Simplified geologic map of a part of northern Minnesota (inset), with plutons discussed in this paper named. Heavy black lines, faults. Single-line pattern, Giants Range batholith; double-line pattern, miscellaneous granite plutons not part of the alkalic suite. Dashed lines: In Coon Lake pluton, boundary between weak and strong magnetic anomalies; in Side Lake pluton, boundary of intercalated monzonite and schist linking pluton and satellites; in Idington pluton, extent of Shannon Lake granite intrusion. Amp, alkalic plutons inferred only from aeromagnetic data. (**B**) Lower image, first vertical derivative shaded-relief aeromagnetic map of same area. Approximate range ± 1,500 nT/km.

Table 1. Modal analyses of alkalic plutonic rocks

[Results in volume percent. Linden analyses from Sims and others (1972, p. 161); samples with KIB and CD prefixes from drill cores, all others from outcrops. Pyroxene—aegerine to augite; *n*, points counted; est, estimate]

	Bello Lake			Coon Lake		Gheen		Idington				Linden		
Sample	KIB-7	KIB-39	KIB-40	DL-61	KIB-6	C027	C029	C551X	C552B	C650	C561A	Gnw7A	Msw2A	Gnw7-2
Quartz	20	-	3	-	-	tr	-	-	41	-	2	tr	-	-
K-feldspar	43	32	46	50	79	8	61	26	3	tr	3	77.6	56.2	37.1
Plagioclase	32	53	40	9	tr	21	7	29	55	32	88	1.9	5.6	0.4
Pyroxene	-	8	-	5	2	12	-	31	-	49	-	16.8	25.9	57.1
Hornblende	2	1	8	-	-	46	19	-	-	8	6	-	-	-
Biotite	1	1	tr	tr	-	7	-	5	-	7	-	-	4.1	0.4
Muscovite	-	-	-	-	tr	-	-	-	-	-	-	-	-	-
Chlorite	tr	1	tr	-	-	4	-	4	-	tr	-	-	-	-
Epidote	tr	-	tr	-	-	-	-	-	-	tr	-	-	-	-
Apatite	tr	tr	tr	tr	tr	1	2	2	-	2	1	0.8	1.1	2.7
Sphene	-	1	tr	tr	tr	1	3	2	-	2	-	2.9	3.7	2.3
Opaques	2	3	3	tr	-	tr	2	-	-	tr	1	-	3.4	-
Calcite, Fl[1]	-	-	-	tr	tr	tr	5	-	2 Fl[1]	-	1	-	-	-
Nepheline	-	-	-	33	15	-	-	-	-	-	-	-	-	-
Cancrinite	-	-	-	2	2	-	-	-	—	-	-	-	-	-
Melanite	-	-	-	-	2	-	-	-		-	-	-	-	-
n	est	est	est	1143	est	1368	1114	989	1157	999	946			

	Linden	L'n sat.	Side Lake		Side Lake satellites					Morcom		Stingy	Rice R.	Cook
Sample	Gnw-7B	CD-4	I242	C706B	C533A	C534A	C543A	C564A	C603A	CD-7[2]	CD-7	CD-9	CD-17	CD-19
Quartz	-	-	-	-	-	-	-	-	-	-	-	26	13	-
K-feldspar	56.3	28	31	tr	13	2	28	1	29	7	20	22	30	-
Plagioclase	0.9	52	30	65	47	33	55	44	20	54	55	47	43	67
Pyroxene	27.1	16	17	22	-	26	-	30	47	21	5	-	-	-
Hypersthene	-	-	14	8	-	-	-	-	-	-	-	-	-	-
Hornblende	-	2	-	-	34	16	9	3	-	8	8	3	6	-
Biotite	9	-	7	4	1	-	3	20	1	7	10	-	1	-
Muscovite	-	-	-	-	-	-	-	-	-	-	-	-	-	-
Chlorite	-	-	-	-	1	14	3	-	1	-	-	1	4	-
Epidote	-	-	-	-	-	5	1	-	-	1	-	1	2	18[3]
Apatite	5.2	1	tr	tr	2	2	1	1	0.5	-	-	-	-	tr
Sphene	1.5	2	-	-	2	1	1	1	0.5	1	1	-	0.5	tr
Opaques	-	-	1	1	-	-	-	-	1	-	-	-	-	tr
Calcite	-	-	-	-	-	-	-	-	-	1	-	-	0.5	tr
n		1166	1151	est	976	1188	947	1-15	1137	988	1-52	836	960	est

[1]Fl, fluorite in sample C552B. [2]Poikilitic and nonpoikilitic phases, sample CD-7. [3]Epidote replacing feldspar in sample DC-19.

(Card and Ciesielski, 1986; Fig. 1A). All were emplaced in the latest stages of the last major regional deformational event (Jirsa and others, 1992) or after it. Several of the alkalic plutons are cut by northwest-trending Late Proterozoic diabase dikes of the Kenora-Kabetogama swarm, which have been dated at 2,125 Ma (Beck, 1988). The plutons are exposed at various levels, and many, such as the Gheen, Side Lake, and Lost Lake, are exposed close to their roof zones. All of the alkalic plutons produce positive aeromagnetic anomalies which generally conform to the pluton shape (Fig. 1B).

The major-element geochemistry of the alkalic plutonic rocks varies greatly as a result of their diverse mineralogy. However, except for minor proportions of felsic differentiates, they are low in SiO_2 (49-62 wt% for syenites, 47 to 58 wt% for monzodiorites, 61-70 wt% for granites; Table 2), and are mostly metaluminous to weakly peralkalic in composition (Fig. 2). The syenitic and monzodioritic rocks are generally quartz-free to nepheline-normative, whereas the granite from the Bello Lake pluton is mostly quartz-normative (Fig. 3). Except for one of the granites and a leucocratic differentiate of the Idington pluton, all plot as alkalic in terms of Na_2O + K_2O vs SiO_2, but as calc-alkalic to weakly alkalic on an AFM diagram (Fig. 4). The syenites tend to be higher in Al and K, similar in Na content, and lower in Ca, Mg, and Fe, compared to the monzodiorites. On Harker diagrams (Fig. 5), the syenitic Linden and Gheen plutons form a linear trend with the monzodioritic group, whereas the more leucocratic nepheline- and cancrinite-bearing Coon Lake pluton departs from it. The Bello Lake pluton of the granitic group has a separate trend on the Harker diagrams in terms of Al, Na, K, and Ca but a continuum in terms of Fe, Mn, Mg, and Ti. In all the plutons, Ba and Sr are in general highly enriched, but vary between the different phases. However, the Coon Lake pluton although slightly enriched, is surprisingly low in Ba and Sr, considering its extremely alkalic composition. The Linden pluton is extremely enriched in Ba and Sr, with Ba values of up to 13,000 ppm and Sr values up to 8,100 ppm reported from company drill cores. Chondrite-normalized REE patterns for the syenites and monzodiorites are fairly consistent, with moderately steep slopes and negligible Eu anomalies (Fig. 6). No REE data are available for any of the granitoid plutons.

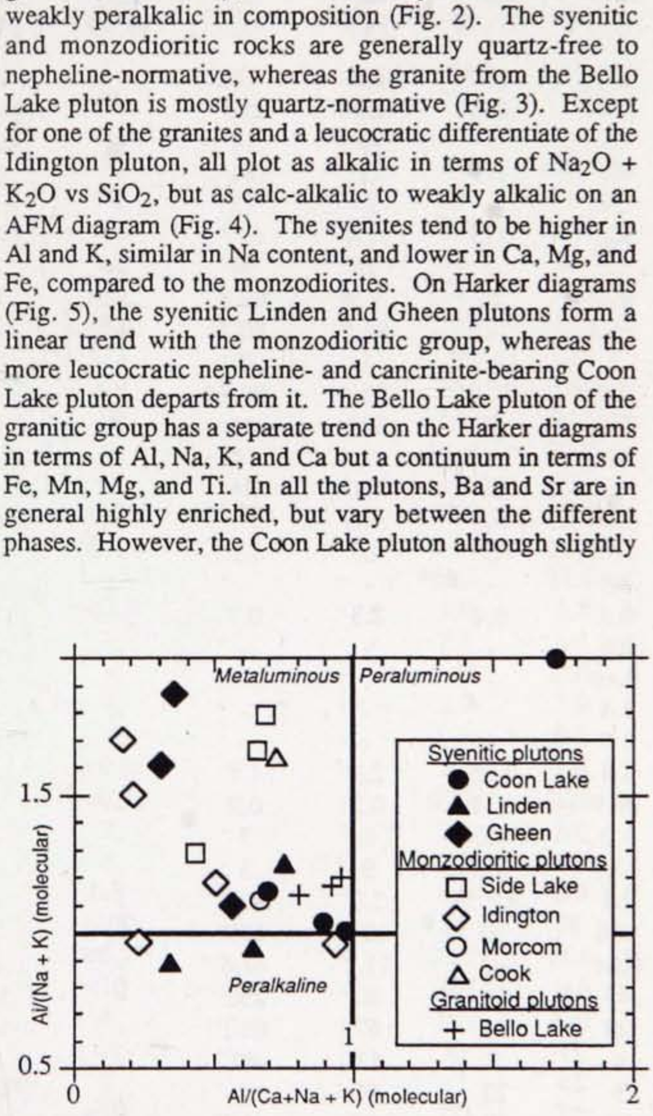

Figure 2. Geochemical classification diagram of the alkalic plutonic rocks.

SYENITIC PLUTONS

Most of the syenitic plutons are northwest of the other plutons (Fig. 1A). The Gheen and Baudette plutons are within the Quetico subprovince, the Coon Lake pluton is in the Wawa subprovince, and the Linden pluton straddles the subprovince border.

These plutons are distinguished by a preponderance of K-rich perthite, typically as trachytic, blocky phenocrysts in an aegerine-rich groundmass, or an amphibole-rich groundmass in the case of the Gheen pluton. The Gheen and Linden plutons contain quartz, chlorite, apatite, epidote, sphene, opaque oxides, and pyrite as ubiquitous but generally minor constituents. The Coon Lake pluton differs from all others in that it contains substantial nepheline and cancrinite; the Baudette pluton lacks both feldspathoids and quartz. Melanite garnet is present in the Coon Lake and Baudette plutons, and in some phases of the Linden. A distinctive phase of spotted monzodiorite with centimeter-size poikilitic feldspar enclosing pyroxene, hornblende, plagioclase, biotite, and sphene is present in both the Linden and Gheen plutons and in plutons of the monzodiorite clan. Although the Gheen and parts of the Linden plutons are texturally similar to rocks of the monzodiorite clan, they differ by having phenocrysts of pink perthite instead of gray antiperthite.

Trachytic fabric in the syenitic intrusions conforms to the pluton edges and dips steeply toward the pluton centers. However, outcrops are generally limited to the pluton borders, and the Baudette and Linden satellite intrusions are seen only in drill core. Aeromagnetic signatures correspond with intrusion shapes, whether it be a consistent oval like the Baudette, Coon Lake, and Linden plutons, or irregular and amoeboid like the Gheen and Linden satellite plutons (Fig. 1B).

Coon Lake Pluton

The Coon Lake pluton (Fig. 1; Jirsa, 1990; Jirsa and Boerboom, 1990) is a 48-mi^2 subcircular pluton which intrudes mafic to felsic volcanic rocks metamorphosed to greenschist grade. A narrow aureole of amphibolite-grade metamorphism accompanied pluton emplacement. The pluton has a strongly magnetic border, and internal lithological zonation is indicated by a circular, weakly positive magnetic anomaly within the pluton. Its north and northeast edges are exposed in scattered outcrops, and a single 10-foot-long vertical drill core was obtained from the pluton center (Boerboom and others, 1989).

Table 2. Major- and selected minor-element geochemical analyses of alkalic rocks
[Major elements in wt% oxides, minor elements in ppm, except Au in ppb; -, not determined]

	Bello Lake			Coon Lake				Gheen			Morcom
Sample	KIB-7	KIB-40	KIB-39	KIB-6	CLP-1	I-561A	DL-61	C029	C027	12, IC-2	CD-7
SiO_2	69.7	63.9	60.2	57.7	62.3	60.3	55.65	56.0	49.2	49.65	58.5
Al_2O_3	15.7	17.4	17.2	17.8	18.9	22.4	21.88	14.1	9.52	9.27	15.4
CaO	1.87	2.16	3.55	5.45	0.33	1.69	1.65	6.48	12.3	13.08	5.01
MgO	0.51	1.28	1.85	0.42	0.35	0.28	1.01	2.55	10.5	8.89	3.58
Na_2O	5.67	6.13	6.30	5.75	5.32	7.1	8.12	3.57	1.51	2.38	5.90
K_2O	3.51	4.47	4.40	5.80	9.3	4.13	7.28	6.56	2.40	1.71	3.80
Fe_2O_3 t	1.84	3.32	3.94	2.71	2.18	2.54	3.67	6.19	10.20	11.76	5.22
FeO	0.4	1.0	1.0	0.3	-	1.6	1.7	-	-	6.08	3.20
Fe_2O_3 c	1.40	2.21	2.83	2.38	-	0.76	1.78	-	-	5.00	1.66
MnO	0.04	0.07	0.08	0.07	0.05	175 ppm	0.08	0.12	0.16	0.56	0.10
TiO_2	0.20	0.35	0.42	0.26	0.18	0.19	0.44	0.71	0.88	0.89	0.48
P_2O_5	0.09	0.18	0.32	0.11	0.02	<10 ppm	0.08	1.03	0.33	0.06	0.29
LOI	0.70	0.77	1.00	2.77	0.85	1.31	0.37	1.85	2.39	1.99	1.08
Total	100.2	100.4	99.8	99.6	100.1	100.1	100.38	99.9	99.5	99.93	99.7
Rb	165	135	129	100	246	132	100	120	60	-	79
Sr	1210	1340	2180	3700	1300	806	926	2520	290	-	1470
Y	<10	41	17	81	<10	10	2	47	14	-	<10
Zr	90	303	253	64	118	404	119	331	84	-	32
Nb	<10	14	14	15	24	27	-	24	13	-	<10
Ba	1340	1470	1970	2530	676	500	215	3710	697	-	1460
Ni	-	-	-	-	8	<1	7	78	94	-	-
Cu	-	-	-	11.2	8.7	9.8	16	5.5	40.8	-	-
Zn	-	-	-	8.18	70.3	46.3	30	84.5	80.1	-	-
Cs	-	-	-	-	9	3	4.5	1	2	-	-
La	-	-	-	-	17.5	79.3	27.0	130	20.8	-	-
Ce	-	-	-	-	33	130	58	328	46	-	-
Pr	-	-	-	-	-	12.8	-	-	-	-	-
Nd	-	-	-	-	11	39.7	33	186	24	-	-
Sm	-	-	-	-	1.7	5.5	5.1	34.7	5.7	-	-
Eu	-	-	-	-	0.4	1.45	1.21	9.3	1.9	-	-
Gd	-	-	-	-	-	3.9	-	-	-	-	-
Tb	-	-	-	-	<0.5	0.5	0.4	2.3	0.7	-	-
Dy	-	-	-	-	-	2.6	-	-	-	-	-
Ho	-	-	-	-	-	0.49	-	-	-	-	-
Er	-	-	-	-	-	1.4	-	-	-	-	-
Tm	-	-	-	-	-	0.5	-	-	-	-	-
Yb	-	-	-	-	0.2	1.4	0.65	2.3	1.7	-	-
Lu	-	-	-	-	<0.1	0.19	0.10	0.2	0.2	-	-
Hf	-	-	-	-	4	9.0	4.0	8	3	-	-
Th	-	-	-	-	10	27.0	1.5	9	3	-	-
U	-	-	-	-	2.3	7.1	<0.5	2.0	1.1	-	-
S	<0.01	<0.01	<0.01	<0.01	1230	<50	30	129	199	-	-
Sc	-	-	-	-	<0.5	0.84	<1	11.2	42.6	-	-
V	-	-	-	-	20	45	10	80	250	-	-
Cr	22	26	36	<10	10	29	11	67	630	-	-
Co	-	-	-	-	2	4	2	11	40	-	-
Au (ppb)	-	-	-	2	6	5	22	16	5	-	-
Li	-	-	-	-	18	74	39	<10	<10	-	-
Be	-	-	-	-	<5	6	<1	<5	<5	-	-
B	-	-	-	-	30	41	<10	<10	<10	-	-
Cl	50	<50	50	150	-	104	28	-	-	-	-
F	-	-	-	-	-	160	850	-	-	-	-

Note: Mn and P are reported as ppm for sample I-561A. KIB samples from Boerboom and others (1989); CD-series from Meints and

Table 2. Major- and selected minor-element geochemical analyses of alkalic rocks—continued
[Major elements in wt% oxides, minor elements in ppm, except Au in ppb; -, not determined]

	Idington					Linden		L'n sat.	SL. sat.	Side Lake		Cook
Sample	C552B	10, IC-2	11, IC-2	C650A	C551X	8, IC-2	MN-10	CD-4-92	C564A	I242	C706B	CD-19
SiO_2	74.5	47.27	50.27	48.3	54.0	60.21	57.1	62.2	52.2	55.2	53.5	53.6
Al_2O_3	14.8	6.99	7.61	7.24	13.1	16.28	10.2	15.0	11.7	14.6	15.4	17.7
CaO	0.08	20.49	13.87	16.6	8.16	4.76	10.1	4.09	9.89	7.38	7.68	7.59
MgO	0.09	9.18	7.92	9.58	4.56	2.21	4.43	1.62	7.08	6.89	6.25	3.26
Na_2O	8.80	1.91	2.41	2.12	4.24	3.78	2.64	6.57	4.04	3.42	3.79	5.40
K_2O	1.08	0.89	3.63	1.23	3.86	6.32	6.52	4.73	2.22	2.95	2.21	1.79
Fe_2O_3 t	0.51	9.15	10.68	10.10	7.05	4.29	6.51	3.98	10.30	7.93	8.37	7.07
FeO	-	5.44	7.04	6.0	3.3	1.62	2.83	1.4	-	-	5.7	2.6
Fe_2O_3 c	-	3.10	2.86	3.43	3.38	2.49	3.36	2.42	-	-	2.04	4.18
MnO	0.03	0.30	0.20	0.19	0.13	0.08	0.15	0.09	0.19	0.14	0.15	0.13
TiO_2	0.03	0.67	1.51	1.00	0.96	0.56	0.64	0.48	0.81	0.77	0.76	0.71
P_2O_5	0.02	1.62	1.46	1.25	0.75	0.23	1.07	0.24	0.45	0.39	0.39	0.36
LOI	0.16	1.33	0.84	0.77	1.23	0.73	-	0.54	1.08	0.23	0.47	1.54
Total	100.1	99.28	99.91	98.6	98.5	99.76	99.1	99.9	100.2	100.2	99.3	99.5
Rb	97	-	-	59	57	-	164	94	67	60	31	39
Sr	43	-	-	772	1770	-	2924	510	1080	1030	1190	1950
Y	<10	-	-	37	26	-	-	10	<10	20	20	<10
Zr	36	-	-	262	181	-	-	246	102	30	82	110
Nb	30	-	-	15	9	-	-	14	21	10	2	15
Ba	81	-	-	817	1830	-	3574	2290	985	1220	1530	882
Ni	<1	-	-	76	64	-	-	-	57	-	61	-
Cu	1.5	-	-	185	54.9	-	-	-	108	-	20.4	-
Zn	28.6	-	-	125	120	-	-	-	128	-	108	-
Cs	7	-	-	9	1	-	-	-	2	-	1	-
La	5.9	-	-	164	134	-	-	-	50.6	-	43.2	-
Ce	10	-	-	348	278	-	406	-	101	-	88.0	-
Pr	-	-	-	41.4	30.8	-	-	-	-	-	11.3	-
Nd	<5	-	-	171	124	-	183	-	46	-	48.8	-
Sm	0.2	-	-	27.9	19.2	-	28.1	-	8.9	-	9.3	-
Eu	0.2	-	-	6.99	5.14	-	6.62	-	2.4	-	2.81	-
Gd	-	-	-	18.2	11.8	-	16.6	-	-	-	6.4	-
Tb	<0.5	-	-	2.0	1.3	-	-	-	0.6	-	0.8	-
Dy	-	-	-	8.8	6.4	-	-	-	-	-	4.1	-
Ho	-	-	-	1.46	1.01	-	-	-	-	-	0.73	-
Er	-	-	-	3.2	1.9	-	-	-	-	-	1.8	-
Tm	-	-	-	0.3	0.2	-	-	-	-	-	0.2	-
Yb	<0.2	-	-	2.6	1.6	-	1.53	-	1.4	-	1.6	-
Lu	<0.1	-	-	0.32	0.22	-	0.262	-	0.2	-	0.23	-
Hf	2	-	-	7.6	5.0	-	-	-	4	-	2.2	-
Th	6	-	-	7.7	4.6	-	-	-	-	-	0.7	-
U	6.8	-	-	1.5	0.9	-	-	-	-	-	0.3	-
S	<100	-	-	56	78	-	-	-	127	-	<50	-
Sc	<0.5	-	-	22.7	11.6	-	-	-	21.1	-	20.8	-
V	<10	-	-	256	148	-	-	-	210	-	208	-
Cr	4	-	-	140	120	-	-	-	80	250	180	-
Co	<1	-	-	56	43	-	-	-	37	-	45	-
Au (ppb)	7	-	-	<1	<1	-	-	-	5	-	<1	-
Li	<10	-	-	231	76	-	-	-	84	-	26	-
Be	10	-	-	6	4	-	-	-	5	-	3	-
B	20	-	-	14	14	-	-	-	<10	-	<10	-
Cl	-	-	-	<50	<50	-	-	-	-	-	<50	-
F	-	-	-	2900	1400	-	-	-	-	-	680	-

others (1993); IC-2 series from Ruotsala and Tufford (1965); sample MN-10 from Arth and Hanson (1975). All others are new data.

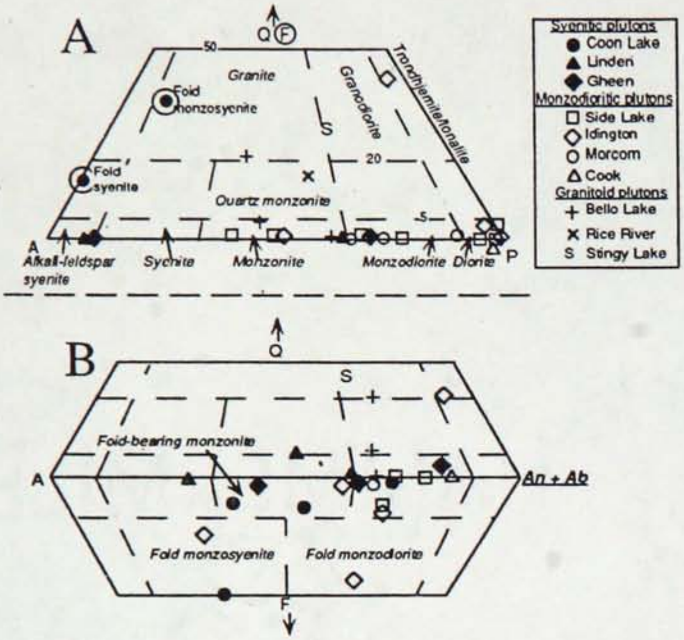

Figure 3. Modal (A) and normative (B) compositions of the alkalic plutonic rocks. Compositional fields from Streckeisen (1973), except "P" corner, which consists of albite and anorthite, used here to emphasize variations in K content. Q, quartz; F, feldspathoids; A, alkali feldspars; P, plagioclase. Circled symbols are feldspathoidal, not quartz.

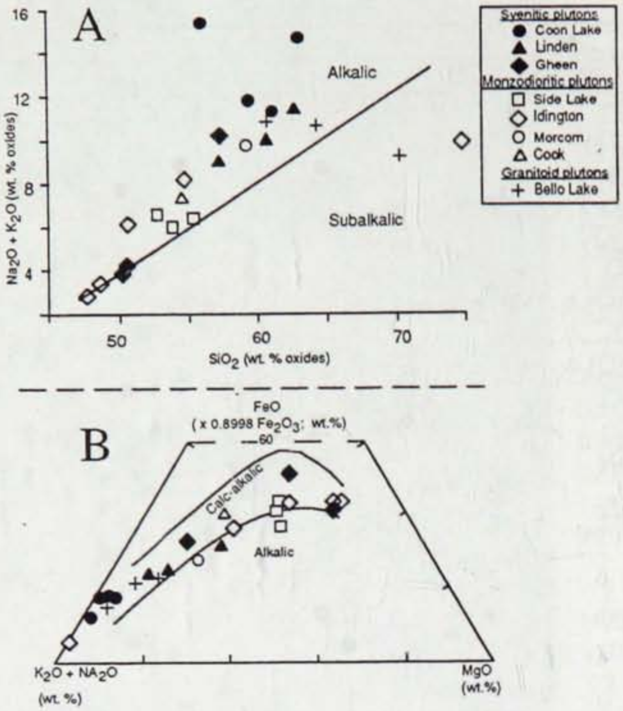

Figure 4. Geochemical discrimination diagrams. (A) Alkalic versus subalkalic discrimination diagram; modified from Irvine and Baragar (1971). (B) AFM diagram for the alkalic plutonic rocks; modified from Barker and Arth (1976).

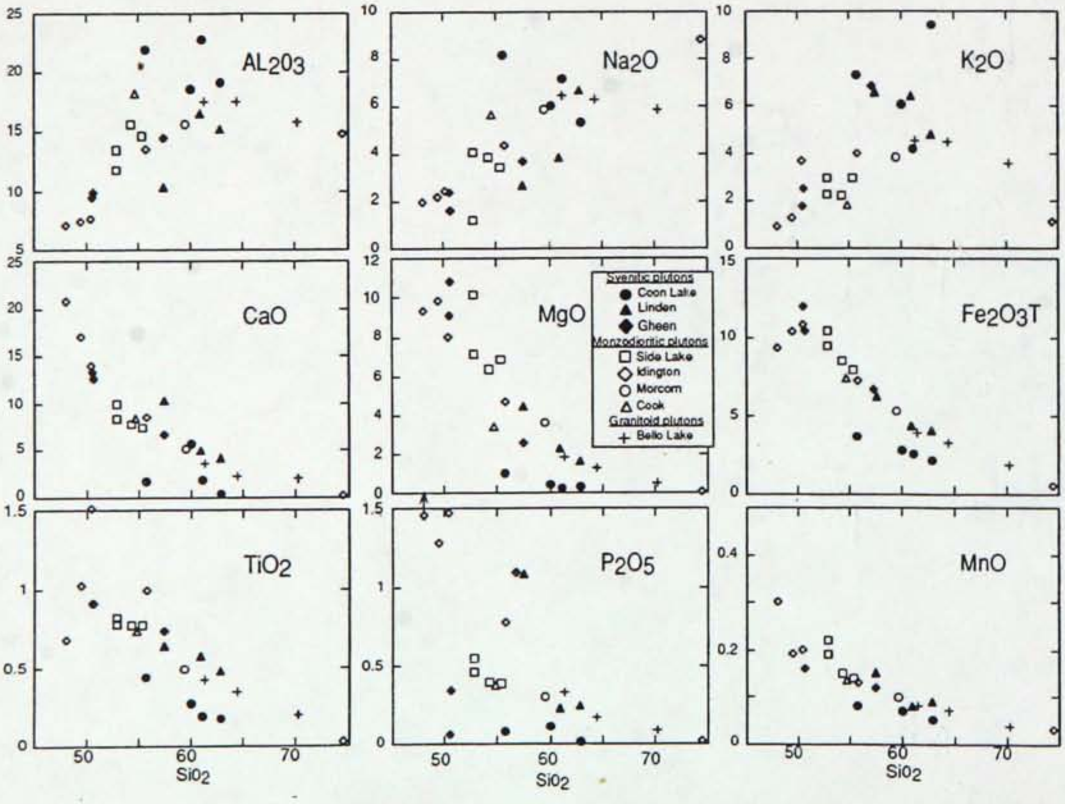

Figure 5. Harker diagrams for the alkalic plutonic rocks, in wt % oxides recalculated to no loss on ignition.

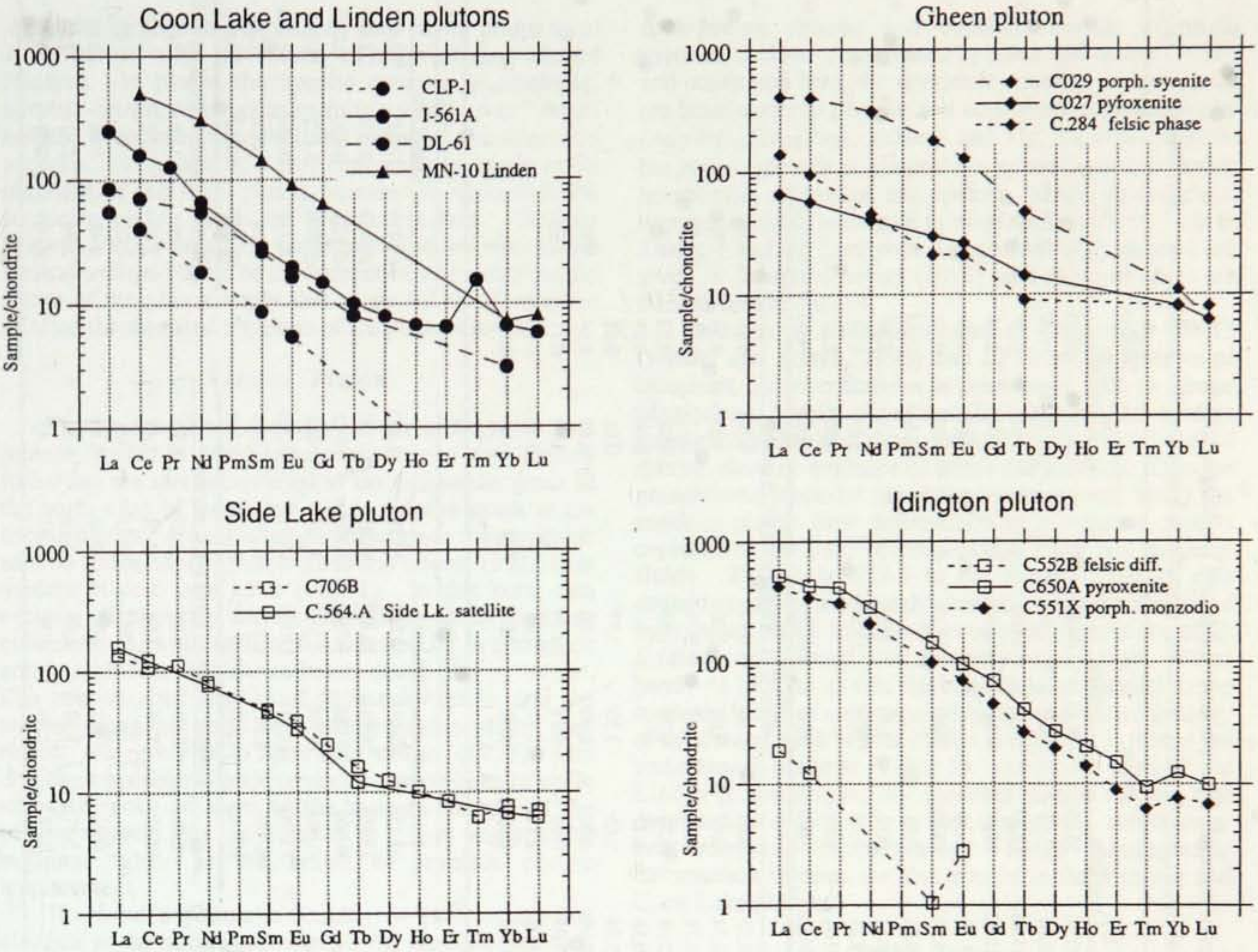

Figure 6. Chondrite-normalized rare-earth-element patterns for the alkalic plutonic rocks for which analyses are available.

The main rock type in the exposed and cored portions of the Coon Lake pluton is pink to gray, medium- to very coarse grained, slightly to strongly porphyritic nepheline syenite, 50-79% microperthite, 15-33% nepheline (Ne_{76-80}), 2-5% aegerine ($Ac_{23}Wo_{18}En_7Fs_{52}$), and as much as 9% plagioclase, 2% cancrinite, and 3% melanite, together with accessory sphene, apatite, biotite, magnetite, muscovite, and zircon (Tables 1 and 3, Fig. 7). Minor proportions of pyroxenite occur in ill-defined dikelets. String- and braid-textured microperthite forms rectangular crystals with minor inclusions of aegerine, sphene, cancrinite, and nepheline. Nepheline is typically anhedral but locally euhedral, up to 2 mm in size, and ranges from fresh to moderately altered to an unknown fibrous mineral of low birefringence. Prismatic, grass-green aegerine formed early in the crystallization sequence and is trachytic. Plagioclase and cancrinite are interstitial, the latter as colorless, highly birefringent fibrous grains.

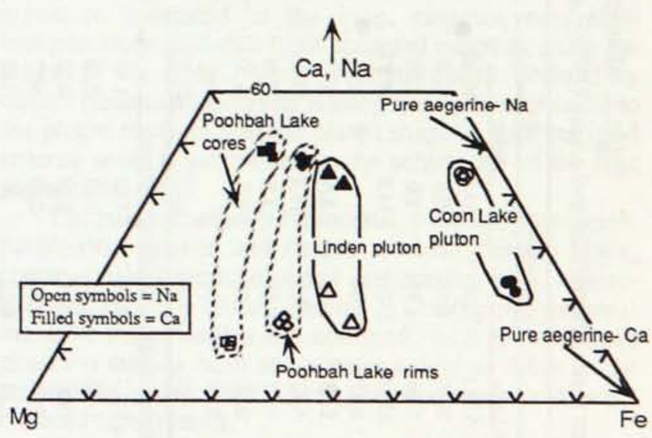

Figure 7. Pyroxene compositions from the Coon Lake and Linden plutons. Pyroxene compositions from Poohbah Lake (Sage, 1988a) and compositions of pure aegerine (Deer and others, 1966, p. 107) shown for comparison.

Table 3. Microprobe analyses of minerals from the Coon Lake and Linden plutons

[Linden results from Sims and others (1972). Chemical analyses in weight percent oxides. Cancrinite totals low due to abundance of volatiles]

	Aegerine				
	Coon Lake			Linden	
SiO2	51.49	51.62	51.80	53.0	46.85
TiO2	0.58	0.54	0.48	0.5	2.13
Al2O3	1.35	1.34	1.38	1.0	2.50
FeO	25.43	25.36	25.74	14.8	16.97
MnO	0.33	0.41	0.44		0.31
MgO	1.96	2.00	1.85	8.6	8.17
CaO	6.74	6.92	6.29	18.8	17.85
Na2O	9.74	9.51	9.88	3.5	2.49
K2O	0.00	0.00	0.00	0.5	0.50
Cr2O3	0.00	0.02	0.00		nd
Total	97.62	97.70	97.85	100.7	99.84
	Number of cations based on 6 oxygen				
Si	2.10	2.10	2.10	2.02	1.88
Ti	0.02	0.02	0.01	0.01	0.06
Al	0.06	0.06	0.07	0.04	0.12
Fe	0.87	0.86	0.87	0.47	0.57
Mn	0.01	0.01	0.02	0	0.01
Mg	0.12	0.12	0.11	0.49	0.49
Ca	0.29	0.30	0.27	0.77	0.77
Na	0.77	0.75	0.78	0.26	0.19
K	0	0	0	0.02	0.03
Cr	0	0	0		

	Biotite				Sphene		
	Coon Lake		Linden		Coon Lake		Linden
SiO2	37.16	35.69	44.0	43.00	30.01	30.65	31.00
TiO2	2.66	3.13	0.5	0.50	37.17	34.62	31.00
Al2O3	13.96	12.34	11.0	13.00	0.55	0.57	3.50
FeO	21.02	18.42	18.0	14.00	2.06	2.34	3.00
MnO	1.13	1.11			0.01	0.06	
MgO	9.32	10.03	14.0	16.20	0.02	0.02	
CaO	0.00	0.01			26.51	25.44	29.00
Na2O	0.14	0.22	1.0	1.00	0.29	0.33	3.30
K2O	9.21	9.34	10.5	11.50	0.01	0.01	
Cr2O3	0.01	0.00			0.00	0.00	
Total	94.60	90.28	99.0	99.20	96.62	94.04	100.80
	Number of cations based on 24 oxygen						
Si	6.31	6.33	6.96	6.71	4.89	5.11	4.91
Ti	0.34	0.42	0.06	0.06	4.55	4.34	3.69
Al	2.79	2.58	2.05	2.39	0.11	0.11	0.65
Fe	2.98	2.73	2.38	1.83	0.28	0.33	0.40
Mn	0.16	0.17			0.00	0.01	
Mg	2.36	2.65	3.30	3.77	0.01	0.01	
Ca	0.00	0.00	0.00	0.00	4.63	4.54	4.92
Na	0.05	0.08	0.31	0.30	0.09	0.11	1.01
K	1.99	2.11	2.12	2.29	0.00	0.00	
Cr	0.00	0.00	0.00	0.00	0.00	0.00	

	Exs. albite	Perthite				
		Coon Lake				Linden
SiO2	72.37	63.422	66.725	67.493	66.235	61.5
Al2O3	19.868	15.347	17.527	18.889	18.612	19
BaO	0.000	0.000	0.132	0.000	0.104	
CaO	0.031	0.000	0.018	0.001	0.000	0.5
Na2O	10.58	0.646	3.055	3.785	0.716	1.5
K2O	1.268	12.139	12.521	12.016	15.932	15.8
Total	104.118	91.553	99.977	102.185	101.598	99.8
	Number of cations based on 8 oxygen					
Si	3.03	3.13	3.04	3.00	3.01	2.92
Al	0.98	0.89	0.94	0.99	1.00	1.06
Ba	0	0	0.01	0	0.01	
Ca	0	0	0	0	0	0.03
Na	0.86	0.06	0.27	0.33	0.06	0.14
K	0.07	0.76	0.73	0.68	0.92	0.96

	Nepheline				
	Coon Lake				
SiO2	46.153	46.641	48.068	46.297	45.345
Al2O3	33.061	34.701	35.152	34.217	33.123
BaO	0.000	0.000	0.000	0.028	0.000
CaO	0.084	0.076	0.116	0.102	0.484
Na2O	15.947	14.848	13.198	15.917	13.574
K2O	6.186	6.211	5.877	6.133	6.068
Total	101.43	102.476	102.412	102.693	98.594
	Number of cations based on 32 oxygen				
Si	8.67	8.62	8.79	8.59	8.70
Al	7.33	7.56	7.58	7.48	7.49
Ba	0	0	0	0.01	0
Ca	0.02	0.02	0.02	0.02	0.10
Na	5.81	5.32	4.68	5.72	5.05
K	1.48	1.46	1.37	1.45	1.49

	Cancrinite		
	Coon Lake		
SiO2	37.455	37.613	37.472
Al2O3	28.053	26.956	28.416
BaO	0.122	0.000	0.000
CaO	5.583	5.432	5.348
Na2O	18.776	18.468	18.201
K2O	0.04	0.052	0.206
Total	90.029	88.52	89.643
	Number of cations based on 12 (O)		
Si	3.02	3.08	3.02
Al	2.67	2.60	2.70
Ba	0.01	0	0
Ca	0.48	0.48	0.46
Na	2.94	2.93	2.85
K	0.00	0.01	0.02

Melanite garnet forms subhedral, dark-brown grains up to 1 cm across with inclusions of aegerine and altered feldspar. In places the syenite consists of trachytic, purplish-brown, rectangular perthite crystals up to 7 cm in length, with minor nepheline, melanite, biotite, and aegerine. A syenite dike that cuts mafic volcanic rocks outboard of the main pluton contains an estimated 1% scolecite and a trace of blue corundum. Netlike anastomosing veinlets of white nepheline parallel to the vertical trachytic fabric of the feldspar in drill core from the center of the pluton imply that a late influx of volatiles affected the magnetic signature of the pluton's interior.

Linden Pluton

The Linden pluton and its smaller satellite to the east intrude mafic to felsic volcaniclastic and sedimentary rocks that are metamorphosed to the sillimanite grade at the north edge of the pluton and to chlorite grade at the southern edge. A narrow amphibolite-grade metamorphic aureole surrounds the pluton (Jirsa and others, 1992), as is evident in drill core LF-1 (Fig. 1). In this core, thin syenitic dikelets cut biotite-amphibole schist that has centimeter-thick green bands dominated by bright-green sodic amphibole and brown bands dominated by biotite. The country rock here is of sillimanite grade, and the aureole along the north edge of the Linden pluton may reflect retrogression. Sims and others (1972), who describe amphibolite-grade contact metamorphism of mafic volcanic rocks adjacent to the western margin of the pluton, suggest that the foliation at a high angle to the regional fabric is the result of forcible pluton emplacement.

The Linden pluton is roughly 54 mi^2 in size and elongate to the northwest, whereas the satellitic intrusion is about 4.5 mi^2 in size and elongate to the northeast (Fig. 1). Exposures are limited to the pluton edges, but ten drill cores from the pluton were obtained by various private and governmental agencies. Records of these cores and the cores themselves are on file at the Minnesota Department of Natural Resources, Division of Minerals in Hibbing. A summary of the cores is given in Table 4. The LF-series of drill cores were subsequently examined by Himmelberg (1973), and thin sections from these cores were briefly reexamined in conjunction with this report. The LP-series descriptions are directly from company logs, and the OB-series descriptions are from the Minnesota Department of Natural Resources, Division of Minerals (Martin and others, 1988). The target of company drilling is not known, but complete metals analyses, together with Na, K, Al, Ca, Ba, and Sr abundances, were obtained by the explorationists. The satellite intrusion is not exposed, but one short drill core was obtained by the Minnesota Geological Survey (Meints and others, 1993).

The main Linden pluton is generally uniform in composition within the exposed portions and in the drill cores. The typical phase consists of trachytic, variably porphyritic, salmon-pink and greenish-black, medium-to coarse-grained aegerine-augite syenite with conspicuous dark-brown sphene and centimeter-scale elliptical pyroxenite clots. As reported by Sims and others (1972), and confirmed here, the dominant minerals of the syenite are braid-textured perthite and dark-green aegerine-augite ($Ac_7Wo_{41}En_{26}Fs_{25}$, Table 3 and Fig. 7), with variable but lesser amounts of plagioclase, sphene, apatite, biotite, hornblende, magnetite, and epidote. Modal analyses and compositions of selected minerals are summarized in Tables 1 and 3. Complete descriptions of exposures are given in Sims and others (1972), and the drill cores are summarized in Table 4.

Textures in the groundmass of drill holes CD-13 (Meints and others, 1993) and LF-2 are suggestive of cataclasis, yet other features in these cores, such as tabular plagioclase, blocky pseudomorphic biotite and epidote (presumably after pyroxene), and euhedral diamond-shaped sphene, show no evidence of brittle deformation. Thus the granoblastic fabric of the groundmass is most likely the result of plastic flow deformation of a viscous, mostly crystallized magma, in conjunction with late deuteric fluids. Drill hole CD-4 in the Linden satellite also contains zones of moderately sheared syenite characterized by rounded, rolled feldspar phenocrysts, suggestions of C-S fabric, and streaky pink and gray segregations. Shear bands <1 inch to 10 feet thick are foliated parallel to the trachytic fabric of unsheared portions, and the mineralogy of the sheared rock in thin section is identical to that of the undeformed portions (Table 1). As is the case in the Linden pluton proper, the annealed texture implies that deformation occurred in a hot, semiplastic state, under near-magmatic temperatures. These submagmatic deformation features are also present in the Idington and Coon Lake plutons.

Gheen Pluton

The Gheen pluton, some 3 miles east of the Linden pluton, intrudes sillimanite-grade metasedimentary rocks. It is currently exposed at a high level, and its magnetic signature conforms to the long, sinuous, northeast-elongate shape deduced from scattered outcrops along the length of the body. Local trachytic fabric defined by tabular perthite phenocrysts is steep and subconformable to the pluton contacts, and the pluton shape at both map and outcrop scale is subcordant to the schistosity of the host supracrustal rocks.

The pluton is chiefly mesocratic, pink and dark-green, porphyritic syenite and ranges to dark-greenish-black, coarse-grained pyroxenite and leucocratic, pink, coarse-grained alkali-feldspar syenite. Conflicting internal intrusive relationships are common, with melanocratic phases occurring both as inclusions and as dikes in the porphyritic phase. However, pink leucosyenite dikelets cross all other phases.

Mesocratic syenite phases contain 1- to 3-cm tabular perthite phenocrysts in a groundmass of fibrous amphibole, euhedral sphene, blocky oxides, stubby prismatic apatite, and minor calcite and epidote. Trace amounts of dark-green pyroxene are present, but most has

Table 4. Descriptions of cores from the Linden pluton
[Bold face, dominant lithology]

Drill Hole	Description	Mineralogy
LF-2	Pink, slightly porphyritic, medium-grained homogeneous leuco-alkali-feldspar syenite. Trachytic foliation defined by aligned mafic minerals. Feldspar varies from coarse blocky phenocrysts with recrystallized edges to granoblastic groundmass.	**Perthite**, biotite, muscovite, aegerine, melanite, sphene, calcite, epidote, oxides, pyrite.
LF-3	Dark-gray, slightly porphyritic, fine- to medium-grained heterogeneous poikilitic syenite to monzonite. Poikilitic feldspar encloses pyroxene, biotite, and sphene. Weak trachytic fabric defined by aligned pyroxenes and feldspar oikocrysts. Feldspathic dikelets and aegerine veinlets.	**Microperthite** that grades to **antiperthite**, **pyroxene**, **biotite**, sphene, apatite.
LF-4	Light-grayish-white, medium-grained, granular to hypidiomorphic hornblende monzonite with 1-cm mafic segregations. Deuteric pyroxene alteration.	**Perthite**, **antiperthite**, **hornblende-biotite-oxide** clusters after pyroxene, epidote, sphene, apatite, calcite in brittle veinlets.
LF-5	Light-pinkish-gray, medium- to coarse-grained, moderately porphyritic syenite; 2- to 4-cm mafic segregations of slightly porphyritic, euhedral aegerine in groundmass of feldspar, hornblende, sphene, etc.	**Perthite**, **aegerine**, sphene, apatite, oxides, hornblende, biotite, chlorite.
OB-207	Pinkish-gray, coarse-grained, trachytic, aegerine syenite.	**Perthite**, **aegerine-augite**, biotite, sphene, apatite, oxides.
OB-212	Coarse-grained, green and pink, trachytic syenite. Deuteric alteration of mafic minerals.	Red-stained **perthite**, fine granular **plagioclase**, stilpnomelane after biotite, chlorite after hornblende or pyroxene, leucoxene after sphene.
LP-1	Pink, coarse-grained syenite with erratic distribution of mafic minerals. Contains a 1-foot-wide dike of melasyenite (biotite-pyroxene-carbonate).	Very coarse **feldspar**, 7-80% **aegerine**, sphene.
LP-2	Upper 20 feet, leucosyenite with 75-90° dipping trachytic fabric; rest is pink and green mesocratic syenite with biotite segregations.	Not described.
CD-13	Pink and green, coarse-grained, weakly trachytic syenite with annealed cataclastic texture. Microperthite phenocrysts, pyroxene altered to tabular clusters of biotite plus epidote. Foliated matrix of fine-grained plagioclase.	**Microperthite**, **plagioclase**, **biotite**, **epidote**, melanite, sphene, sericite.
CD-4 Satellite	Gray, coarse-grained, trachytic, porphyritic syenite with narrow pink and green, fine-grained shear bands. Granoblastic-recrystallized texture in shear bands grades into unsheared rock, contains rolled feldspar phenocrysts. Sheared portions of same mineralogy as unsheared.	In unsheared portion, tabular **perthite** rimmed by granular **plagioclase**, zoned euhedral **aegerine-augite** rimmed by pale-green fibrous amphibole. Apatite, chlorite, sphene, allanite, oxides.

been deuterically altered to bright-green fibrous amphibole. Calcite occurs both in irregular veinlets with amphibole and as magmatic, interstitial grains against sharp corners of feldspar phenocrysts. The melanocratic monzodiorite phase consists predominantly of relict pale-green pyroxene up to 2.5 mm across and lesser amounts of sericitized plagioclase, fine-grained, euhedral sphene, and apatite. The pyroxene is variably replaced by euhedral, pale-green hornblende. Biotite occurs as brown books within hornblende, and is slightly altered to chlorite. Unaltered microperthite occupies a late anhedral interstitial position.

Sills of pink, leucocratic, coarse-grained syenite up to 10 feet wide emanate from the Gheen pluton and cut adjacent metasedimentary rocks. This phase is characterized by irregular microcline phenocrysts in a seriate groundmass of macroscopically identified, pink microcline, fine-grained biotite, and minor white albite. Local planar miariolitic cavities lined with K-feldspar crystals are consistent with the interpretation that the pluton is exposed at a high level.

The Gheen pluton differs from the other alkalic intrusions by its pervasive deuteric alteration and relatively abundant chalcopyrite. Modal analyses of the melanocratic and porphyritic mesocratic phases are listed in Table 1 and shown on Figure 3.

Baudette pluton, Lake of the Woods County

The Baudette pluton is not exposed, but is seen in a drill core obtained by the Minnesota Geological Survey (hole 1986-CUSMAP-1; Mills and others, 1987). It is located 8 miles south of the town of Baudette, in Lake of the Woods County, and intrudes felsic schists. As judged from geophysical data, the pluton is approximately 1 mile long and half a mile wide, but the best resolution of available geophysics is only 1:250,000 (USGS data in Chandler, 1991).

The core consists of coarse-grained, green and pink, porphyritic garnet-biotite syenite. Trachytoid phenocrysts of pink perthite up to 2 cm long with irregular granular borders are in a groundmass of green biotite, melanite garnet, plagioclase, lesser epidote, sphene, and aegerine-augite, and accessory apatite and zircon or monazite. The brownish-yellow melanite varies from small euhedral crystals to large granular masses enclosed within coarser green biotite. The biotite varies greatly in grain size from fine-grained mats to medium-grained books with a decussate intergrown fabric.

MONZODIORITE CLAN

The monzodioritic group includes the Side Lake, Morcom, Idington, Lost Lake, and Cook plutons, as well as the Daisy Bay pluton (Sims and Mudrey, 1972), which is shown on Figure 1 but not discussed here. All are within the Wawa subprovince, adjacent to the north edge of the Shannon Lake granite phase of the Giants Range batholith (Jirsa and others, 1991).

These plutons tend to be irregular in shape and elongate to the northeast, parallel to the regional D_2 fabric (Jirsa and others, 1992) of the supracrustal country rocks. The rock is largely pink and green porphyritic monzodiorite, but varies erratically to dark-green pyroxenite and pink granite, granodiorite, and Na-rich trondhjemite. The pyroxenite tends to occur in small irregular pods and segregations, whereas the felsic differentiates occur in thin, straight dikes and in larger segregations. In addition, the monzodiorite group contains minor dark-green poikilitic phases in which antiperthite is grown over pyroxene, sphene, apatite, and hornblende.

Porphyritic phases typically have strong trachytoid fabrics, defined by aligned feldspar phenocrysts, that are subconformable to the borders but more erratic in the centers of the intrusions. The typical porphyritic phase is characterized by coarse, blocky, pink to gray phenocrysts of Na-rich antiperthite in a groundmass of predominantly fine-grained euhedral aegerine-augite, along with sphene, perthite, polygonal plagioclase, lesser proportions of hornblende, biotite, apatite, epidote, chlorite, opaque oxides, and rare quartz. Feldspar phenocrysts are typically antiperthitic, but range from albitic plagioclase to strongly perthitic K-feldspar. The normative composition is commonly midway between the K-rich and Na-rich end members in contrast to the compositions implied by point counting, because of difficulties in properly quantifying modal abundances of the strongly exsolved feldspars (Fig. 3B).

Idington Pluton

The Idington pluton is located in west-central St. Louis County near the former village of Idington. Its irregular horseshoe shape, roughly 8 mi^2 in size, is elongate to the northeast (Fig. 1). Trachytic foliations are predominantly northeast-oriented, subcordant to the pluton boundary, and dip generally more than 70°. However, exposures are limited to central parts of the pluton, where trachytic fabrics are less likely to conform to the pluton shape. The pluton has a rather irregular magnetic anomaly (Fig. 1), but the magnetic pattern has been somewhat obscured by a 150-foot-wide, strongly magnetic diabase dike and possibly by late north-trending brittle faults. No contact relationships with country rocks were observed, except at the southwestern edge of the pluton, where it is intruded by the 2,674-Ma Shannon Lake granite of the Giants Range batholith (Jirsa and others, 1991; Boerboom and Zartman, 1993).

Rock types in the Idington pluton are consistent in mineralogy but extremely erratic in modal proportions. Mesocratic, porphyritic pyroxene monzonite predominates, but dark-green aegerine-augite pyroxenite is common, and a small proportion of pink, sodic leucotrondhjemite occurs in aplopegmatite dikes 1 to 10 cm wide in the heart of the pluton. A mappable segregation of leucotrondhjemite exposed at the pluton's northeast corner contains minor flat-lying vuggy fractures lined with purple fluorite and a dark-brown translucent tetragonal mineral tentatively identified as zircon or cassiterite.

Modal analyses from four samples of the Idington pluton (porphyritic phase—C.551.X, pyroxenite phase—C.650.A, and two felsic differentiates—C.552.B and C.561.A) are listed in Table 1. In the porphyritic phase, feldspar phenocrysts are mostly gray, rectangular, 1- to 4-cm crystals of coarsely exsolved antiperthite, but small intergrown polygonal grains of plagioclase and perthite also are abundant in the groundmass. Aegerine-augite crystals are prismatic, weakly pleochroic, and zoned with darker green rims. Apatite inclusions are common near the edges of pyroxene crystals. Euhedral, dark-brown sphene is prominent in hand sample and is microscopically associated with biotite. Melanocratic diorite is medium to coarse grained, with trachytically aligned aegerine-augite prisms in a groundmass dominated by fresh, zoned, anhedral plagioclase. Hornblende in this phase occurs as dark-green patches of secondary origin within pyroxene and as larger subpoikilitic grains with inclusions of apatite, pyroxene, and plagioclase. Green biotite forms clusters of euhedral blocky grains aligned parallel to the trachytic fabric. Sphene is mostly euhedral, but locally is subpoikilitic-anhedral and partially encloses pyroxene and other mafic minerals. Accessory minerals include allanite and secondary chlorite, calcite, and epidote. The leucocratic differentiate contains albitic feldspar as large as 40 cm across, which is characterized by graphic intergrowths with quartz. Aplitic parts of the leuco phase contain radial-plumose sheaves of albite as long as 3 cm.

The erratic distribution between phases, which typifies exposures of this intrusion, can be documented on an outcrop scale to have formed by filter-pressing of a mafic liquid out of a feldspar-phenocryst slurry. The groundmass in the porphyry is identical to the melanocratic pyroxenite, which occurs as irregular amoeboid to net-vein segregations as large as several feet. However, at the southwestern end of the pluton, cumulus modal layering is also present in the form of melanocratic layers tens of centimeters thick interlayered with mesocratic, porphyritic diorite. This diorite itself shows layering by changes in phenocryst size and abundance and trachytoid foliation parallel to layering. The layering and trachytic fabric have been drag-folded into widely spaced, crosscutting ductile shear bands, which lack cleavage or schistosity, but instead have an annealed, granoblastic habit similar to that in the Linden pluton. Pink granite pegmatite dikelets (Shannon Lake granite?) commonly occupy these shear planes. In these bands, elliptical deformed relict feldspar phenocrysts are recrystallized into granoblastic aggregates, and the pyroxenes have been replaced by bright-green hornblende. The annealed textures and lack of through-going fabric development imply that ductile deformation, recrystallization, and annealment, caused by self-induced strain during emplacement or the last vestiges of regional deformation, occurred while the rock was still hot. These features may be analagous, on a smaller scale, to those in the Mortagne granite pluton in France, which was emplaced in a pull-apart structure along a regional-scale shear zone. There, shear deformation was documented to have begun before solidification of the granite, probably along transcurrent faults in the floor of the magma chamber, and to have persisted throughout cooling (Guineberteau and others, 1987), as shear zones became more constricted and solid-state, ultimately forming narrow orthogneiss bands. The Idington pluton and some other alkalic plutons in northern Minnesota may have been emplaced in a similar, but less localized and less intense, transcurrent shear regime, resulting in the preferred E-NE en echelon map patterns, in addition to the deformational features described above.

In a series of exposures along Highway 53 at the south edge of the Idington pluton a sharp line of demarcation exists whereby outcrops of Shannon Lake granite have inclusions only of Idington monzodiorite north of an east-west line, and those south of it have inclusions only of granodiorite derived from the Britt pluton, an early, D_2-deformed intrusion (Jirsa and others, 1991, 1992). This implies that the earlier intrusive contact of the Idington pluton into the Britt granodiorite was overprinted but preserved by upward stoping of the Shannon Lake granite (Boerboom and Zartman, 1993).

Side Lake Pluton

The long, arcuate Side Lake pluton, roughly 27 mi^2 in dimension, extends eastward from Side Lake in western St. Louis County. The pluton crops out only at its very western and eastern limits. Two exposed satellitic plugs off the eastern tip of the main pluton (Fig. 1) are identical in mineralogy to, and conterminous with, the eastern end of the Side Lake pluton. These satellites have complex intrusive relationships with the country rocks, and are described in a separate section below. The main pluton intrudes metamorphosed basaltic and felsic sedimentary rocks along most of its length. It is just north of the Shannon Lake granite, but intrusive relationships with the granite are unknown because of lack of exposure. Crosscutting Proterozoic diabase dikes have lowered the magnetism along their length, in contrast to the Idington pluton, where the diabase dikes have enhanced the magnetism.

Rocks from the exposures of the Side Lake pluton range from mesocratic biotite-hypersthene-clinopyroxene diorite on the west to hornblende monzodiorite on the east. Trachytic fabrics in most outcrops are generally conformable to the margins of the pluton. Segregations of melanocratic pyroxenite to hornblendite occur throughout the intrusion, but are more abundant to the west, where they occur as irregular dikelets, segregations, and small inclusions in mesocratic diorite. In addition, dikes of diorite and pyroxenite up to 150 feet wide, which emanate from the western margin of the pluton, are parallel to the pluton boundary and intrude metabasaltic rocks. These dikes are clearly discordant to the regional metamorphic fabric in the intruded basalts; some of them contain wispy felsic stringers parallel to their walls produced by flow segregation. Thin, straight, late-stage pink granitic to syenitic dikelets are common within and adjacent to the pluton,.

Mesocratic, medium-grained, pinkish-gray diorite, which predominates at the western end, contains 5-10% tiny euhedral grains of pleochroic pale-pink to green hypersthene, and at least 20% euhedral, pale-green clinopyroxene with light-colored rims. These pyroxenes range in size from less than 1 to 3 mm; the hypersthene is generally finer grained, and the clinopyroxene is variably phenocrystic. Plagioclase is the predominant feldspar. A sample from the pluton 200 feet from the western contact contains strongly zoned, subhedral, trachytic plagioclase, with fuzzy grain boundaries. Another thin section 500 feet from the contact has fine-grained granoblastic plagioclase, orthoclase, and quartz between larger augite phenocrysts. Apatite is abundant as fine-grained euhedral prismatic grains included within pyroxene and feldspar. Oxides occur both within augite as wormy blebs of apparent secondary origin and as scattered blocky, fine-grained crystals. Sphene is rare or lacking at the western end. Brown biotite is a generally minor component at the western end of the pluton, but in some outcrops composes up to 5% of the rock. It locally forms vertically oriented poikilitic plates that are up to 2 cm long and oriented parallel to the trachytic fabric of the monzodiorite.

The eastern outcrops consist of moderately heterogeneous, medium- to coarse-grained, pink and green pyroxene-hornblende monzodiorite. Here moderately developed trachytic foliation plunges 20-30° to the southwest, down the axis of the pluton. Fine-grained, centimeter-sized, angular cognate xenoliths of mafic monzodiorite, in addition to dark-green mafic stringers, are common.

Side Lake Pluton Satellites

Two small plugs are exposed northeast of the Side Lake pluton. One, about 1/4 mile east of the Side Lake pluton, is round and 3/4 mile in diameter. It consists of medium- to coarse-grained, trachytic, weakly porphyritic, green and pink hornblende-pyroxene monzodiorite. Subhedral 5-mm orangish-white antiperthite and scattered 2-mm aegerine-augite phenocrysts are set in a fine-grained groundmass of green prismatic pyroxene, fine-grained anhedral feldspar of unknown composition, minor hornblende, and brownish-green biotite mostly replaced by chlorite. Apatite, biotite, opaques (oxides and pyrite), and sphene each compose about 1% (Table 1). Clots and irregular segregations of pyroxenite are common, as are late dikelets of pink syenite up to 10 cm wide which cut across trachytic fabrics. The trachytic fabric is locally variable and inconsistent in orientation, but generally has a shallow southwest plunge toward the main Side Lake pluton.

The next satellite is a horseshoe-shaped body, 0.75 mi^2 in size, located 1.5 miles east of the Side Lake pluton (Fig. 1). Its linear trachytic fabrics are subconformable to the edges of the plug, and again plunge shallowly southwest toward the Side Lake pluton. This small intrusion is highly varied in texture and mafic content, but dark-green poikilitic diorite and white leucocratic monzodiorite with small inclusions of pyroxenite predominate. The poikilitic diorite has 1-cm, oval-shaped antiperthitic to perthitic poikilitic feldspar with inclusions of aegerine-augite, biotite, sphene, and apatite. The long axes of the poikilitic feldspars and prismatic pyroxenes are parallel and define a primary trachytic fabric. The dark poikilitic phase is sharply cut by sills of the white monzodiorite. However at one location, the two rocks are commingled in a pillow-like fashion that suggests mixing of immiscible liquids. Thus the field relationships, as well as mineralogy, indicate that the dark poikilitic and leucocratic phases are comagmatic.

Relationship of Satellitic Intrusions to the Side Lake Pluton

Their similar lithological and textural attributes and aligned trachytic fabrics imply that the Side Lake pluton and the two satellites are derived from a common source at depth to the west. Further evidence of comagmatism is the presence of numerous thin anastamosing sills of white monzodiorite, identical to the white phase in the small plugs, which are parallel to the schistosity of the surrounding metasedimentary country rocks and intercalated with them. The intercalated monzodiorite and schist define a mappable unit along a discrete zone (dashed area on Fig. 1) that links the two satellitic plugs to the Side Lake pluton. This zone continues past the eastern satellite for at least 2.5 miles, where it merges back into a magnetic anomaly interpreted as another alkalic intrusion (Jirsa and others, 1991).

At the intersection of Highway 73 and the Sturgeon River east of the Side Lake pluton, the intercalated monzodiorite and metasedimentary rocks are transected by a late, north-trending brittle shear zone, which has minimal offset but has reduced the rocks to a fine-grained cataclasite.

Morcom Pluton

The Morcom pluton is just north of the Side Lake pluton and may be related to it at depth, because a large positive gravity anomaly underlies the area between the two. The Morcom pluton, which intrudes metasedimentary rocks, has a bulbous shape with a long narrow appendage to the east (Fig. 1). Scattered outcrops exist at the eastern limit of the pluton, and a drill core was obtained from the western end, near the north side. Trachytic foliation near the southeast edge dips 80°N, and at the eastern tip plunges 40°SW. In the drill core, the foliation dips 40-45°, presumably toward the pluton center.

Rock types are similar in the Morcom pluton, the eastern Side Lake pluton and its satellites, and the Idington pluton. However, the major-element geochemistry of the Morcom is very similar to that of the Linden pluton (Fig. 5). The drill core consists of multiphase, medium-grained, weakly porphyritic biotite-hornblende-pyroxene monzodiorite, with a trachytoid foliation defined by alignment of plagioclase phenocrysts and prismatic mafic minerals. Dark-green, poikilitic monzodiorite occurs in the core as 15-cm inclusions or layers; small miariolitic cavities lined with fine-grained crystalline biotite, pyroxene, and pyrite are also present. Late brittle slickensided faults and fractures, oriented obliquely to foliation, locally transect the core. Feldspar compositions vary from clean plagioclase with narrow twin lamellae to untwinned plagioclase, and from antiperthite to perthite, the latter confined to anhedral grains in the groundmass. Euhedral, light-green, aegerine-augite has hornblende rims and alteration patches; hornblende is also present as subhedral to prismatic, brownish- to bluish-green grains with patchy color zonation and rare deuteric overgrowths of colorless actinolite. Biotite is dark green and pleochroic, and is associated with hornblende. Accessory minerals include sphene, allanite, apatite, epidote, calcite, and minor secondary oxides within pyroxene. The nonpoikilitic and poikilitic phases have similar mineralogy (Table 1).

Exposures at the eastern tip of the pluton consist of pink to gray, medium-grained monzodiorite with abundant 5- to 10-cm, elongate xenoliths of foliated felsic to pelitic schist, together with cognate xenoliths of fine-grained melanocratic monzodiorite. Some of the intrusive-breccia xenoliths are themselves an intrusive breccia. Pink monzonitic dikelets are abundant and cut all the earlier intrusive phases and xenoliths. The monzodiorite contains scattered sericitized plagioclase phenocrysts in a fine-grained groundmass consisting of up to 5% quartz intergrown with granular K-feldspar and plagioclase, along with hornblende, actinolite, sphene, chlorite, apatite, and minor oxides and secondary calcite. Melanocratic clots are of similar mineralogy but with a higher proportion of mafic minerals. Elsewhere at the eastern terminus, the rock lacks xenolithic inclusions but is still heterogeneous and cut by late, pink felsic differentiates. This inclusion-free monzodiorite has a trachytic fabric defined by aligned feldspars and mafic clots, and is similar in mineralogy to the core from the western end of the pluton.

Lost Lake Pluton

The Lost Lake pluton, the "pluton southwest of Lost Lake" of Sims and Mudrey (1972), was described as a circular pluton composed of heterogeneous syenite with a local, conspicuously porphyritic facies, a pegmatitic facies with miarolitic cavities, and small bodies of pyroxene-biotite lamprophyre. They noted that the borders of the pluton tend to be quartzose and contain small angular inclusions of metagraywacke and slate of the Lake Vermilion Formation.

Based on detailed remapping, the authors have redefined the shape of the pluton as a long, sinuous and bulbous, northeast-trending body that is 1 mile or less wide but approximately 9 mi^2 in size. The eastern tip of the pluton lies 1/4 mile south of Lost Lake, and the western terminus is just south of Angora on State Highway 53, about half a mile north of the Idington pluton (Fig. 1). The uniform magnetic signature of the pluton has been lowered locally by late, north-south, brittle faults which have minimal offset. The western end of the Lost Lake pluton is not exposed and its shape is inferred from aeromagnetic data, whereas the central portion is very well exposed, and scattered outcrops exist over the eastern end, mainly adjacent to more resistant crosscutting Proterozoic diabase dikes. Two mappable intrusions of quartz monzonite 1/4 mile in diameter occur adjacent to the main body (Jirsa and others, 1991). These small plugs are similar in composition to leucocratic dikes within the main pluton, and are related to the pluton.

Subvertical trachytic fabric, which is defined by both phenocrysts and elongate poikilitic feldspar, strikes generally northeast, subparallel to the length of the intrusion. The small, separate bodies of pink monzonite also possess a northeast-oriented trachytic fabric, defined by orbicular clots of biotite, disseminated biotite, or aligned feldspar crystals.

The Lost Lake pluton is mineralogically similar to the Idington and eastern Side Lake plutons, but contains a higher proportion of pink leucocratic phases. The main rock types range from pink and green, porphyritic monzodiorite to dark-green, poikilitic biotite-pyroxene monzodiorite to pink monzonite, syenite, and quartz monzonite. Pyroxenite occurs in small segregations, in the same fashion as in the Idington pluton. In general, the poikilitic and porphyritic phases are earliest and are cut by the pink rock varieties. Small dikes of pink granitic pegmatite cut all other rock types, but it is unclear whether these dikes are related to the pluton or are from an external source, such as the Shannon Lake granite of the Giants Range batholith. The pink monzodiorite and syenite differentiates are medium grained, equigranular to weakly porphyritic, and commonly aplitic to pegmatitic, with pyroxene, hornblende, and biotite as the predominant mafic phases.

The two small felsic plugs of quartz monzonite to granodiorite contain a mafic mineral assemblage of varied proportions of biotite, chlorite, and hornblende, and up to 30% quartz. The margins of these plugs contain abundant inclusions of felsic volcanic country rocks up to 15 feet across which were clearly deformed prior to incorporation, and small dikes emanating from these plugs cut across fold axes in the supracrustal rocks. One of the plugs contains a unique medium-grained, pink, orbicular granodiorite with trachytically aligned discs of black, concentrically foliated biotite that are as much as 0.5 cm thick and 5 cm long. The biotite orbs which contain intergrown sphene, apatite, plagioclase, quartz, and magnetite, compose as much as 15% of the rock. The orbicular rock grades into a non-orbicular phase with the same proportion of biotite, but as medium-grained, uniformly disseminated flakes. In addition to the typical phases, related rocks in the small plugs include coarse-grained, dark-green biotite-hornblende lamprophyre; green poikilitic monzodiorite; and pink monzonitic pegmatite.

Cook Pluton

The Cook pluton (Cook Airport pluton on Southwick, 1993), 1 mile south of the town of Cook (Fig. 1), is inferred from aeromagnetic data to be 1.5 mi^2 in size, elongate to the east. No outcrops of this pluton are known, but a drill hole in the western margin of the pluton recovered core of uniformly coarse-grained, peppery, dark-greenish-black and light-green, epidote-altered hornblende-biotite diorite. Strong trachytic foliation, which is defined by tabular plagioclase and mafic minerals, dips 50° from horizontal. One fine-grained cognate xenolith, 1 cm x 3 cm in size, is present near the bottom of the 10-foot core. The rock has a primary hypidiomorphic-granular texture, but pervasive, small euhedral crystals of secondary epidote are overprinted on all primary minerals, preferentially in the cores of plagioclase, and as fine-grained granular masses in biotite. Pale-green hornblende is rimmed by green biotite, and zoned plagioclase is clean and well-twinned, despite the pervasive epidote alteration. Accessory minerals include apatite, sphene, oxides, calcite, and interstitial orthoclase. Scattered late, brittle fractures which dip as much as 20° from horizontal are lined with coarse, lineated chlorite, pink-altered feldspar, and a crust of epidote and white carbonate. The pristine trachytic igneous texture and lack of metamorphic fabric indicate that the pervasive epidotization is the result of deuteric alteration, rather than regional metamorphism.

GRANITOID PLUTONS

The granitoid group includes the Stingy Lake, Rice River, and Bello Lake plutons, all within the Wawa subprovince. These plutons tend to be oval in shape and elongate to the northeast. Rocks in this group are characterized by substantial quantities of quartz and are vaguely to strongly porphyritic and trachytic. Hornblende is the predominant mafic phase, along with biotite and rare pyroxene. These plutons are considered part of the alkalic group on the basis of their similarity to the other alkalic plutons in size, shape, high Ba and Sr content, magnetic signature, and trachytic fabric.

Stingy Lake Pluton

The Stingy Lake pluton is a 9 mi^2 circular pluton located 3 miles south of Sturgeon Lake, adjacent to the Giants Range granite, and is inferred to intrude mafic volcanic rocks (Fig. 1). Although unexposed, its round shape is well defined by its aeromagnetic anomaly (magnetic rim and nonmagnetic core). A 10-foot drill core was obtained from the northwest side of the pluton (Meints and others, 1993). The intrusion is cut by two Proterozoic diabase dikes.

The rock in the core is uniformly coarse-grained, porphyritic, pink granodiorite to quartz monzodiorite. Tabular phenocrysts of string-and-braid microperthite up to 7 mm long, together with weakly zoned plagioclase up to 2 mm long having narrow twin lamellae and weakly sericitized cores, define the 45°-dipping trachytoid foliation. The perthite contains small blocky plagioclase inclusions, and the areas between abutting perthite grains are also stuffed with small blocky plagioclase grains. Light-gray anhedral interstitial quartz with shadowy extinction has been recrystallized into coarse polycrystalline aggregates. Hornblende is mostly altered to green biotite, epidote, and granular oxides; however, fresh, dark-green, euhedral hornblende is locally preserved within quartz and feldspar. Accessory minerals include blocky primary oxides, sphene, zircon, and apatite (Table 1). Late closely spaced, vertical brittle fractures lined with epidote and chlorite are pervasive in the 10-foot core.

Rice River Pluton

The Rice River pluton, about 5 miles west of Cook, intrudes metamorphosed sedimentary rocks. It is inferred to be approximately 15 mi^2 in size, although its magnetic signature (Fig. 1B) of magnetic rim and nonmagnetic core is irregular and overprinted at the western edge by a north-trending Proterozoic diabase dike. A drill hole in the magnetic eastern rim of the pluton recovered core of gray, coarse-grained, porphyritic quartz monzonite to monzodiorite. Steeply inclined trachytic foliation is defined by euhedral, strongly zoned, 1- to 2-cm perthite phenocrysts and small elliptical melanocratic clots that are fine-grained cognate xenoliths. Groundmass to the phenocrysts consists of 3- to 6-mm subhedral microcline, zoned plagioclase, hornblende, and anhedral interstitial quartz; the phenocrysts are rimmed by fine-grained plagioclase and myrmekitic quartz-feldspar intergrowths. Plagioclase grains are heavily sericitized, preferentially in the cores. Hornblende is weakly zoned and slightly altered to biotite, chlorite, and opaques. Euhedral sphene, allanite rimmed by epidote, and secondary calcite occur in minor proportions. Scattered chlorite-pyrite veinlets dip 5-10° from horizontal and occupy brittle fractures; some have slickensides that dip shallowly in the fracture planes.

Bello Lake Pluton

The Bello Lake pluton (Jirsa, 1990; Jirsa and Boerboom, 1990) is just southwest of the Coon Lake pluton. It is approximately 60 mi^2 in size, elongate to the northeast parallel to the regional strike of the mafic to felsic supracrustal rocks that it intrudes. The Bello Lake pluton is unexposed, but three 10-foot drill cores were obtained by the Minnesota Geological Survey, two near the western end, and one near the eastern end of the pluton (Fig. 1). The intrusion is magnetically quiet relative to the mafic volcanic rocks around it, but the pluton margins are strongly magnetic locally.

As judged from the cores, the Bello Lake pluton is uniform in color and texture, but moderately variable in composition, ranging from pyroxene monzonite to hornblende granite. The pyroxene-bearing phase occurs close to the pluton margin, whereas the hornblende monzonite occurs near the center of the pluton at its western end, and the hornblende granite is near the eastern end of the pluton. Data are insufficient to properly judge spatial variation of rock types, but the observed distribution suggests that the pluton may be zoned from a pyroxene-bearing phase at the rim, to a more differentiated, quartz-bearing phase near the center.

Pyroxene monzodiorite near the pluton border (KIB-39; Table 1) is green and pink, medium grained, and seriate in texture with a strong trachytic fabric defined by rectangular, zoned plagioclase and subhedral, weakly uralitized augite crystals. Accessory oxides, sphene, hornblende, chlorite, biotite, and apatite all formed late in the crystallization sequence, and tend to occur together.

Green and pink, medium-grained, slightly porphyritic hornblende monzonite (KIB-40; Table 1) on the western side of the pluton contains subhedral-prismatic hornblende and small phenocrysts of grayish-pink, blocky microperthite in an allotriomorphic-granular to weakly seriate groundmass of plagioclase, perthite, and minor quartz. This rock is similar to the pyroxene monzodiorite in hole KIB-39, except that hornblende occupies the position of pyroxene.

Hornblende granite from the eastern part of the pluton (drill hole KIB-7; Table 1) is characterized by strongly zoned, blocky plagioclase with sericitized cores surrounded by poikilitic microperthite. Myrmekitic feldspar-quartz intergrowths occur along perthite-plagioclase grain boundaries. Quartz is coarse and anhedral intersitial, and hornblende forms dark-green, irregular grains with abundant tiny quartz inclusions near the edges and granular oxide inclusions in the cores. Accessory green biotite, epidote, and chlorite are associated with hornblende as alteration products, and blocky apatite crystals are associated with mafic phases.

PETROGENETIC AND GEOCHRONOLOGICAL STUDIES

Arth and Hanson (1975), using data on major, trace, and rare earth elements, and isotopic data from the Linden pluton, concluded that the magma formed from 5 to 10% partial melting of a mixed eclogite and garnet peridotite source at mantle depth. Stern and others (1989) believe that the Linden originated by partial melting of a LILE-enriched mantle peridotite at shallow depths under hydrous conditions created by mantle metasomatism from rapid subduction of oceanic lithosphere. However, they have lumped the Linden pluton in with the "sanukatoid suite," a very broad suite of rocks of variable size, timing, and associations throughout the Superior Province.

The age of D_2 deformation of the supracrustal rocks at the southern edge of the area from Cook to Side Lake (Jirsa and others, 1991) was bracketed by U-Pb zircon geochronology to between 2,685 and 2,669 Ma (Boerboom and Zartman, 1993). The alkalic plutons lack significant D_2 fabrics, and thus could not have been emplaced until approximately 2,669 Ma. The Idington pluton is intruded by a granite pegmatite inferred to have originated from the Shannon Lake granite, which was dated by Boerboom and Zartman (1993) at 2,674 $\pm$ 5, or a minimum of 2,669. Catanzaro and Hanson (1971) obtained a discordant Pb^{207}/Pb^{206} age of 2,740 $\pm$ 10 Ma on sphene from the Linden pluton. Prince and Hanson (1972) obtained a similar age of 2,740 Ma, based on a Rb/Sr isochron through apatite and two whole-rock samples. These older ages on the Linden pluton relative to the younger age implied for the Idington pluton indicate that the syenitic rocks may be slightly older than the monzodioritic group, or that pluton emplacement may have progressed from north to south. Clearly, modern high-precision U-Pb zircon dates on the alkalic plutons are needed.

CONCLUSIONS

The alkalic intrusions in northern Minnesota can be generally subdivided into a syenitic group, a monzodioritic group, and a granitoid group. The syenitic plutons are somewhat north of the monzodioritic intrusions, whereas the granitoid plutons are interspersed with the monzodiorites. Although these groups differ in mineralogy, they are all similar in terms of size, texture, map pattern, geochemistry (e.g., high Ba and Sr), aeromagnetic signature, and timing of emplacement. All of the alkalic plutons have porphyritic textures, and the syenitic and monzodioritic plutons typically contain abrupt phase transitions from predominantly mesocratic, porphyritic rocks to dark-green pyroxenites and pink felsic differentiates. The granitoid plutons are more uniform in composition and texture.

The plutons are eroded to various levels. The northeastward-elongation and en-echelon map pattern of the Gheen and Lost Lake plutons and the eastern Side Lake pluton and its satellites indicate exposure at high levels, whereas the broad, rounded map shapes of the Linden, Coon Lake, and Bello Lake plutons indicate a deeper level of erosion. The map patterns of the relatively well exposed Side Lake, Idington, and Lost Lake plutons indicate a similar style of emplacement, in which the plutons have penetrated the supracrustal rocks to different levels. The Side Lake pluton plunges to the west, as indicated by the deeper level of erosion at the western end of the pluton and the west-plunging linear trachytic fabrics in the Side Lake satellites. This westward plunge may be either a primary emplacement feature or the result of tilting of the pluton prior to unroofing.

Several other plutons of alkalic affinity are suggested by the aeromagnetic data, but they are not exposed and their existence has not been verified by drilling.

ACKNOWLEDGMENTS

Field work and geochemical analyses for this project were funded by the Minerals Diversification Program administered by the Minerals Coordinating Committee for the Minnesota Legislature. The Minerals Division of the Minnesota Natural Resources Research Institute (also

supported by the Minerals Diversification Program) coordinated the analytical work for several of the geochemical samples.

REFERENCES CITED

Arth, J.G., and Hanson, G.N., 1975, Geochemistry and origin of the early Precambrian crust of northeastern Minnesota: Geochimica et Cosmochimica Acta, v. 39, p. 325-362.

Barker, J.G., and Arth, J.G., 1976, Generation of trondhjemite-tonalite liquids and Archean bimodal trondhjemite-basalt suites, Geology, v. 4, p. 596-600.

Beck, J.W., 1988, Implications for Early Proterozoic tectonics and the origin of continental flood basalts, based on combined trace element and neodymium/strontium isotopic studies of mafic igneous rocks of the Penokean Lake Superior belt, Minnesota, Wisconsin, and Michigan: Unpublished Ph.D. dissertation, University of Minnesota, Minneapolis.

Boerboom, T.J., Jirsa, M.A., Southwick, D.L., Meints, J.P., and Campbell, F.K., 1989, Scientific core drilling in parts of Koochiching, Itasca, and Beltrami Counties, north-central Minnesota, 1987-1989: Summary of lithological, geochemical, and geophysical results: Minnesota Geological Survey Information Circular 26, 159 p.

Boerboom, T.J., and Zartman, R.E., 1993, Geology, geochemistry, and geochronology of the central Giants Range Batholith, northeastern Minnesota: Canadian Journal of Earth Sciences, v. 30, p. 2510-2522.

Card, K.D., and Ciesielski, A., 1986, DNAG #1. Subdivisions of the Superior Province of the Canadian Shield: Geoscience Canada, v. 13, p. 5-13.

Catanzaro, E.J., and Hanson, G.N., 1971, U-Pb ages for sphene in northeastern Minnesota-northwestern Ontario: Canadian Journal of Earth Sciences, v. 8, p. 1319-1324.

Chandler, V.W., 1991, Aeromagnetic map of Minnesota: Minnesota Geological Survey State Map Series S-17, scale 1:500,000.

Deer, W.A., Howie, R.A., and Zussman, J, 1966, An introduction to the rock-forming minerals: London, Longman Group Limited, 528 p.

Geldon, A.L., 1972, Petrology of the lamprophyre pluton near Dead River, *in* Sims, P.K., and Morey, G.B., eds., Geology of Minnesota: A centennial volume: Minnesota Geological Survey, p. 153-159.

Guineberteau, B., Bouchez, J.L., and Vigneresse, J.L., 1987, The Mortagne granite pluton (France) emplaced by pull-apart along a shear zone: Structural and gravimetric arguments and regional implication: Geological Society of America Bulletin, v. 99, p. 763-770

Himmelberg, G.R., 1973, Geologic descriptions of drill core from greenstone belts in northeastern Minnesota: Minnesota Geological Survey Open-File Report.

Irvine, T.N., and Baragar, W.R.A., 1971, A guide to the chemical classification of the common volcanic rocks: Canadian Journal of Earth Sciences, v. 8, p. 523-548.

Jirsa, M.A., 1990, Bedrock geologic map of northeastern Itasca County, Minnesota: Minnesota Geological Survey Miscellaneous Map M-68, scale 1:48,000.

Jirsa, M.A., and Boerboom, T.J., 1990, Bedrock geologic map of parts of Koochiching, Itasca, and Beltrami Counties, north-central Minnesota: Minnesota Geological Survey Miscellaneous Map series M-67, scale 1:250,000 .

Jirsa, M.A., Boerboom, T.J., Chandler, V.W., and McSwiggen, P.L., 1991, Bedrock geologic map of the Cook to Side Lake area, St. Louis and Itasca Counties, Minnesota: Minnesota Geological Survey Miscellaneous Map Series M-75, scale 1:48,000.

Jirsa, M.A., Southwick, D.L., and Boerboom, T.J., 1992, Structural evolution of Archean rocks in the western Wawa subprovince, Minnesota: Refolding of pre-cleavage nappes during D_2 transpression: Canadian Journal of Earth Sciences, v. 29, p. 2146-2155.

Martin, D.P., Meyer, G.N., Lawler, T.L., Chandler, V.W., and Malmquist, K.L., 1988, Regional survey of buried glacial drift geochemistry over Archean terrane in northern Minnesota: Minnesota Department of Natural Resources, Division of Minerals Report 252, v. 1, 74 p.; v. 2, 386 p.

Meints, J.P., Jirsa, M.A., Chandler, V.W., and Miller, J.D., Jr., 1993, Scientific core drilling in parts of Itasca, St. Louis, and Lake Counties, northeastern Minnesota, 1989-1991: Summary of lithologic, geochemical, and geophysical results: Minnesota Geological Survey Information Circular 37, 159 p.

Mills, S.J., Southwick, D.L., and Meyer, G.N., 1987, Scientific core drilling in north-central Minnesota: Summary of 1986 lithologic and geochemical results: Minnesota Geological Survey Information Circular 24, 48 p.

Prince, L.A., and Hanson, G.N., 1972, Rb-Sr isochron ages for the Giants Range granite, northeastern Minnesota: Geological Society of America Memoir 135, p. 217-225.

Ruotsala, A.P., and Tufford, S.P., 1965, Chemical analyses of igneous rocks: Minnesota Geological Survey Information Circular 2, 87 p.

Sage, R.P., 1988a, Geology of carbonatite-alkalic rock complexes in Ontario: Poohbah Lake alkalic rock complex, district of Rainy River: Ontario Geological Survey Study 48, 68 p.

Sage, R.P., 1988b, Geology of carbonatite-alkalic rock complexes in Ontario: Sturgeon Narrows and Squaw Lake alkalic rock complexes, district of Thunder Bay: Ontario Geological Survey Study 49, 117 p.

Sage, R.P., 1988c, Geology of carbonatite-alkalic rock complexes in Ontario: Wapikopa Lake alkalic rock complex, district of Kenora: Ontario Geological Survey Study 52, 63 p.

Sims, P.K., and Mudrey, M.G., Jr., 1972, Syenitic plutons and associated lamprophyres: *in* Sims, P.K., and Morey, G.B., eds., Geology of Minnesota: A centennial volume: Minnesota Geological Survey, p. 140-152.

Sims, P.K., Morey, G.B., Ojakangas, R.W., and Viswanathan, S., 1970, Geologic map of Minnesota, Hibbing Sheet: Minnesota Geological Survey, scale 1:250,000.

Sims, P.K., Sinclair, D., and Mudrey, M.G., Jr., 1972, Linden pluton: *in* Sims, P.K., and Morey, G.B., eds., Geology of Minnesota: A centennial volume: Minnesota Geological Survey, p. 160-162.

Southwick, D.L., 1993, Geologic map of Archean bedrock, Soudan to Bigfork area, northern Minnesota: Minnesota Geological Survey Miscellaneous Map Series M-79, scale 1:100,000.

Stern, R.A., Hanson, G.N., and Shirey, S.B., 1989, Petrogenesis of mantle-derived LILE-enriched Archean monzodiorites and trachyandesites (sanukitoids) in southwestern Superior Province: Canadian Journal of Earth Sciences, v. 26, p. 1688-1712.

Streckeisen, A.L., 1973, Plutonic rocks: Classification and nomenclature recommended by the IUGS Subcommission on the Systematics of Igneous Rocks: Geotimes, v. 18, no. 10, p. 26-30.

ANTHRAXOLITE IN THE EARLY PROTEROZOIC BIWABIK IRON FORMATION, MESABI RANGE, NORTHERN MINNESOTA

By

G.B. Morey

ABSTRACT

Anthraxolite is one of a number of natural bitumens, broadly defined as allochthonous, localized, more or less solid masses of organic matter formed in or closely associated with a variety of sedimentary rocks of all ages. It is a minor but widely distributed constituent in the Biwabik Iron Formation (Animikie Group, Early Proterozoic) of the Mesabi iron range, northern Minnesota. Samples typically are black and have a pronounced vitreous luster and conchoidal fracture; as such they resemble obsidian. It has a narrow compositional range, containing 95 percent or more carbon. It yields an X-ray diffraction pattern indicative of amorphous organic material and suggestive of asphaltic affinity. As characterized, anthraxolite in the Biwabik Iron Formation is physically and chemically similar to material from the Sudbury, Ontario area, the "type locality" for anthraxolite.

The anthraxolite occurs as obviously remobilized material in crosscutting veins and as small spherically-shaped bodies both in stratigraphic units just beneath the Intermediate slate, an ashfall tuff that contains measurable quantities of carbonaceous material, mostly as reduced carbon. The abundance of reduced carbon in the Intermediate slate and the presence of anthraxolite just beneath it imply that the two are interrelated. It is suggested here that the organic material in the slate reflects a mass-kill phenomenon and that the precursor to the anthraxolite was a liquid that migrated from the source bed to its present locations where anthraxolite itself formed as various volatile constituents were driven off over time.

INTRODUCTION

Fractures filled with natural bitumens are relatively common in Early Proterozoic sedimentary rocks of the Lake Superior region (Mancuso and Seavoy, 1981). The term anthraxolite has been applied to most of these occurrences. The name was first proposed by Chapman (1888, p.143) for "anthracite-like materials," consisting predominantly of fixed or reduced carbon in veins and disseminated masses. He suggested that it was the alteration product of petroleum or asphalt. Ellis (1897) determined the chemical composition of anthraxolite from the Sudbury, Ontario, area as 94.92% carbon, 0.52% hydrogen, 1.04% nitrogen, 0.31% sulfur, 1.69% oxygen and 1.52% ash. Subsequently, the Sudbury area became the "type locality" for anthraxolite (Coleman, 1928).

Ongoing studies have established that anthraxolite is one of a number of natural bitumens broadly defined as allochthonous, localized, more or less solid masses of organic matter found in or closely associated with sedimentary rock (Curiale, 1986). Traditional classification schemes for solid bitumens are entirely generic, relying upon the solubility, fusibility, and hydrogen/carbon ratio of the sample for naming purposes (Abraham, 1945; Hunt and others, 1954; King and others, 1963; Hunt, 1979). In those schemes, the term anthraxolite applies to pyrobituminous material (insoluble in carbon disulfide) with a hydrogen/carbon ratio of less than unity.

Anthraxolite is common in the Early Proterozoic Animikie Group of northern Minnesota and adjoining parts of Ontario. It has been described by Ellsworth (1934) and Kwiatkowski (1975) as veins in iron-formation and associated argillaceous strata of the group from the Thunder Bay area of Ontario, Canada. Hayatsu and others (1983) reported that material collected by them from that area was derived from two different sources. They thought that one component, consisting of heavier, aromatic ring compounds and associated graphic carbon, was a residual product derived from a much older tar or asphalt that formed from organic remains contemporaneous with enclosing iron-rich strata. They believed that a lighter, aliphatic component probably was derived from overlying sediments deposited in latest Jurassic or in Cretaceous time.

In the late 1960s I acquired samples of anthraxolite from three sites along the strike length of the Early Proterozoic Biwabik Iron Formation on the Mesabi range, northern Minnesota (Fig. 1). These materials were physically and chemically characterized at that time, but the results were never published. Since then, anthraxolite has been identified at other localities along the range, and thus may be relatively common in the iron-formation.

The anthraxolite of the Biwabik Iron Formation differs somewhat from that in the Thunder Bay area, and this communication will expand the record of natural bitumens in the Precambrian rocks of the Lake Superior reigon. It will also contribute data as part of a renewed interest in the genesis of natural bitumens (Meyer and de Witt, 1990).

GEOLOGIC SETTING

The Biwabik Iron Formation crops out as a narrow belt, about a quarter mile to 3 miles wide, that extends for 120 miles along strike in northern Minnesota. The iron is underlain by quartz arenitic rocks assigned to the Pokegama Quartzite and is overlain by a thick sequence of shale and graywacke assigned to the Virginia Formation. These rock units collectively constitute the Animikie Group in northern Minnesota (Fig. 1).

The Animikie Group unconformably overlies an Archean basement complex of sedimentary and volcanic rocks that was intruded and metamorphosed by granitic rocks at 2,650 Ma during the time of the Algoman orogeny (Morey and Van Schmus, 1988). Basal units of the Animikie Group truncate a swarm of diabase dikes that are dated at 2,125 $\pm$ 45 Ma (Southwick and Day, 1983; Beck, 1988). The Animikian rocks in northern Minnesota have yielded a Rb-Sr whole-rock isochron age of 1,630 Ma (Morey and Van Schmus, 1988), an age similar to the 1,635 $\pm$ 24 Ma that has been obtained from the correlative Gunflint Iron Formation in Canada (Faure and Kovach, 1969). Similar 1,600-Ma ages, which are widespread throughout the Lake Superior region, seem to reflect a low-grade metamorphic event unrelated to any obvious tectonic or igneous activity (Morey and Van Schmus, 1988). Although argillaceous rocks on the Mesabi range have a reset Rb-Sr whole-rock isochron age, oxygen-isotopic data for quartz-magnetite pairs indicate that the main part of the underlying Biwabik Iron Formation was never subjected to temperatures of more than 150°C to 170°C (Perry and others, 1973; Perry, 1983).

The Biwabik Iron Formation from Mesaba eastward (Fig. 1) was metamorphosed in Middle Proterozoic time, with the emplacement at about 1,100 Ma, of the Duluth Complex, a large batholithic body of generally mafic composition. Broad features of the metamorphic aureole include mineral assemblages in the iron-formation which are dominated by fibrous amphiboles on the outer fringes and by olivine and pyroxene near the complex.

Strata within the Biwabik Iron Formation are classified by texture into two fundamentally different kinds of iron-formation. There are cherty materials, which are granular or peloidal, massive, and typically rich in quartz and iron oxide; and slaty materials, which are generally fine grained, finely laminated, and composed mostly of iron silicate and iron carbonate. Beds or groups of beds having cherty or slaty attributes are interlayered on all scales. Despite the heterogeneity of the formation, it has been divided into four major lithostratigraphic "divisions" (Wolff, 1917) or members (White, 1954), which are from bottom to top: (1) Lower Cherty, (2) Lower Slaty, (3) Upper Cherty, and (4) Upper Slaty (Fig. 2). Except for an ash-fall tuff, locally called the "Intermediate slate" at the Lower Cherty-Lower Slaty contact, contacts between adjacent members are gradational and arbitrary. In general, however, stratigraphic units included in the slaty members contain 40 percent or more slaty material; locally that proportion may be less. The cherty members, on the other hand, contain 10 to 30 percent slaty strata.

The members contain several unnamed subunits in the eastern half of the Mesabi range. Two are stromatolite- and oncolite-bearing intervals ranging in thickness from a few feet to several tens of feet. The thicker and more persistent is at the base of the Lower Cherty member; the other is in the middle part of the Upper Cherty member. The stromatolitic structures occur in original growth positions and as intraformational fragments and are commonly laminated red and white chert set in a jasper matrix that also contains granules, oolites, and other intraformational conglomeratic clasts.

Anthraxolite occurs widely in the eastern half of the Biwabik Iron Formation, even in highly metamorphosed strata in close proximity to the Duluth Complex. Generally the anthraxolite is restricted to the stromatolite-bearing units and to just beneath the Intermediate slate. The anthraxolite samples described here are from the Lower Cherty member. The two samples from near Keewatin and Buhl (Fig. 1) were from diamond drill core, and their stratigraphic positions, just a few inches beneath the Intermediate slate, are well constrained. The third sample, from near Hoyt Lakes, was acquired from a taconite mine developed in the outer part of the contact metamorphic aureole associated with the Duluth Complex. Unfortunately, we know only that this sample was collected from the uppermost part of the Lower Cherty member.

PHYSICAL PROPERTIES

Anthraxolite samples from the Biwabik Iron Formation at Keewatin and Buhl are black and have a pronounced vitreous luster and conchoidal fracture (Fig. 3A). Like anthraxolite in general, the samples superficially resemble obsidian. In contrast, the Hoyt Lakes sample has a very dark gray color and somewhat duller luster, probably owing to subaerial weathering that occurred at the open-pit mine face. Anthraxolite from the Buhl site occurs as large, irregularly shaped fragments that were as much as 1 to 2 cm in diameter before fracturing. The fragments are enclosed in a vein of quartz and calcite (Figs. 3B and 3C). Figure 3B also shows that individual fragments can be easily restored to their prefracture configurations. It is obvious that breakage occurred after the anthraxolite had been solidified.

At Buhl, veins containing anthraxolite cut an easily identified stratigraphic unit consisting predominantly of large green silicate granules set in a matrix of white, fine-grained chert, diagenetically modified in places by patches and mottles of ankerite (Fig. 3D). The anthraxolite from the Keewatin site (Figs. 3E and 3F) occurs as elliptical grains generally 3 mm to as much as 5 mm in diameter in the same stratigraphic unit. However, at this site the anthraxolite is indigenous to the iron-formation. The grains are set in a chert-rich matrix, in areas interstitial to large grains of diagenetic ankerite. Furthermore, fractured grains are filled with euhedral ankerite, carbonate, and some quartz. The textural relationships imply that the anthraxolite was solidified and fractured early in the diagenetic history of the rock.

At the Hoyt Lakes site, anthraxolite also is an indigenous component of the iron-formation and occurs in a somewhat recrystallized and coarsened chert-rich matrix that also contains small grains of cummingtonite and grunerite. The individual anthraxolite grains have an irregular outline (Fig. 3G) that apparently formed as the matrix was recrystallized, presumably under low-grade metamorphic conditions.

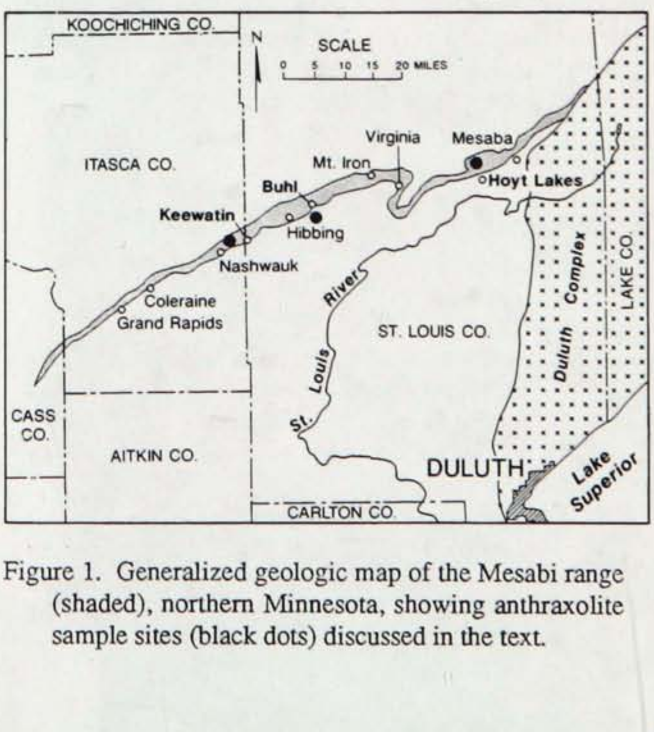

Figure 1. Generalized geologic map of the Mesabi range (shaded), northern Minnesota, showing anthraxolite sample sites (black dots) discussed in the text.

Physical properties are summarized in Table 1. These properties are remarkably constant from sample to sample. In addition, these properties are very much like those described for other anthraxolitic material as characterized over the years by Coleman (1928), Dietrich (1956), and Runnells (1965).

In an attempt to further characterize some of the physical aspects of anthraxolite from the Biwabik Iron Formation, each sample was ground to -200 mesh, mounted on a glass slide with a water slurry, and X-rayed with a Norelco diffractometer using CuKα radiation and a nickel filter. The patterns (Fig. 4) obtained are characterized by a low-angle intensity maximum, a broad peak with its highest point at approximately d = 3.56 Å (2θ = 25°), and several minor peaks in the region between d = 2.04 Å and d = 2.06 Å (2θ = 42° to 44°). Such patterns are indicative of amorphous organic material and suggestive of asphaltic material (French, 1964). Anthraxolite from other localities, as well as anthracite and semi-anthracite coal, give similar diffractograms (Dietrich, 1956, p. 655), as does carbonaceous material from samples of Biwabik Iron Formation collected from the outer part of the metamorphic aurole of the Duluth Complex (French, 1968, p. 70).

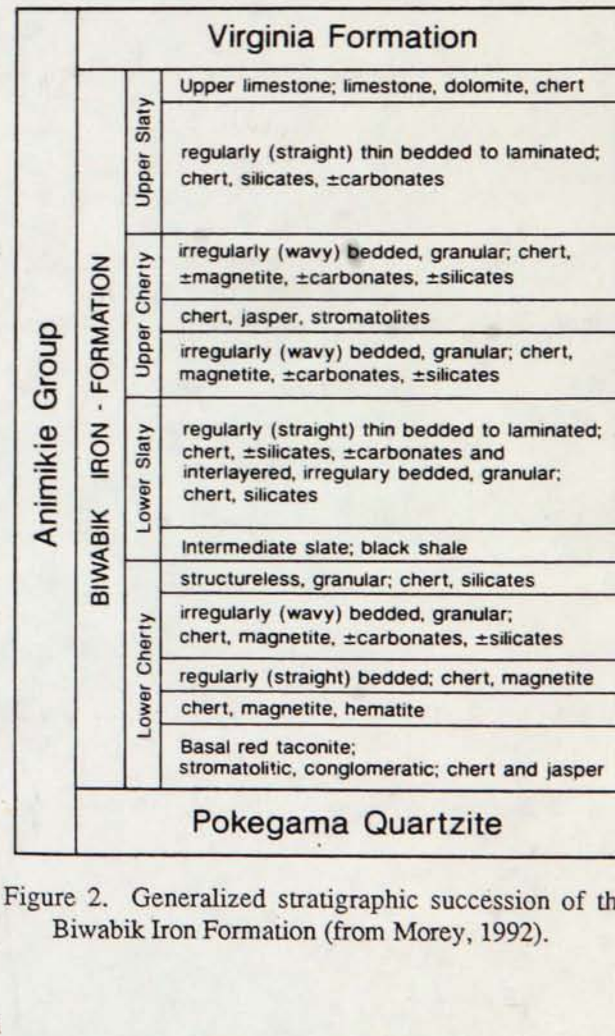

Figure 2. Generalized stratigraphic succession of the Biwabik Iron Formation (from Morey, 1992).

Differential thermal analyses also were performed with material ground to -100 mesh and heated in open and covered containers to approximately 1,040°C in a three-point thermocouple system attached to two X-Y recorders (Fig. 5). A heating rate of approximately 10°C/minute was used between 50° and 1,040°C. No differences between the open and covered experiments were detected. The results obtained from the Biwabik anthraxolites were very similar to those obtained from other anthraxolites (Dietrich, 1956, p. 658) and generally reflect devolatilization reactions and graphitization. The only notable difference was the temperature at which the first major exothermic devolatilization reaction occurs. This reaction occurs at 550°C to 600°C in the Biwabik samples, whereas it occurs at 480°C to 530°C in the samples studied by Dietrich. A similar reaction occurs in the temperature range 420°C to 470°C in anthracite coals (Glass, 1954, p. 297). This relationship implies either that volatiles are more tightly attached in the Biwabik samples or that these samples contain much less volatile material. Sample material X-rayed after being heated to 1,100°C in covered containers during differential thermal analysis showed no structural changes other than slightly reduced peak heights on the diffractogams.

CHEMICAL PROPERTIES

Anthraxolites from the Biwabik Iron Formation have similar chemical attributes (Table 1), which are broadly similar to those associated with anthraxolite from the type locality at Sudbury, as well as to analogous substances from elsewhere in the United States, Canada, and the former USSR.

Some anthraxolite from the Thunder Bay area has been reported to be slightly radioactive and nickeliferous (Ellsworth, 1934), but the Biwabik anthraxolite showed no anomalous radioactivity. Samples from Buhl and Hoyt Lakes were analyzed spectrographically to determine the presence of metallic elements present in trace amounts. The elements in Group I of Table 1 are major constituents of the iron-formation and may well reflect contamination, even though the samples analyzed were hand-picked for purity under a binocular microscope. In contrast, the elements in Group II occur only in trace quantities in the Biwabik Iron Formation and therefore presumably could either represent contamination or constituents indigenous to the anthraxolite. However, other elements potentially associated with natural bitumens in general, such as V, Be, Co, Ag, Sn, Ge, In, Ga, Pb, Cr, Ba, and Sc, were specifically sought, but not detected.

Little has been done regarding the organic geochemical attributes of the Biwabik anthraxolite. However, in a study of material from the Buhl site, trace quantities ($<1.0 \times 10^{-9}$ moles/grain) of the amino acids serine and glycine were found in one of several samples analyzed by Niehaus (1969) and Niehaus and Swain (1972). No particular conclusion was drawn from these results.

DISCUSSION

The Biwabik anthraxolite is characterized by a large fixed-carbon content and a relatively small proportion of hydrocarbon compounds, as shown by its low volatile content, hydrogen/carbon values of less than unity, and insolubility in carbon disulfide. As such it is one of a large number of solid bitumens of variable color and hardness composed principally of the elements carbon and hydrogen, but having subordinate sulfur, oxygen, nitrogen, and trace amounts of various metals, especially iron and nickel, in the carbon network (Yen, 1984). Various origins have been suggested for these materials, ranging from thermally immature to thermally postmature crude oil, and including several stages of possible alteration (e.g., devolatilization, biodegradation) between these two extremes. Regardless of the specific details, there is a general consensus that solid bitumens are the alteration products of a once-liquid oil (Curiale, 1986).

Figure 3. Photographs and photomicrographs of anthraxolite from the Mesabi range.

A. Sample from Buhl, interval perpendicular to core axis, showing the vitreous luster and conchoidal fracture characteristic of anthraxolite from the Biwabik Iron Formation. The diameter of the core is about 6 cm (2-1/8 inches).
B. Buhl material parallel to core axis, showing the fractured nature of anthraxolite enclosed in a vein of quartz and calcite.
C. Same as Figure 3B rotated 90° in a counterclockwise direction.
D. Rounded grains of anthraxolite from the Buhl site in transmitted light. Note that the grains are set in a matrix of ankerite and chert.
E. Rounded grains of anthraxolite from the Keewatin site in reflected light.
F. Enlargement of part of Figure 3E.
G. Anthraxolite from the Hoyt Lakes site in transmitted light. Note the recrystallized nature of the matrix and the irregular outlines of anthraxolite grains.

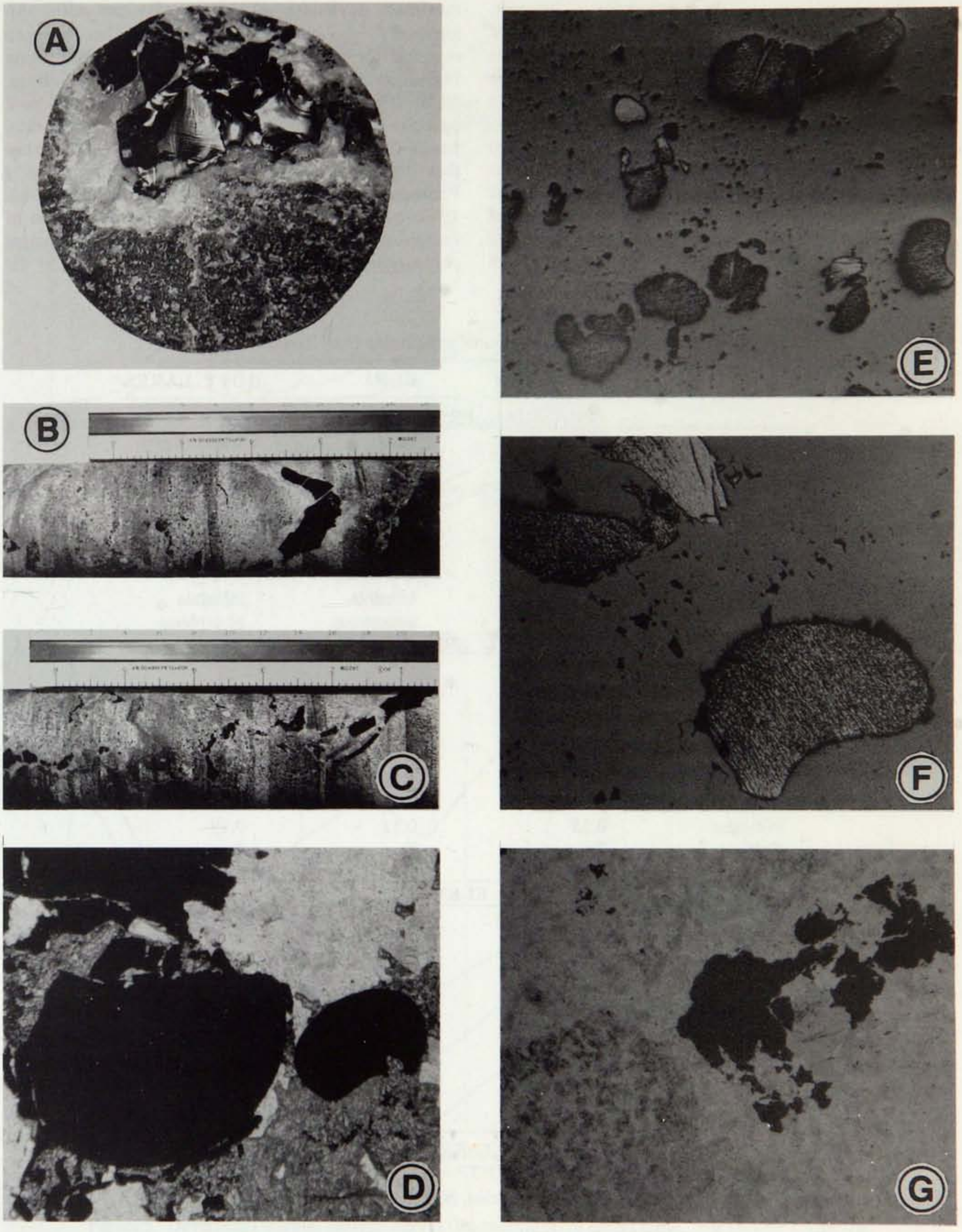
A
B
C
D
E
F
G

The spherical shapes in the Buhl sample, in particular, imply that the anthraxolite or its precursor was a liquid that migrated from some organic-rich source bed to its present location, although the identity of that source bed is problematic. However, the Biwabik Iron Formation contains measurable quantities of carbonaceous material, mostly as reduced carbon. It averages about 0.20% reduced carbon overall (Lepp, 1966), and Gruner (1946) reported as much as 3.20% reduced carbon in the lower part of the Intermediate slate. Perry and others (1978) reported that six samples of reduced carbon from two cores—including Buhl—had an average δ^{-13} value of -33.1 per mill, with maximum deviations of -1.4 to +2.4 per mill. An identical δ^{-13} value of -31.3 per mill also has been reported for reduced carbon from the Gunflint Iron Formation in the Thunder Bay area (Smith and others, 1970). This evidence, together with the presence of fossil proalgae and budding bacteria and a variety of chemical fossils (Darby, 1972; Swain and others, 1976), indicates that organic life was well established in the Early Proterozoic seas in Biwabik time. Indeed Cloud (1983, 1988) has championed the idea that the deposition of Proterozoic iron-formation was enhanced by proalgal photosynthetic activity in shallow water, and also by the

Table 1. Physical and chemical properties of anthraxolite from Biwabik Iron Formation

		KEEWATIN	BUHL	HOYT LAKES
		PHYSICAL PROPERTIES		
Color		black	black	very dark gray
Color transmitted light		golden brown	golden brown	golden brown
Hardness		3.2	3.0	3.5
Luster		vitreous	vitreous	dull
Fracture		conchoidal	conchoidal	conchoidal
Streak		black	black	black
Specific gravity		1.79 ± .07	1.75 ± .03	1.78 ± .03
Fusibility		infusible	infusible	infusible
Crystal form		amorphous	amorphous	amorphous
		CHEMICAL PROPERTIES		
Solubility				
Carbon disulfide		insoluble	insoluble	insoluble
Chloroform		insoluble	insoluble	insoluble
Composition (%)[1]				
Carbon		96.35	95.21	96.60
Hydrogen		1.01	1.59	0.79
Oxygen		1.29	1.89	1.42
Nitrogen		0.35	0.31	0.19
Sulfur		Tr	Tr	Tr
Ash		Tr	Tr	n.d.
		TRACE ELEMENTS[2]		
Si		-	1.	2.
Al		-	.2	.2
Fe		-	.2	2.
Mn	Group I	-	.03	.5
Mg		-	.1	1.
Ca		-	.2	3.
Ni		-	.04	.08
Ti		-	.002	.01
Cu	Group II	-	<.0002	.002
Sr		-	<.001	.01

1. Analyses by microanalytic laboratory, University of Minnesota, February 1968. Tr, trace; n.d., not detected.
2. Analyses in ppm; written communication, N.H. Suhs, Pennsylvania State University, July 1968.

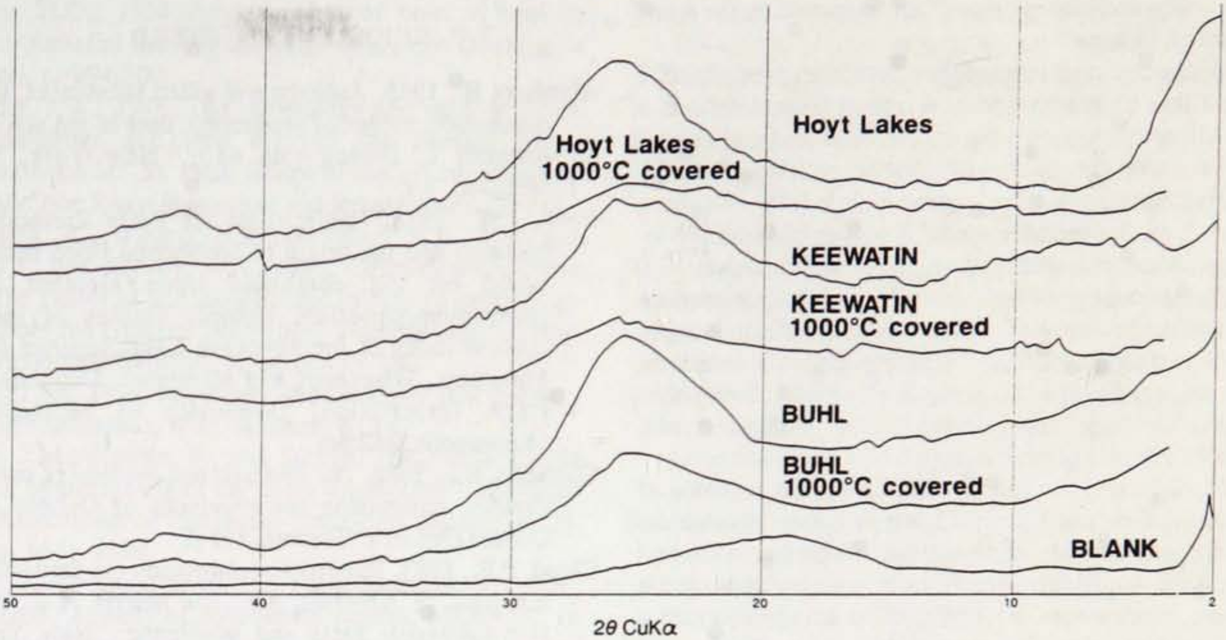

Figure 4. X-ray diffraction patterns of anthraxolite. See text for discussion.

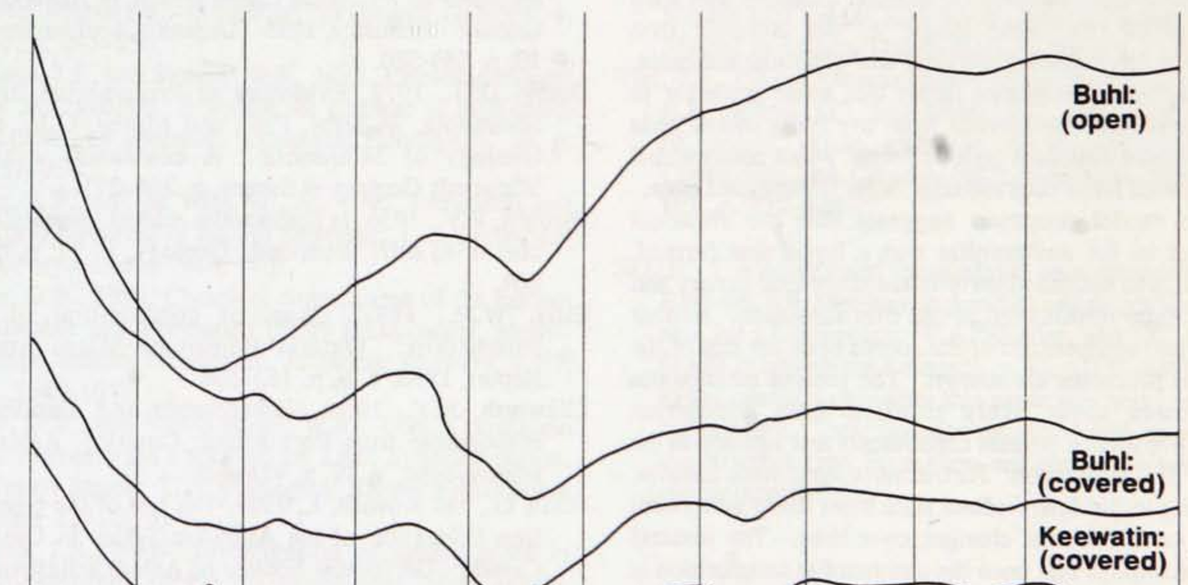

Figure 5. Differential thermal analysis curves (thermograms) of anthraxolite. See text for discussion.

decay on the seafloor of organic debris formed by the death of proalgal blooms.

Inasmuch as the Intermediate slate is an ash-fall tuff, I suggest that its present reduced carbon content reflects a mass-kill phenomenon where tuffaceous material caused the catastrophic death of proalgae living in the photosynthetic zone. The organic debris from that event collected on the seafloor where it was quickly buried by tuffaceous material settling through the water column.

The abundance of reduced carbon in the Intermediate slate and the presence of anthraxolite just beneath it imply that the two are interrelated. This implication is consistent with the suggestion of King and others (1963) that anthraxolite is generally found closely associated with primary cemented organic material.

Three inferences can be made from the presence of anthraxolite in the Lower Cherty member beneath its potential source bed: (1) the liquid oil precursor formed early in the diagenetic history of the iron-formation, and it or some intermediate precursor of the anthraxolite had a specific gravity somewhat greater than unity; (2) it moved and solidified well before the enclosing sediments were completely lithified; and (3) once solidified, the precursor material must have been sufficiently rigid to retain its original shape in spite of subsequent metamorphism.

CONCLUSION

Anthraxolite samples from three localities that span 80 miles of the strike length of the Biwabik Iron Formation have similar physical and chemical attributes. Stratigraphic relationships imply that some precursor to the anthraxolite was derived from overlying source beds that contained abundant organic debris, which accumulated together with tuffaceous material in the Intermediate slate.

The model proposed suggests that the chemical precursor to the anthraxolite was a liquid that formed, migrated, and solidified early in the diagenetic history and prior to final lithification of the iron-formation. Neither the original composition of the source beds nor that of the chemical precursor are known. The present anthraxolite composition most likely resulted from concurrent progressive loss of volatile constituents and increase in the amount of fixed carbon. Furthermore syngenetic material remaining in the Intermediate slate most likely underwent similar compositional changes over time. The textural evidence implies that once the anthraxolite composition is achieved, it is relatively stable over a long period of time and a wide range of temperature. Therefore processes leading to the development of anthraxolite in Early Proterozoic time are analogous to those that produced crude oils and associated bitumens in more modern sedimentary sequences.

REFERENCES CITED

Abraham, H., 1945, Asphalts and allied substances, their occurrence, modes of production, uses in the arts and methods of testing (5th ed.): New York, Van Nostrand, 2 v.

Beck, J.W., 1988, Implications for Early Proterozoic tectonics and the origin of continental flood basalts, based on the combined trace element and neodymium/strontium isotopic studies of mafic igneous rocks of the Penokean Lake Superior belt, Minnesota, Wisconsin, and Michigan: Unpublished Ph.D. dissertation, University of Minnesota, Minneapolis, 262 p.

Chapman, E.J., 1888, The minerals and geology of central Canada, comprising the provinces of Ontario and Quebec (3rd ed.): Toronto, 371 p.

Cloud, P.E., 1983, Banded iron-formation—a gradualist's dilemma, *in* Trendall, A.F., and Morris, R.C., eds., Iron-formation facts and problems: New York, Elsevier, p. 401-416.

_____1988, Oasis in space—earth history from the beginning: New York, W.W. Norton, 508 p.

Coleman, A.P., 1928, The anthraxolite of Sudbury: American Journal of Science, 5th ser., v. 15, p. 25–27.

Curiale, J.A., 1986, Origin of solid bitumens, with emphasis on biological matter results, *in* Advances in Organic Chemistry, 1985: Organic Geochemistry, v. 10, p. 559-580.

Darby, D.G., 1972, Evidences of Precambrian life in Minnesota, *in* Sims, P.K., and Morey, G.B., eds., Geology of Minnesota: A centennial volume: Minnesota Geological Survey, p. 264–271.

Dietrich, R.V., 1956, Is anthraxolite related genetically to coal or to oil?: Economic Geology, v. 51, p. 649–664.

Ellis, W.H., 1897, Chemical composition of the anthraxolite: Ontario Bureau of Mines Annual Report, 1896, v. 6, p. 162–166.

Ellsworth, H.V., 1934, Nickeliferous and uraniferous anthraxolite from Port Arthur, Ontario: American Mineralogist, v. 19, p. 426–428.

Faure, G., and Kovach, J., 1969, The age of the Gunflint Iron Formation of the Animikie Series in Ontario, Canada: Geological Society of America Bulletin, v. 80, p. 1725–1736.

French, B.M., 1964, Graphitization of organic material in a progressively metamorphosed Precambrian iron formation: Science, v. 146, p. 917–918.

_____1968, Progressive contact metamorphism of the Biwabik Iron-formation, Mesabi range, Minnesota: Minnesota Geological Survey Bulletin 45, 103 p.

Glass, H.D., 1954, Investigation of rank in coal by differential thermal analysis: Economic Geology, v. 49, p. 294-309.

Gruner, J.W., 1946, The mineralogy and geology of the taconites and iron ores of the Mesabi range, Minnesota: St. Paul, Office of the Commissioner of the Iron Range Resources and Rehabilitation, 127 p.

Hayatsu, R., Winans, R.E., Newman, D.E., Mancuso, J.J., and Seavoy, R.E., 1983, Correlations between the chemical and the geologic origins of anthraxolite from the Gunflint Formation, Thunder Bay, Ontario: Economic Geology, v. 78, p. 175–180.

Hunt, J.M., 1979, Petroleum geochemistry and geology: San Francisco, W.H. Freeman, 617 p.

Hunt, J.M., Stewart, F., and Dicken, P.A., 1954, Origin of hydrocarbons of the Uinta Basin, Utah: American Association of Petroleum Geologists Bulletin, v. 38, p. 1671–1698.

King, L.H., Goodspeed, F.E., and Montgomery, D.S., 1963, A study of sedimented organic matter and its natural derivatives: Canada Department of Mines and Technical Surveys, Mines Branch Research Report R114, 68 p.

Kwiatkowski, D., 1975, The geology and geochemistry of the Kakabeka Falls anthraxolite: Unpublished master's thesis, Lakehead University, Thunder Bay, Ontario, 103 p.

Lepp, H., 1966, Chemical composition of the Biwabik Iron Formation, Minnesota: Economic Geology, v. 61, p. 243–250.

Mancuso, J.J., and Seavoy, R.E., 1981, Precambrian coal or anthraxolite: A source for graphite in high-grade schists and gneisses: Economic Geology, v. 76, p. 951–954.

Meyer, R.F., and de Witt, W., Jr., 1990, Definition and world resources of natural bitumens: U.S. Geological Survey Bulletin 1944, 14 p.

Morey, G.B., 1992, Chemical composition of the eastern Biwabik Iron-Formation (Early Proterozoic), Mesabi range, eastern Minnesota: Economic Geology, v. 87, p. 1649-1658.

Morey, G.B., and Van Schmus, W.R., 1988, Correlation of Precambrian rocks of the Lake Superior region, United States: U.S. Geological Survey Professional Paper 1241-F, 31 p.

Niehaus, J.R., 1969, Investigation of amino acids in Precambrian rocks: Unpublished M.S. thesis, University of Minnesota, Minneapolis, 75 p.

Niehaus, J.R., and Swain, F.M., Jr., 1972, Amino acids in some Middle Precambrian rocks of northern Minnesota and southern Ontario, *in* Sims, P.K., and Morey, G.B., eds., Geology of Minnesota: A centennial volume: Minnesota Geological Survey, p. 272–277.

Perry, E.C., Jr., 1983, Part C. Oxygen isotope geochemistry of iron-formation, *in* Trendall, A.F., and Morris, R.C., eds., Iron-formation facts and problems: Amsterdam, Elsevier, p. 359-371.

Perry, E.C., Jr., Tan, F.C., and Morey, G.B., 1973, Geology and stable isotope geochemistry of the Biwabik Iron Formation, northern Minnesota: Economic Geology, v. 68, p. 1110-1125.

Runnells, D.D., 1965, Anthraxolite derived from indigenous organic matter in Middle Devonian dolomite, Cosmos Hills, Alaska: Journal of Sedimentary Petrology, v. 35, p. 599–603.

Smith, J.W., Schapf, J.W., and Kaplan, I.R., 1970, Extractable organic matter in Precambrian cherts: Geochimica et Cosmochimica Acta, v. 34, p. 659-675.

Southwick, D.L., and Day, W.C., 1983, Geology and petrology of Proterozoic mafic dikes, north-central Minnesota and western Ontario: Canadian Journal of Earth Sciences, v. 20, p. 622-638.

Swain, F.M., Jr., Baysinger, J., and Bratt, J.M., 1976, Hydrocarbons obtained by pyrolysis of some Precambrian rocks of Minnesota: Origins of Life, v. 7, p. 239–257.

White, D.A., 1954, The stratigraphy and structure of the Mesabi range, Minnesota: Minnesota Geological Survey Bulletin 38, 92 p.

Wolff, J.F., 1917, Recent geologic developments on the Mesabi Iron Range, Minnesota: American Institute of Mining Engineers Transactions, v. 56, p. 142-169.

Yen, T.F., 1984, Characterization of heavy oils, *in* Meyer, R.F., Wynn, J.C., and Olson, J.C., eds., The future of heavy crude and tar sands—International Conference, 2nd, Caracas, 1982: New York, McGraw-Hill, p. 412–423.

NOTE: The paper titled Precambrian vein pyrobitumens: Evidence for petroleum generation and migration 2 Ga ago, by J.J. Mancuso, W.A. Kneller, and J.C. Quick (1989, *Precambrian Research*, v. 44, p. 139-146) came to my attention only after this paper was being readied for printing. Their findings regarding anthraxolite in the Biwabik Iron Formation are consistent with the results reported here.

MANGANESE-RICH ONCOLITES IN THE BIWABIK IRON FORMATION, EVELETH MINE, MESABI IRON RANGE, MINNESOTA

By

A.M. Zielinski(1), J.J. Mancuso(2), J P. Frizado(2), and R.J. Waidler(3)

ABSTRACT

The middle part of the Upper Cherty member of the Biwabik Iron Formation on the Mesabi iron range in northern Minnesota is marked by a thin, but areally extensive, hematite-rich algal unit characterized by finger-sized algal stromatolites. However, in the main part of the range at the Eveleth South (formerly Thunderbird South) mine, the algal unit uniquely contains rhodochrosite-rich oncolites that range from <1 mm to 6 cm in long diameter. The oncolites most likely formed in a high-energy, oxygenated environment, such as a tidal channel, where strong surges prevented the algal and bacterial growths from becoming attached to the substrate. The original mineralogy was marked mainly by rhodochrosite, together with lesser amounts of siderite, magnetite, chert, hematite, and organic material. Chemical changes in the diagenetic environment resulted in the replacement of some carbonates by chert, the oxidation of ferrous iron to ferric iron, and the precipitation of hematite. Biogenic processes that can be attributed to the algae and bacteria that formed the oncolites most likely caused the high concentration of manganese carbonate in the algal unit at this location.

INTRODUCTION

The Early Proterozoic Animikie Group includes the Biwabik Iron Formation, the principal source of iron ore on the Mesabi range in northern Minnesota. Mineralogical, textural, and sedimentological attributes of the Biwabik Iron Formation have been studied in considerable detail (Gruner, 1946; White, 1954; Morey, 1972; Bayley and James, 1973; Morey, 1983; LaBerge and others, 1987), although original mineral compositions and paragenetic sequences are uncertain because of considerable diagenetic and postdiagenetic modifications.

Algal stromatolites are common primary depositional features in iron-formations and are well documented (Grout and Broderick, 1919; Gruner, 1922; Barghoorn and Tyler, 1965; Cloud and Licari, 1968; Darby, 1972; Lougheed, 1983; Walter and Hofmann, 1983). However, little documentation exists in the literature for the rhodochrosite-rich algal pisolites (oncolites) exposed in the relatively unaltered Upper Cherty member of the Biwabik Iron Formation in the Eveleth South mine near Eveleth, Minnesota. This paper presents the first description of these manganese-bearing minerals in unoxidized Biwabik strata (G.B. Morey, 1991, written communication).

GEOLOGIC SETTING

The Early Proterozoic tectonic framework in east-central and northern Minnesota is now envisioned by Southwick and Morey (1991) as the product of a collisional event—the Penokean orogeny of Goldich and others (1961)—between 1,900 and 1,760 Ma with most activity in the interval between 1,870 and 1,850 Ma (Morey and Van Schmus, 1988). In this view, the Penokean orogen—the zone of deformed rocks produced by the Penokean orogeny and earlier tectonic events in Early Proterozoic time—consists of an allochthonous fold-and-thrust belt that includes the Cuyuna iron range and contiguous areas to the south and east (Fig. 1). The fold-and-thrust belt contains several structural discontinuities that are probable zones of thrusting and that bound discrete structural panels or enclaves having small-scale structural features consistent with large-scale north-northwest-verging nappes. The belt of strongly deformed rocks flanks a tectonic foredeep which extends to the Mesabi range in northern Minnesota where rocks of the Animikie Group are exposed. Because the basin is filled with strata that can be assigned to the Animikie Group, Southwick and others (1988) have referred to the foredeep as the

(1) Engineering Science, Inc.
Buffalo, NY 14202

(2) Department of Geology
Bowling Green State University
Bowling Green, OH 43403

(3) Eveleth Mines
Eveleth, MN 55734

Animikie basin, a usage somewhat at odds with that in the earlier literature (e.g., Morey, 1983a). Correlative rocks underlie a much smaller area in far northeastern Minnesota and adjoining parts of Ontario where they comprise the Gunflint iron range.

Stratigraphy and Structure

The Animikie Group comprises a conformable sedimentary sequence which thickens to the south. On the Mesabi range, the group consists of three conformable units, the Pokegama Quartzite at the base, the Biwabik Iron Formation, and the overlying Virginia Formation (Fig. 2). The Pokegama Quartzite (about 150 feet thick at Eveleth) consists of a basal conglomerate overlain by shale and siltstone, which grades upward into sandstones and quartzite. Ojakangas (1983) concluded that this sequence is the result of transgression onto an Archean peneplain and subsequent deposition in subtidal and intertidal environments. The Biwabik Iron Formation (about 750 feet thick at Eveleth) consists of alternating cherty and slaty intervals believed by Ojakangas (1983) to represent environments of high and low energy, respectively. The terms "cherty" and "slaty" are descriptive, not morphological. "Slaty" refers to iron-formation that is dark, nongranular, and has a flaggy nature. "Cherty" refers to the blocky nature and granular texture of units, not to an increased chert content (Gruner, 1922). Beds or groups of beds having cherty or slaty attributes are interbedded on all scales in the iron-formation. Nonetheless, lithostratigraphic units that extend over long distances along the range can be recognized. Wolff (1917) was the first to divide the iron-formation into four major lithostratigraphic units which he referred to as "divisions." The cherty-slaty nomenclature has been retained as members—from bottom to top, (1) Lower cherty, (2) Lower slaty, (3) Upper cherty, and (4) Upper slaty. In general, stratigraphic units included in the slaty members contain 40 percent or more slaty strata, although locally less (White, 1954). The slaty strata characteristically contain sparse iron oxides, and the associated cherty beds commonly are silicate-rich. The cherty members, on the other hand, contain between 10 and 30 percent slaty strata; the cherty beds are rich in magnetite (or locally hematite), although they also contain abundant silicates or carbonates. The overlying Virginia Formation (>2,000 feet thick) is an orogenic turbidite deposit (Morey and others, 1989), which includes interbedded graywacke, siltstone, and shale or mudstone.

The gross structure of the Mesabi range is a gently dipping homocline that strikes east-northeast and dips 5° to 15° southeast. This general trend is interrupted by several noticeable bends in the Animikie strata. The most prominent of these structural features is the "Virginia Horn," a broad, gentle fold consisting of the southwest-plunging Virginia syncline and the parallel Eveleth anticline. The Eveleth South mine is located near the axis of the Eveleth anticline.

ALGAL UNIT IN THE EVELETH SOUTH MINE

Layers containing algal structures are common features in the Upper and Lower Cherty members in the Biwabik Iron Formation throughout the Mesabi range and in the equivalent stratigraphic level of the Gunflint Iron Formation on the Gunflint range. In the Gunflint Iron Formation, the algal structures range in size from reeflike mounds (Goodwin, 1956; Hoffmann, 1967) to finger-size algal stromatolites (Barghoorn and Tyler, 1965). In the Upper Cherty member of the Biwabik Iron Formation in the Mary Ellen mine and the Erie mine, east of the Eveleth mine, the algal structures are finger-size algal stromatolites (Fig. 3), which have the appearance of stacked, inverted thimbles (Grout and Broderick, 1919). Well-preserved coccoidal and filamentous algal microfossils have been found in algal stromatolites of the Biwabik and Gunflint Iron Formations (Lougheed, 1983; Cloud, 1972; LaBerge, 1973; Robbins and others, 1987). At the Eveleth South mine the algal structures are in the form of oncolites (Fig. 4), which range in size from less than 1 mm to more than 6 cm in long diameter.

The algal structures at the Eveleth South mine form part of an easily recognizable stratigraphic unit in the middle part of the Upper Cherty member of the Biwabik Iron Formation. The unit is 1.5 to 5 feet thick and appears to be a single sedimentation unit marked by a disconformable lower contact and a gradational upper contact. In addition to oncolites, the unit contains pisolites, oolites, and algal hash set in a groundmass of red and green chert. Irregular layers and lenses of green opaline chert occur at the extreme base of the algal unit, and pass gradationally upward into similar masses of red opaline chert. Bedding within the algal unit is defined by gradational changes in mineralogy and by indistinct erosional surfaces. The peloidal structures typically have long axes roughly parallel to bedding. Other primary sedimentary features include cross-bedding, graded bedding, soft-sediment deformation structures, pressure-solution textures, and desiccation cracks.

Red and green chert-rich parts of the algal unit have been extensively reworked. Syneresis cracks are prominent and have fragmented the red chert; these fragments form the nucleus of many oncolites. The unit contains numerous bedding-parallel slickenside surfaces and horizontal fractures; the latter are filled with secondary quartz and a pyrobitumen (Mancuso and others, 1989).

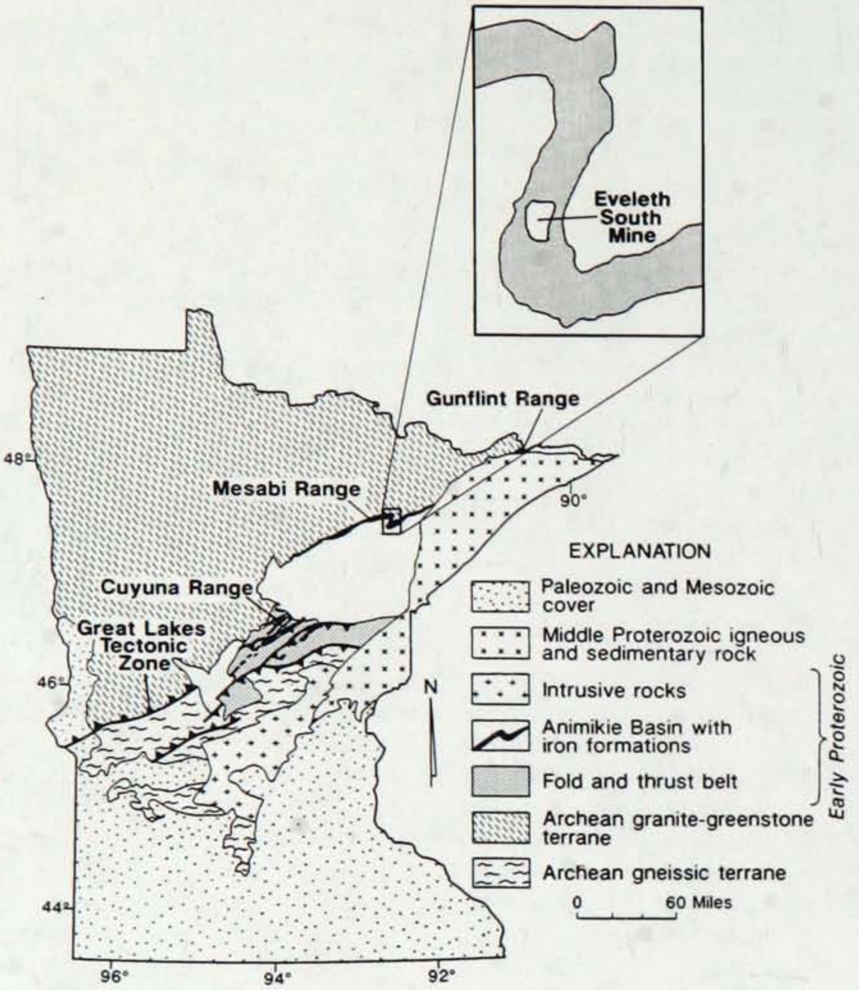

Figure 1. Locations of the Eveleth South (formerly Thunderbird South) mine and Minnesota iron ranges.

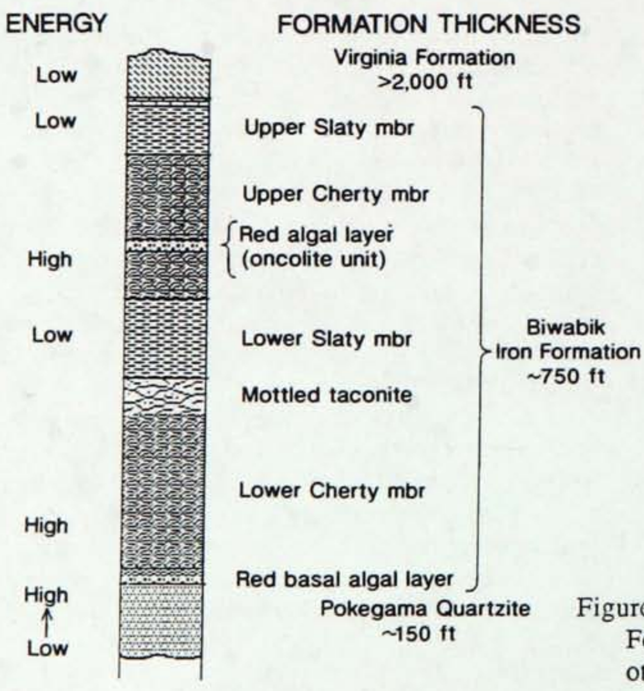

Figure 2. Stratigraphic section of the Biwabik Iron Formation at Eveleth (modified from Morey and others, 1989).

Physical Characteristics

Peloidal structures, including pisolites, oncolites, and oolites, typically have long axes roughly parallel to bedding. Oolites ranging in size from 0.5 mm to 2 mm in diameter are the most abundant peloidal structure in the algal unit. Those composed of chert and iron oxides have well-preserved concentric and radial fabrics. Those composed of carbonate minerals have been recrystallized, preserving no original structure.

The oncolites range in size from less than 1 mm to more than 6 cm in long diameter. In any given sample the number of oncolites decreases with an increase in size (Fig. 5). They range in shape from spherical and pear-shaped to ellipsoid or disk-shaped; their external shape typically mimics that of the core grain. Most of the oncolites larger than 2 mm in diameter are ellipsoid (Figs. 6, 7). In detail, the oncolites are composed of a core grain surrounded by concentric laminae that range in thickness from 0.01 mm to 0.1 mm. Fragments of red chert, green chert, broken pisolites, and detached layers of algal stromatolites form core grains for the oncolites (Figs. 6, 7). Some oncolites are markedly asymmetric in that laminae on one side are thicker than laminae on the opposite side. Many oncolites having this asymmetry have growths of small-scale finger algae on their thicker sides and oolites between the algal columns (Fig. 8). Other oncolites have erosionally truncated laminae overlain by complete laminae. In some samples, large oncolites incorporate small oncolites within their laminated fabric (Fig. 9).

Several generations of vein-filling materials occur within and cut across the oncolites. Some veins cut only the core grains, others cut the core grains and surrounding laminae, and some cut both the oncolites and surrounding matrix. Veins inside the core grains are shrinkage cracks filled with calcite and quartz. Larger veins are fractures related to postdepositional stresses that are filled with quartz and a hematite-stained carbonate.

Mineralogical and Chemical Characteristics

The algal unit is composed mineralogically of three distinct assemblages as determined by X-ray diffraction, energy-dispersive X-ray analysis, and optical microscopy (Fig. 10, Table 1). One heretofore unrecognized assemblage consists mainly of rhodochrosite with subordinate amounts of siderite, magnetite, hematite, organic material, and calcite. A second assemblage consists of manganese-rich siderite, chert, hematite, magnetite, and organic matter. A third assemblage consists mainly of red chert (jasper) and hematite. The first two assemblages have gradational paragenetic relationships, and a single oncolite may contain both

Table 1. Chemical analyses of mineral assemblages

Assemblage	1	2	3
SiO_2 (wt%)	9	11	77
Fe_2O_3	16	27	7
FeO	18	31	7
MnO	31	14	7
CaO	1	0	0
CO_2	25	18	2
Total	100	101	100

assemblages. The two differ principally by the presence of rhodochrosite and siderite in one assemblage and manganiferous siderite in the other. The third assemblage, which lacks carbonates, composes as much as 80 percent of the algal unit and replaces or cuts the first two assemblages.

Oncolites of the first mineral assemblage are composed mainly of rhodochrosite (Fig. 11 A-D) with laminations of organic material, magnetite, and hematite, which are subordinate to laminations of rhodochrosite in the oncolite shells (Fig. 12). Individual laminae may contain as much as 25 to 45% euhedral magnetite, which is only sparingly present in core grains (<1 to 5%). Individual laminae also contain hematite, but it is considerably less abundant (<1 to 35%) than magnetite. Chert (<1 to 10%) occurs as isolated patches throughout many oncolites, as does calcite (generally less than 4%). The matrix in the first assemblage is dominated by siderite, but euhedral magnetite is sparingly present (generally less than 5%), as are isolated patches of chert. The carbonates are recrystallized, as is shown by pronounced rhombohedral crystal forms.

Oncolites of the second mineral assemblage consist of alternating laminae of manganese-rich siderite and chert (Fig. 13). In these oncolites, hematite (15 to 30%) is restricted to the siderite-rich laminae. Organic matter is sparingly present (~15%) in siderite-rich laminae, but abundant (15 to 40%) in the chert-rich laminae. Magnetite (10 to 25%) in both kinds of laminae occurs as individual euhedra and as clusters of interlocking grains. It is somewhat coarser grained in the siderite-rich laminae. Recrystallization of the siderite lamellae obscures their fine-scale algal features. Such features are better preserved in chert and include fine laminae, stylolites, erosion surfaces, fractures (Fig. 14), and broken laminae. In fractures filled with siderite and hematite, the siderite is rhombohedral and extends beyond the walls of the fractures into the matrix. In contrast, in fractures filled with quartz, the quartz is confined within the walls of the fracture. Oncolites of the second mineral assemblage are set in a matrix of chert, anhedral quartz, which has replaced sparry calcite, and carbonate rhombohedrons that contain inclusions of pisolites or microspherules of uncertain derivation.

In the third mineral assemblage, both the oncolites and the matrix consist of red chert (jasper), hematite, and magnetite. In the oncolites, chert (75%) occurs as microlaminae alternating with laminae composed of hematite, fine-grained magnetite, and manganese oxides (Fig. 15). Carbonate minerals occur as rare (less than 1%), fine-grained inclusions in chert. Radiating crystals of minnesotaite are present in trace amounts (less than 1%) in the red chert matrix.

DISCUSSION

Questions raised by the presence of rhodochrosite-bearing oncolites in the algal layer in the Upper Cherty member of the Biwabik Iron Formation include: (1) the nature of the depositional environment in which iron-formation in general and the algal layer in particular accumulated; (2) the nature of the tectonic framework and how it may have influenced the depositional environment; (3) the nature of the processes that led to the separation of iron and manganese and concentrated rhodochrosite in the algal layer; and (4) the nature of the processes that led to the observed mineral paragenesis.

Tectonic Models

Specific tectonic settings not only influenced the physical placement of iron-rich strata, but also influenced chemical and physical attributes of specific deposits. Following the ideas of many previous authors, Schulz and Ojakangas (1989) expanded on a depositional model where iron-rich strata were deposited on a shelf below low-tide level, whereas quartz-rich strata like those in the Pokegama Quartzite were deposited in a shoreward, supratidal environment, and pelagic muds like those in the Virginia Formation were deposited on the slope outboard of the shelf. Thus units of cherty iron-formation were deposited in a shallow-water, agitated environment, and units of slaty iron-formation were deposited in deeper, less active, and possibly more reducing waters. In the model, the interlayering of cherty and slaty strata reflects repeated transgressive and regressive events, possibly related to the tectonic development of the foredeep basin.

Paragenesis

Following the model of Schulz and Ojakangas (1989), we infer that the Upper Cherty member was most likely deposited on a shallow shelf under regressive conditions, when the depositional environment changed from deep water to shallow water, and the oxygen content throughout the water column increased because of more complete mixing with atmospheric oxygen and photosynthesis by algae (Schopf, 1983). Increased oxygen led to an increase in ferric iron and the transition from gray and green cherty layers in "ordinary" iron-formation to red chert in the algal layer. We also infer that the sediments in that transition zone, possibly a shallow tidal channel, were reworked locally to fragment the red chert and produce an algal hash, fragments of which served as nuclei for oncolites now found at the Eveleth South mine. Last, we also infer that mineral assemblage one, consisting of rhodochrosite and subordinate siderite, is a primary assemblage which was stable in the pH range inferred for seawater in Early Proterozoic time (Schopf, 1983). A slight lowering of the pH would have led to the dissolution of rhodochrosite and siderite, and the free oxygen would have destroyed organic material and led to the precipitation of iron and manganese oxides. The new chemical environment would also be optimal for the precipitation of silica and replacement of carbonate minerals by chert, i.e., mineral assemblage three. Mineral assemblage two, which is most restricted, most likely formed in an environment where oxidation and replacement by silica were incomplete.

Separation of Iron and Manganese

Separation of iron and manganese in iron-formations is problematic but may be explained as a result of several processes. Morey and Southwick (1993) and Morey and others (1991) proposed an epigenetic origin for manganiferous zones in the Emily district of the Cuyuna iron range. They suggested that manganese oxides were deposited by a refluxing process where manganese was leached from older rocks of the North Range Group by reducing solutions that were subsequently oxidized just below the sediment-water interface. Along similar lines, Sugisaki and others (1991) suggested that manganese-rich pore fluids with a low Eh will migrate upward during sediment compaction and precipitate manganese dioxide at the sediment-water interface where higher Eh conditions are encountered. However, neither of these processes applies to the Upper Cherty algal unit, because the manganese there was precipitated as a primary carbonate phase.

The presence of rhodochrosite and siderite as primary phases suggests that iron and manganese were chemically separated during deposition. Krauskopf (1979) and Sugisaki and others (1991) have suggested several possible ways in which that may occur. Krauskopf (1979) concluded that manganese and iron may be naturally separated if the pH of a solution that contains both is slowly increased, because iron will reach the solubility limit before manganese and will precipitate as either a ferric oxide or an iron carbonate, depending on the chemical potential and concentrations of iron, carbon dioxide, and oxygen. The two phases also may separate because of

Figure 3. Hand specimen from the Upper Cherty member at the Mary Ellen mine, Minnesota, showing finger-like algal stromatolites. Scale in millimeters.

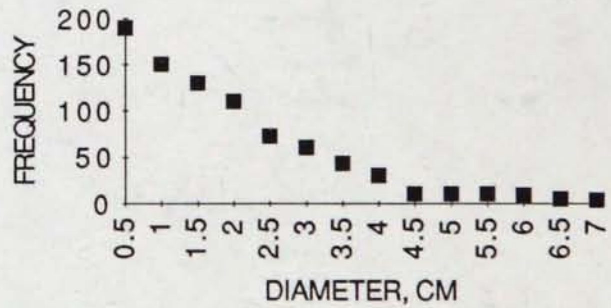

Figure 5. Graph illustrating decrease in frequency of oncolites with increase in size.

Figure 4. Hand specimen showing oncolites from the Upper Cherty member of the Biwabik Iron Formation at the Eveleth South mine, Minnesota. Scale in millimeters.

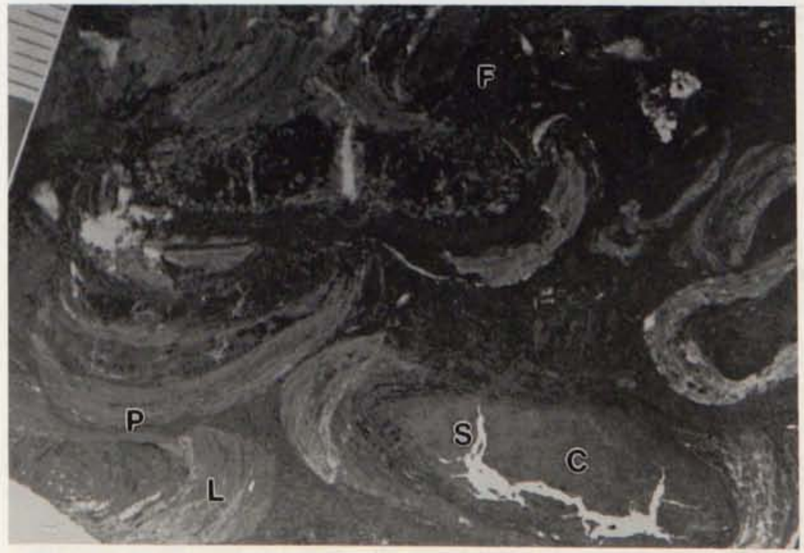

Figure 6. Hand specimen showing disk-shaped oncolites with nuclei of red chert (C), algal laminae (L), and a shrinkage crack (S) filled with calcite in a nucleus. Fragmented oncolites are also present (F), as is evidence of pressure solution (P). Scale in millimeters.

Figure 7. Photomicrograph showing portion of large oncolite as well as several smaller oncolites and pisolites. Bar is 0.5 mm.

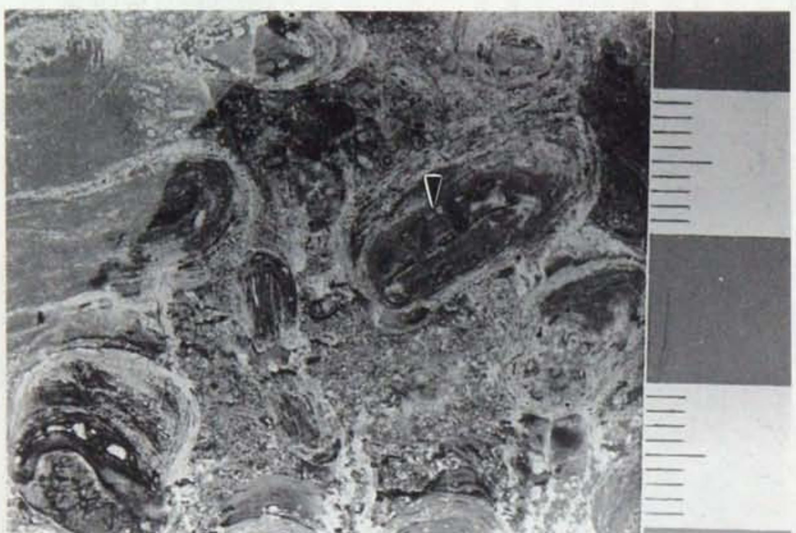

Figure 8. Hand specimen showing finger-type algal growth (arrow) on one side of the oncolite. Scale in millimeters.

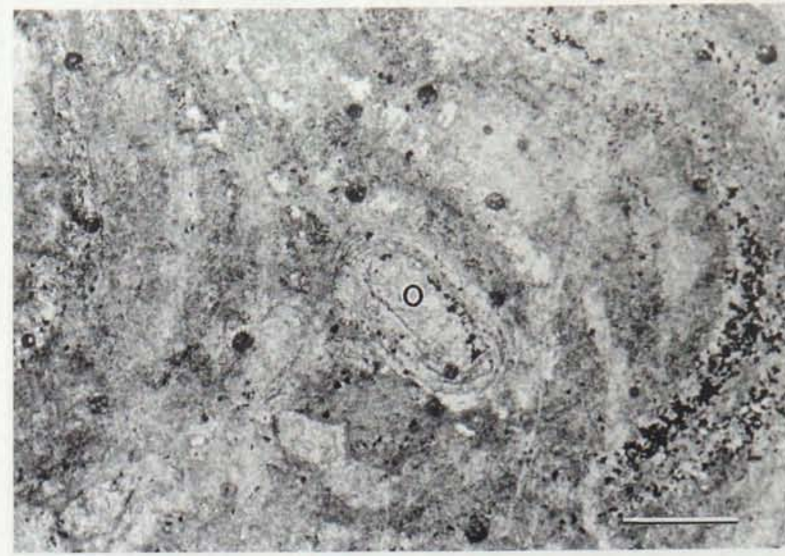

Figure 9. Photomicrograph showing smaller oncolite (O) incorporated between laminae of larger oncolite. Bar is 0.5 mm.

Figure 10. Hand specimen showing the three mineral assemblages: (1) rhodochrosite and siderite, (2) siderite and chert, and (3) mostly red chert (jasper). Bar is 1 cm.

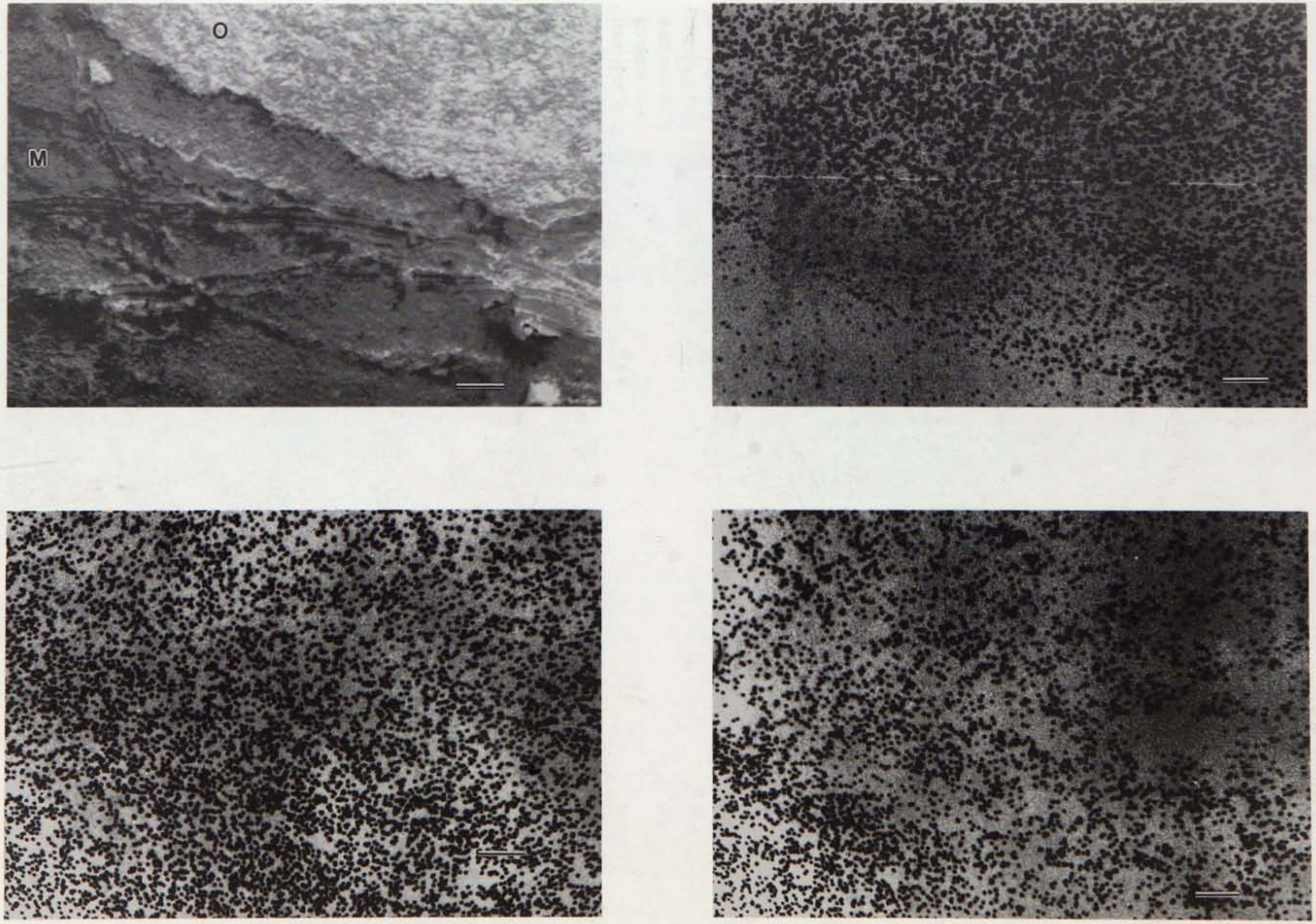

Figure 11. Photomicrograph and energy-dispersive X-ray dot maps of same area (bar, 0.05 mm).
(**A**) Part of oncolite (O) of mineral assemblage one and matrix (M). (**B**) FeKα dot image. (**C**) MnKα image. (**D**) SiKα image.

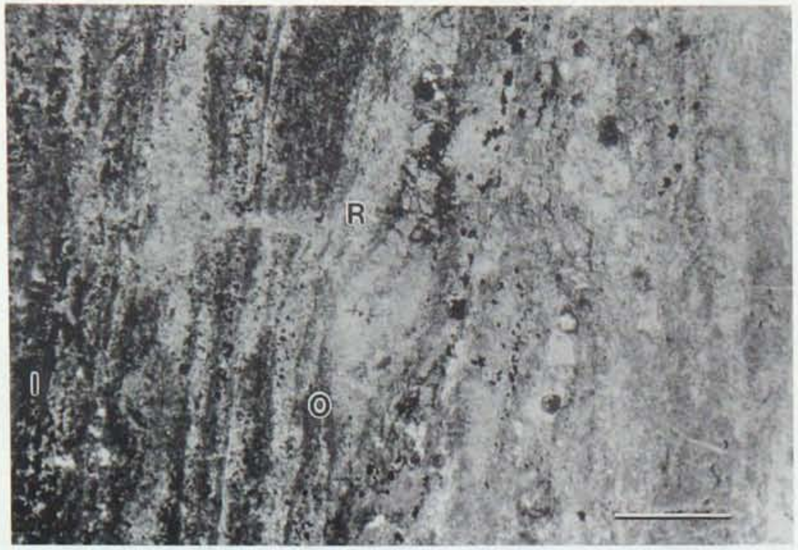

Figure 12. Photomicrograph showing algal laminae of assemblage one, consisting of alternating rhodochrosite (R), organic material (O), and magnetite and hematite (I). Bar is 0.5 mm.

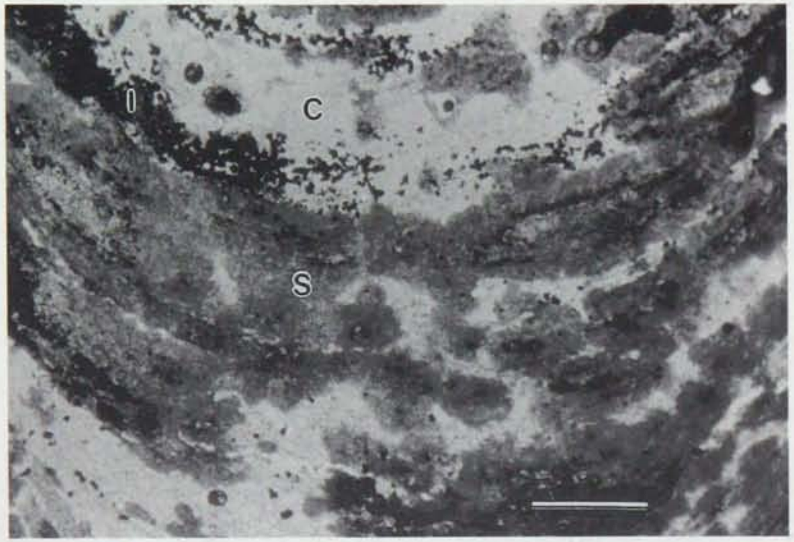

Figure 13. Photomicrograph of oncolite composed of mineral assemblage two showing alternating siderite (S), chert (C), and iron oxides (hematite and euhedral magnetite) (I). Bar is 0.5 mm.

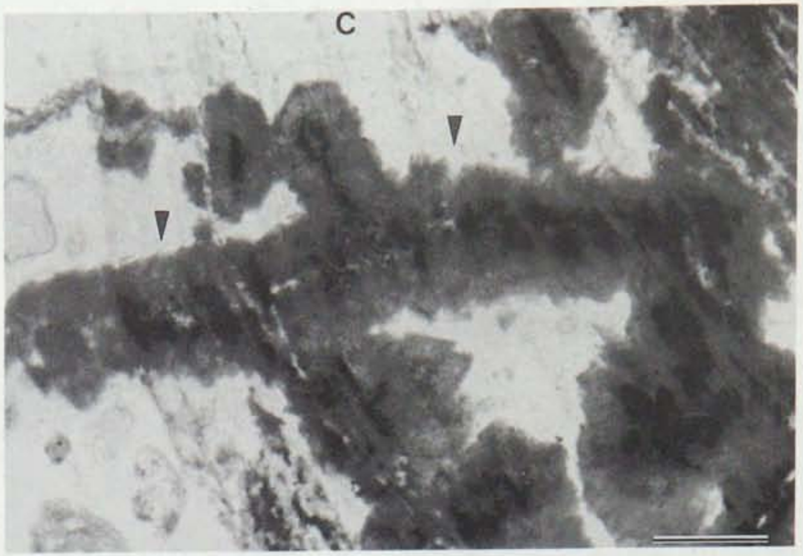

Figure 14. Photomicrograph showing late-stage carbonate along fracture (arrows) crossing white chert (C) in matrix and laminae. Bar is 0.5 mm.

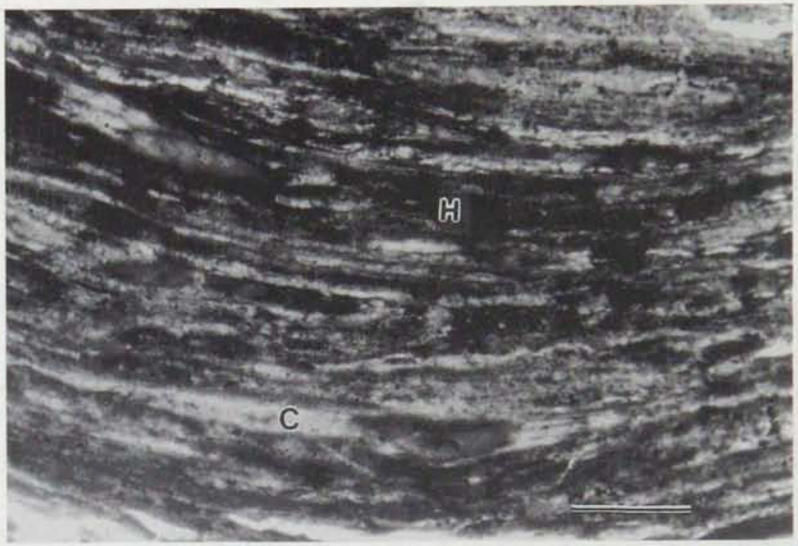

Figure 15. Photomicrograph of oncolite composed of mineral assemblage three; laminae of chert (C), interlayered with laminae of admixed hematite and manganese oxides (H). Bar is 0.5 mm.

differences in the oxidation potential of iron and manganese (Krauskopf, 1979). When iron and manganese are carried to the sea, manganese is less readily oxidized than iron in the presence of organic matter and would remain in solution for a longer time. However, because iron was an abundant constituent in Early Proterozoic seawater and because rhodochrosite is present in shallow-water, siderite-rich, red, oxidized algal sediments, these purely chemical scenarios seem to be unlikely explanations to account for the rhodochrosite in the algal unit.

Biogenic activity by algae and bacteria seems a more plausible explanation for the rhodochrosite. Precambrian species of algae and bacteria, like some modern forms, utilized manganese in their metabolic processes (Krauskopf, 1979; Ehrlich, 1981; Baturin, 1988). Modern algal structures, including stromatolites and oncolites, are composed of successive mats of coccoidal and filamentous algae which precipitate carbonate and trap and bind sediment in successive layers or laminae. It is likely that Precambrian stromatolites and oncolites formed in a similar manner (Barghoorn and Tyler, 1965; Hoffman, 1967; Cloud and Licari, 1968; Gebelein, 1969; Darby, 1972; Lougheed, 1983), although there is little evidence that the Precambrian organisms trapped particulate matter. It is more likely that the structures in the Biwabik and Gunflint Iron Formations formed by the precipitation of successive layers of carbonate (Darby, 1972). Many modern micro-organisms utilize cations, such as carbon, iron, and in this case, manganese, to remove free oxygen generated by metabolic processes. Combined iron, carbon, and oxygen or combined manganese, carbon, and oxygen, under appropriate chemical conditions, can then precipitate as siderite or rhodochrosite as part of the metabolic process.

The presence of rhodochrosite as a discrete phase in these circumstances requires that manganese be concentrated at values much above normal background levels. It is well established that certain modern microbial organisms concentrate manganese (Cloud and Licari, 1968; Walter, 1977; Sugisaki and others, 1991), in some cases to levels as much as 2,000 times greater than that of the surrounding environment (Baturin, 1988). Furthermore, organisms that directly precipitate rhodochrosite have been noted in modern anoxic pore waters (Holdren, 1977). Lastly, certain organisms known to concentrate manganese as well as iron, such as *Metallogenium personatum*, have been found in oncolites of the Early Proterozoic Frere Formation of the Nabberu basin in Australia where a microbiota similar to that of the Biwabik and Gunflint Iron Formations has been described (Walter and others, 1976; Walter, 1977).

CONCLUSIONS

Oncolites in the Upper Cherty member exposed in the Eveleth South mine were similar in origin to algal stromatolites found elsewhere in the Biwabik and Gunflint Iron Formations, but were mobile rather than attached to a substrate; most likely they formed in a shallow tidal channel. The oncolites had an original mineral composition consisting mainly of rhodochrosite with lesser amounts of siderite, magnetite, chert, hematite, and organic material. Biogenic processes, which can be attributed to the algae and bacteria that formed the oncolites, most likely caused the high concentrations of manganese now found as rhodochrosite. Chemical changes in the diagenetic environment resulted in replacement of manganese and iron carbonate by chert and caused the oxidation of ferrous to ferric iron and the precipitation of hematite.

ACKNOWLEDGMENTS

Financial support for this project was provided by the Graduate College and the Department of Geology at Bowling Green State University.

REFERENCES CITED

Barghoorn, E.S., and Tyler, S.A., 1965, Microorganisms from the Gunflint chert: Science, v. 147, p. 563-577.

Baturin, G.N., 1988, The geochemistry of manganese and manganese nodules in the ocean: D. Reidel, 342 p.

Bayley, R.W., and James, H.L., 1973, Precambrian iron-formations of the United States: Economic Geology, v. 68, p. 934-959.

Cloud, P.E., Jr., 1972, A working model of the primitive earth: American Journal of Science, v. 272, p. 537-548.

Cloud, P.E., Jr., and Licari, G.R., 1968, Microbiotas of the banded iron-formations: National Academy of Science Proceedings, v. 61, p. 779-786.

Darby, D.G., 1972, Evidences of Precambrian life in Minnesota, *in* Sims, P.K., and Morey, G.B., eds., The geology of Minnesota: A centennial volume: Minnesota Geological Survey, p. 264-271.

Ehrlich, H.L., 1981, Geomicrobiology: New York, M. Dekker, 393 p.

Gebelein, C.D., 1969, Distribution, morphology, and accretion rate of recent subtidal algal stromatolites, Bermuda: Journal of Sedimentary Petrology, v. 39, p. 49-69.

Goldich, S.S., Nier, A.O.C., Baadsgaard, H., Hoffman, J.H., and Krueger, H.W., 1961, The Precambrian geology and geochronology of Minnesota: Minnesota Geological Survey Bulletin 41, 193 p.

Goodwin, A.A., 1956, Facies relations in the Gunflint iron formation: Economic Geology, v. 51, p. 565-595.

Grout, F.F., and Broderick, T.M., 1919, Organic structures in the Biwabik Iron-bearing Formation of the Huronian in Minnesota: American Journal of Science, v. 198, p. 199-205.

Gruner, J.W., 1922, The origin of sedimentary iron-formations: The Biwabik Formation of the Mesabi Range: Economic Geology, v. 22, p. 407-460.

_____1946, The mineralogy and geology of the taconites and iron ores of the Mesabi Range, Minnesota: Iron Range Resources and Rehabilitation Commission, 127 p.

Hoffman, P., 1967, Algal stromatolites: Use in stratigraphic correlation and paleocurrent determination: Science, v. 157, p. 1043-1045.

Holdren, R.H., Jr., 1977, Distribution and behavior of manganese in the interstitial waters of Chesapeake Bay sediments during early diagenesis: Unpublished Ph.D. dissertation, The Johns Hopkins University, 190 p.

Krauskopf, K.B., 1979, Introduction to geochemistry (2d ed.): McGraw Hill, 617 p.

LaBerge, G.L., 1973, Possible biological origin of Precambrian iron-formations: Economic Geology, v. 68, p. 1098-1109.

LaBerge, G.L., Robbins, E.G., and Han, T.-M., 1987, A model for the biological precipitation of Precambrian iron-formations—A: Geological evidence, *in* Appel, P.W.U., and LaBerge, G.L., eds., Precambrian iron formations: Athens, Greece, Theophrastus, p. 69-96.

Lougheed, M. S., 1983, Origin of Precambrian iron-formations in the Lake Superior Region: Geological Society of America Bulletin, v. 94, p. 325-340.

Mancuso, J.J., Kneller, W.A., and Quick, J.C., 1989, Precambrian vein pyrobitumens: Evidence for petroleum generation and migration 2 Ga ago: Precambrian Research, v. 44, p. 139-146.

Morey, G. B., 1972, Mesabi range, *in* Sims, P.K., and Morey, G.B., eds., The geology of Minnesota: A centennial volume: Minnesota Geological Survey, p. 204-217.

_____1983, Animikie basin, Lake Superior region, USA, *in* Trendal, A.F., and Morris, R.C., eds., Iron-formation facts and problems: Elsevier, p. 13-67.

Morey, G.B., and Van Schmus, W.R., 1988, Correlation of Precambrian rocks of the Lake Superior region, United States: U.S. Geological Survey Professional Paper 1241-F, 3 p., 1 plate.

Morey, G.B., Southwick, D.L., and Ojakangas, R.W., 1989, The Penokean orogen in east-central and northern Minnesota, *in* Early Proterozoic rocks of the Great Lakes region: Field Trip Guidebook T145: American Geophysical Union, p. 43-54.

Ojakangas, R.W., 1983, Tidal deposits in the early Proterozoic basin of the Lake Superior region—the Palms and the Pokegama Formations: Evidence for subtidal-shelf deposition of Superior-type banded iron-formation, *in* Medaris, L.G., Jr., ed., Early Proterozoic geology of the Great Lakes region: Geological Society of America Memoir 160, p. 49-66.

Robbins, E.I., LaBerge, G.L., and Schmidt, R.G., 1987, A model for the biological precipitation of Precambrian iron-formations—B: Morphological evidence and modern analogs, *in* Appel, P.W.U., and LaBerge, G.L., eds., Precambrian iron-formations: Athens, Greece, Theophrastus, p. 97-139.

Schopf, J.W., ed., 1983, Earth's earliest biosphere, its origin and evolution: Princeton University Press, 543 p.

Schulz, K.J., and Ojakangas, R.W., 1989, Wisconsin magmatic terrane and Marquette Range Supergroup in Wisconsin and the western part of northern Michigan, *in* Early Proterozoic Rocks of the Great Lakes region: Field Trip Guidebook T145: American Geophysical Union, p. 31-42.

Southwick, D.L. and Morey, G.B., 1991, Tectonic imbrication and foredeep development in the Penokean orogen, east-central Minnesota: An interpretation based on regional geophysics and the results of test-drilling, *in* Sims, P.K., and Carter, L.M.H., eds., Contributions to Precambrian geology of Lake Superior region: U.S. Geological Survey Bulletin 1904-C, p. C1-C17.

Southwick, D.L., Morey, G.B., and McSwiggen, P.L., 1988, Geologic map (scale 1:250,000) of the Penokean orogen, central and eastern Minnesota, and accompanying text: Minnesota Geological Survey Report of Investigations 37, 25 p., 1 pl.

Sugisaki, R., Sugitani, K., and Adachi, M., 1991, Manganese carbonate bands as an indicator of hemipelagic sedimentary environments: Journal of Geology, v. 99, p. 23-40.

Walter, M.R., 1977, Interpreting stromatolites: American Scientist, v. 65, p. 563-571.

Walter, M.R., and Hofmann, H.J., 1983, The palaeontology and palaeoecology of Precambrian iron-formations, *in* Trendall, A.F., and Morris, R.C., eds., Iron-formation facts and problems: Elsevier, p. 373-400.

Walter, M.R., Goode, A.D.T., and Half, W.D.M., 1976, Microfossils from a newly discovered Precambrian stromatolitic iron formation in Western Australia: Nature, v. 261, p. 221-223.

White, D.A., 1954, The stratigraphy and structure of the Mesabi Range, Minnesota: Minnesota Geolological Survey Bulletin 38, 92 p.

Wolff, J.F., 1917, Recent geologic developments on the Mesabi range, Minnesota: American Institute of Mining and Metallurgical Engineers Transactions, v. 56, p. 142-169.

REVISED STRATIGRAPHIC NOMENCLATURE FOR THE UPPER CAMBRIAN (ST. CROIXAN) JORDAN SANDSTONE, SOUTHEASTERN MINNESOTA

By

Anthony C. Runkel

ABSTRACT

The Jordan Sandstone is one of several well-known cratonic sheet sandstones that are part of the type and reference area of Late Cambrian (St. Croixan) age in North America. Borehole cuttings and natural gamma logs, in combination with outrops, were used to determine lithic attributes within the Jordan Sandstone, and to clear up some long-standing nomenclature problems.

The Jordan Sandstone consists of two distinct facies—a quartzose, fine- to coarse-grained, cross-stratified sandstone, and a feldspathic, very fine grained, mostly burrowed sandstone. The feldspathic facies is the regionally continuous basal part of the Jordan, which passes transitionally upward into the quartzose facies. It also occurs at higher stratigraphic levels within the quartzose facies as disconformable tongues that climb diagonally up-section from the base of the Jordan Sandstone.

I formally recommend abandonment of all formal member nomenclautre for the Jordan Sandstone, because the distinction between a quartzose and a feldspathic facies is the only practical lithic division of the Jordan Sandstone. Both facies are recognizable in outcrop, as well as by subsurface geophysical methods. Furthermore, the stratigraphic setting of the feldspathic and quartzose facies relative to one another is such that formal definition of lithostratigraphic units is neither useful nor proper.

INTRODUCTION

The term Jordan Sandstone was formally applied by Winchell (1874) to sandstone exposed in a quarry near the town of Jordan in Scott County, Minnesota. These rocks were originally assigned to the uppermost parts (units F1e and F1f) of the Lower Sandstone of Owen (1852). The Jordan Sandstone is one of several well-known cratonic sheet sandstones that are part of the type and reference area of Late Cambrian (St. Croixan) age in North America. Strata assigned to the Jordan have been studied by many workers over the past 120 years, mostly in scattered outcrops along the Mississippi River and its tributaries (Fig. 1). The best descriptions are those by Stauffer (1925), Stauffer and others (1939), Nelson (1956), and Odom and Ostrom (1978).

In general the Jordan Sandstone ranges in thickness from 50 to 115 feet and consists mostly of very fine grained to coarse-grained sandstone (Fig. 2) that gradationally overlies the St. Lawrence Formation. The contact with the St. Lawrence is generally drawn above a siltstone bed and at the base of a continuous sandstone bed (Berg and others, 1956). The Jordan in turn is sharply overlain by the Coon Valley Member of the Oneota Dolomite of Early Ordovician (Ibexian) age.

Internal stratigraphic attributes of the Jordan Sandstone are poorly understood because of a paucity of subsurface data and because studies have been local rather than regional in scope. Traditionally the Jordan Sandstone has been divided into a lower and an upper member. The lower or Norwalk Member was named from outcrops near Norwalk in Monroe County, Wisconsin, by Ulrich (1924), who assigned it as the uppermost member of his Trempealeau Formation. Stauffer (1925) subsequently revised the nomenclature of the Jordan and suggested that the Norwalk be considered its lowermost member. Stauffer described the Norwalk as medium- to fine-grained, cross-bedded or massive sandstone. The term Van Oser, now widely applied to the upper part of the Jordan, was mentioned by Winchell (1874). It was first defined as a formal member by Stauffer and others (1939), who described it as a coarse-grained sandstone between the Norwalk Member below and the Oneota Dolomite of Ordovician age above.

The Norwalk-Van Oser nomenclature has been difficult to apply with consistency, because it relies on subtle differences in grain size. In addition, many sections of the Jordan Sandstone do not contain beds composed dominantly of coarse-grained sandstone. Consequently, most workers have not strictly adhered to the original definitions of these units. The Norwalk is commonly described as very fine grained, and mostly structureless, whereas the Van Oser is described as fine grained or coarser and mostly cross-stratified (Fig. 2) (e.g., Odom and Ostrom, 1978; Witzke and McKay, 1987). However, measured sections published by some of these workers

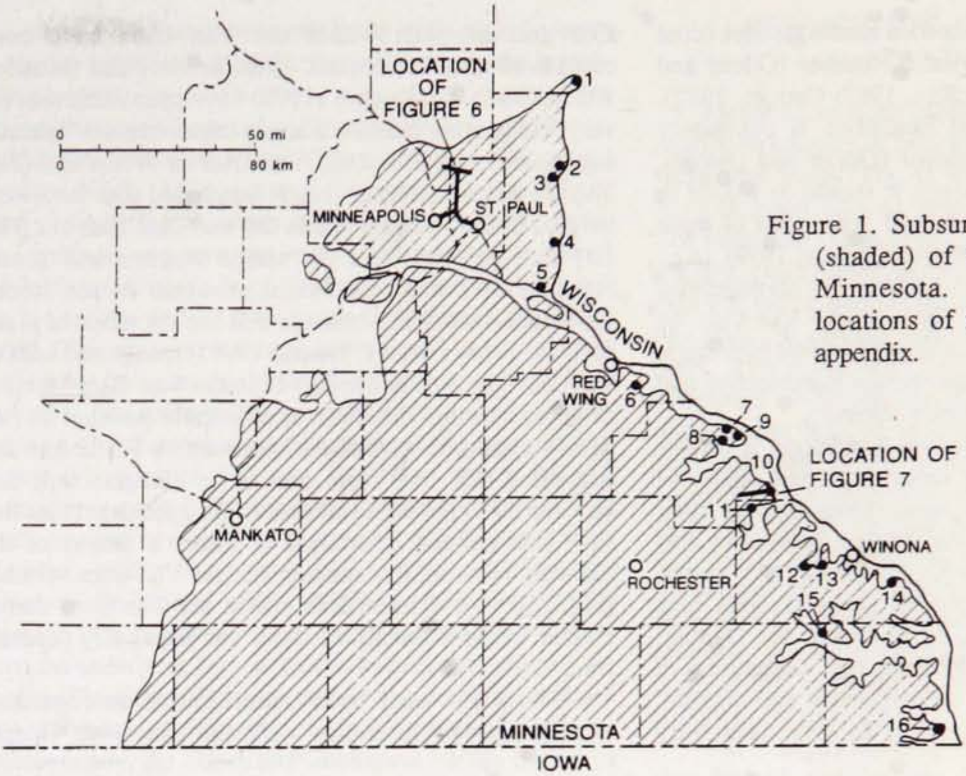

Figure 1. Subsurface and outcrop extent (shaded) of the Jordan Sandstone in Minnesota. Numbered dots show locations of measured sections in the appendix.

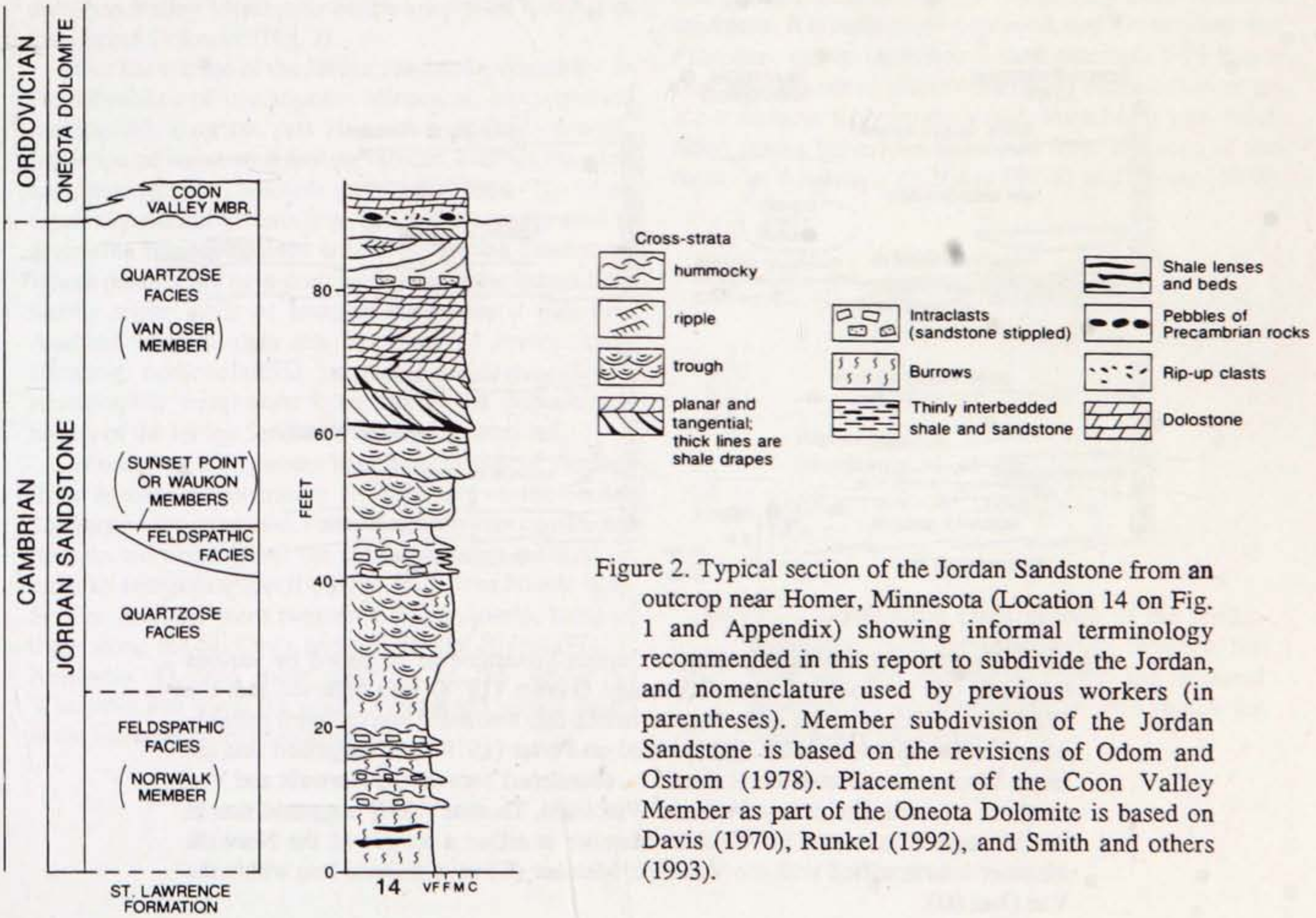

Figure 2. Typical section of the Jordan Sandstone from an outcrop near Homer, Minnesota (Location 14 on Fig. 1 and Appendix) showing informal terminology recommended in this report to subdivide the Jordan, and nomenclature used by previous workers (in parentheses). Member subdivision of the Jordan Sandstone is based on the revisions of Odom and Ostrom (1978). Placement of the Coon Valley Member as part of the Oneota Dolomite is based on Davis (1970), Runkel (1992), and Smith and others (1993).

indicate that fine-grained, cross-bedded sandstone does occur in the upper part of the Norwalk Member (Odom and Ostrom, 1978; Witzke and McKay, 1987; Ostrom, 1987). Furthermore, medium-grained sandstone is commonly assigned to the Van Oser Member (Odom and Ostrom, 1978; Ostrom, 1987), even though it should be placed in the Norwalk according to the formal definitions of these members (Stauffer, 1925; Stauffer and others, 1939). In an attempt to resolve these problems, Porter (1978) suggested that the contact between the Norwalk and Van Oser be placed at the base of the stratigraphically lowest high-angle cross-strata in the Jordan. This criterion is subjective and therefore has also been applied inconsistently.

The stratigraphy of the Jordan Sandstone is further complicated by the presence of very fine grained sandstone units within the Van Oser Member. Even though their stratigraphic setting within the Jordan Sandstone was poorly understood, these units have been formally named (Fig. 2) the Sunset Point Member for exposures near Madison, Wisconsin (Raasch, 1951; Odom and Ostrom, 1978) and the Waukon Member for exposures in southwestern Wisconsin and Iowa (Odom and Ostrom, 1978; Anderson and others, 1979). In Minnesota, very fine grained units within the Van Oser have been considered to be "analogous" to the Sunset Point (Mossler, 1987). Odom and Ostrom (1978) have speculated that the very fine grained units are discrete lenses that are "laterally equivalent" to parts of the Van Oser in Wisconsin (Fig. 3A). In contrast, Porter (1978) concluded that they were tongues of the Norwalk within the Van Oser Member (Fig. 3B) and suggested that the names Waukon and Sunset Point be abandoned as formal members of the Jordan Sandstone—a recommendation that has not received much support. More recently, Thomas (1991) recognized beds of very fine grained sandstone within the Van Oser Member in approximately the same stratigraphic position at two widely separated localities in southeastern Minnesota and suggested that they were part of an elongate unit that exceeds 60 miles in lateral extent. He speculated that this very fine grained unit could be either a tongue of the Norwalk Member that extends into the Van Oser Member (Fig. 3C) or a discrete lens within the Van Oser that is similar to the Norwalk Member but physically separate from it (Fig. 3D).

There has also been some confusion regarding stratigraphic relationships with the overlying Oneota

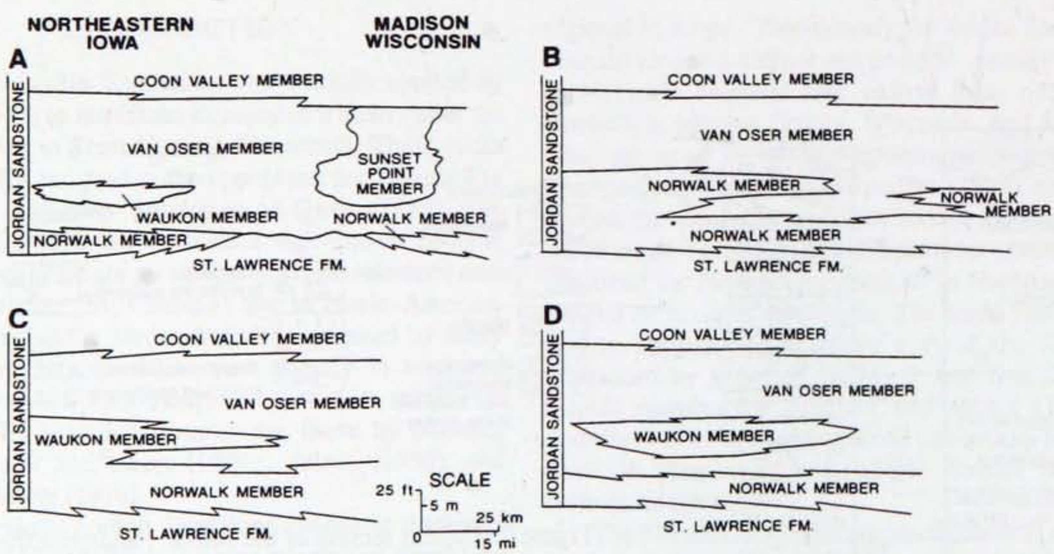

Figure 3. Generalized lithostratigraphy of Jordan Sandstone as proposed by various workers. (**A**) is modified from Odom and Ostrom (1978) who believed that the Waukon and Sunset Point were discrete lenses that warranted two different member names in two different areas. (**B**) is based on Porter (1978) who suggested that the terms Waukon and Sunset Point should be abandoned because the Norwalk and Van Oser are interstratified in southwestern Wisconsin. Thomas (1991) suggested that in southeastern Minnesota the Waukon Member is either a tongue of the Norwalk Member interstratified with the Van Oser Member (**C**) or a discrete lens within the Van Oser (**D**).

Dolomite. The contact was originally defined as between sandstone below and dolomite above. However, the Jordan-Oneota contact is transitional in most places, marked by a heterolithic unit of intercalated sandy dolostone, sandstone, and shale termed the Coon Valley Member (Odom and Ostrom, 1978). All or parts of this transitional unit have been given different names at different times and places, and assigned as a member in both the uppermost part of the Jordan Sandstone (e.g., Odom and Ostrom, 1978) and the lowermost part of the Oneota Dolomite (e.g., Davis, 1970). The situation is further complicated by the fact that the contact between the Jordan Sandstone and the Oneota Dolomite was understood to correspond to the boundary between the Cambrian and Ordovician Systems in the Upper Mississippi Valley. Therefore much of the controversy over lithostratigraphic nomenclature arises from uncertainty as to the age of the Coon Valley Member, rather than its lithic properties. Recently however, Smith and others (1993) and Runkel (1992) reported that an unconformity separates the Coon Valley from the underlying fine- to coarse-grained sandstone of the Jordan. The Coon Valley in turn is overlain gradationally by the pure dolostone of the Oneota Dolomite. Consequently, the Minnesota Geological Survey considers the Coon Valley Member to be the lowermost member of the Oneota Dolomite (Fig. 2).

Our knowledge of the Jordan Sandstone, especially in the subsurface of southeastern Minnesota, has improved considerably over the past 20 years with the systematic collection of water-well drilling records, cuttings samples, and, more recently, borehole geophysical logs. The latter, especially natural gamma logs, are now routinely used to determine lithic attributes within the Jordan Sandstone. Where possible we have correlated them with cuttings from nearby water wells or samples from natural outcrops. Analysis of these data sets has resolved several long-standing nomenclatural problems, and provides a stratigraphic framework from which the depositional history of the Jordan Sandstone can be reconstructed.

More than 400 gamma logs and 58 sets of cuttings from boreholes penetrating at least part of the Jordan Sandstone were examined. Fence diagrams were constructed for selected areas where the subsurface data sufficed, in order to extrapolate specific lithic units from hole to hole. Sixteen sections were measured in Minnesota, most of them along the St. Croix and Mississippi Rivers (Fig. 1; Appendix 1), and most outcrops of the Jordan in Wisconsin and Iowa, for which a measured section exists in the literature, were re-examined.

DESCRIPTION OF THE JORDON SANDSTONE

Measured sections (Appendix 1) reveal that the Jordan Sandstone consists of two distinct facies, a quartzose and a feldspathic facies (Fig. 4), which can be recognized on the basis of grain size, as well as mineralogic composition. The quartzose facies (Fig. 5A) is friable, fine- to coarse-grained, cross-stratified sandstone that generally is more than 98 percent quartz (Odom, 1978) and is as much as 60 feet thick. It can be subdivided into two subtly different parts. The lower 10 to 20 feet of the quartzose facies is composed mostly of fine- to medium-grained sandstone with wedge sets of trough cross-strata that range in thickness from 10 to 30 cm. *Skolithos* and *Arenicolites* burrows are common, and shale drapes are rare. The upper 20 to 40 feet of the quartzose facies consists mostly of medium- to coarse-grained sandstone with sets of trough, planar, and tangential cross-strata as thick as 5 feet. Scour surfaces with intraclastic lags define sandstone units that range in thickness from 1 to 13 feet. Shale drapes, reactivation surfaces, and herringbone cross-strata are common. Burrows are rare.

The feldspathic facies (Fig. 5B) is dominated by very fine grained, structureless, or hummocky cross-stratified sandstone. It is extensively burrowed, and *Arenicolites* and *Planolites* can be identified at most outcrops. Very thin to thin, tabular beds of siltstone and shale are common, as are scour surfaces with poorly sorted, intraclastic lags. Sand-filled cracks have been described from outcrops of this facies in Wisconsin by Byers (1978) and Porter (1978).

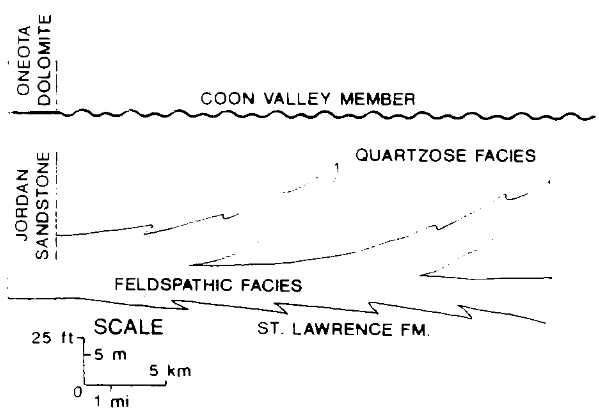

Figure 4. Generalized cross section of the Jordan Sandstone showing relationship between the quartzose and feldspathic facies, the informal terminology recommended in this report for subdividing the Jordan.

Thomas (1991) has described this facies as arkose or subarkose consisting mostly of subangular to subrounded grains of quartz and potassium feldspar of both detrital and authigenic origin. Odom (1978) and Thomas (1991) have shown that the total feldspar content of this facies is between 10 and 65 modal percent of the rock, an attribute in marked contrast to the feldspar content of the quartzose facies of less than 2 modal percent.

The feldspathic facies occurs at several stratigraphic levels in the Jordan Sandstone. It forms a regionally continuous interval, 5 to 20 feet thick, that gradationally overlies the St. Lawrence Formation and passes transitionally upward into the quartzose facies. At higher stratigraphic levels, intervals having similar sedimentologic attributes are intercalated in the quartzose facies (e.g., sections 1-4, 7, 13-14 in Appendix 1). In outcrops, these intercalated units overlie erosion surfaces having as much as 5 feet of relief over about 100 feet of horizontal distance, which are overlain by a poorly sorted lag of very fine to coarse-grained sandstone. The lag in turn is overlain by an interval of very fine grained, hummocky cross-stratified sandstone that passes transitionally upward

A

B

Figure 5. Representative exposures of the quartzose facies (A) and feldspathic facies (B) of the Jordan Sandstone.

into mostly structureless, burrowed, very fine grained sandstone. Each of these intercalated intervals passes gradationally upward into the quartzose lithofacies.

Borehole geophysical logs show that sharp lower contacts and gradational upper contacts are persistent attributes of the intercalated feldspathic intervals across the entire subsurface extent of the Jordan Sandstone. They can be distinguished easily on natural gamma logs because of their large potassium feldspar content as compared to the surrounding quartzose facies (Fig. 6). Gamma responses across the feldspar-rich intervals are typically asymmetric. The lower part of the profile is nearly horizontal, reflecting the abrupt lithic change across the scour surface at the base. In contrast, the upper part of each profile is characterized by a diagonal signature, reflecting the gradational transition from the feldspathic to the quartzose facies. A single vertical section of the Jordan can contain as many as three successive feldspathic units separated from one another by about 80 feet of the quartzose facies.

The pronounced natural gamma signature makes it possible to trace units of the feldspathic facies laterally in the subsurface and to construct fence diagrams (Figs. 7 and 8) that illustrate the relationship between the feldspathic and quartzose facies. As these fence diagrams show, the intercalated units of feldspathic facies are disconformable tongues that climb diagonally up-section from the base of the Jordan Sandstone. Individual tongues are as wide as 9 miles and have a shallow, crescentic shape in cross sections oriented perpendicular to strike. They are as much as 40 feet thick near the base of the Jordan, but they thin as they climb stratigraphically up-section. The tongues typically pinch out about 10 to 20 feet below the top of the Jordan. In contrast, individual tongues maintain a fairly constant thickness along strike, and several tongues can be traced in the subsurface for distances of 12 miles or more in areas where closely spaced borehole geophysical logs are available. Unfortunately, the data base is not yet sufficient to trace individual tongues for greater distances, and so their true regional extent has not been established.

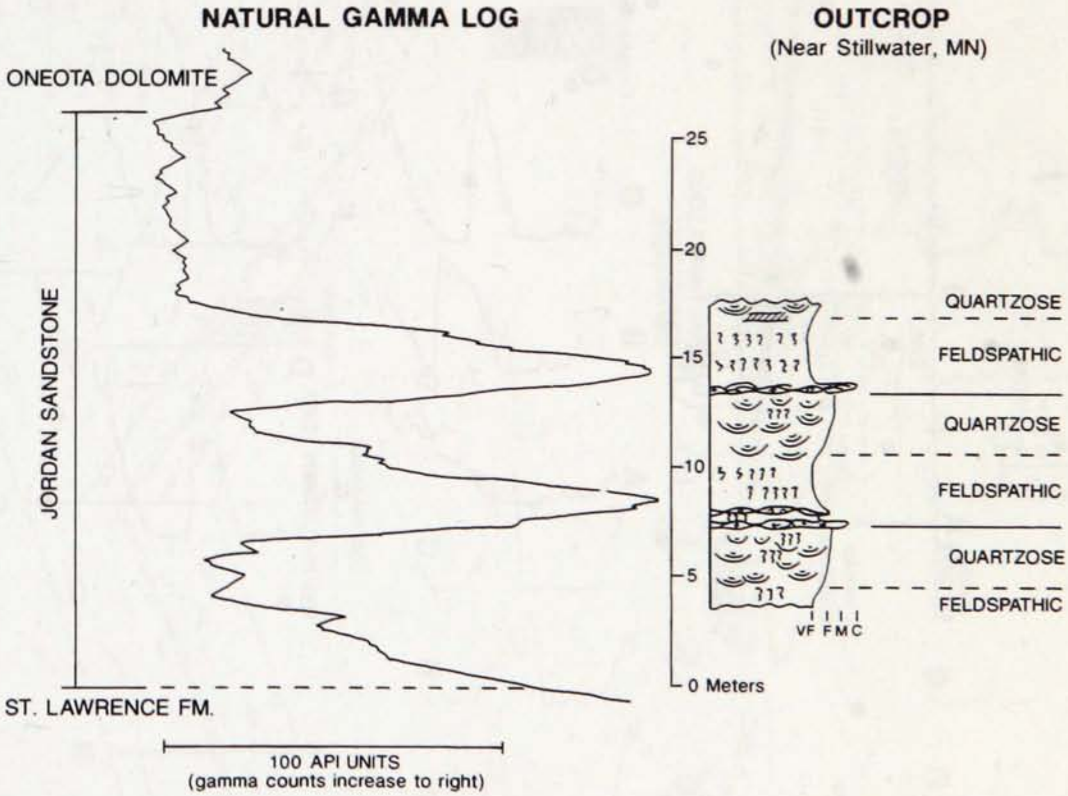

Figure 6. Measured section of Jordan Sandstone showing feldspathic and quartzose facies and corresponding gamma response. Natural gamma log is from water well about 500 yards from outcrop and shows the pronounced positive signatures associated with the feldspathic facies in contrast to the quartzose facies.

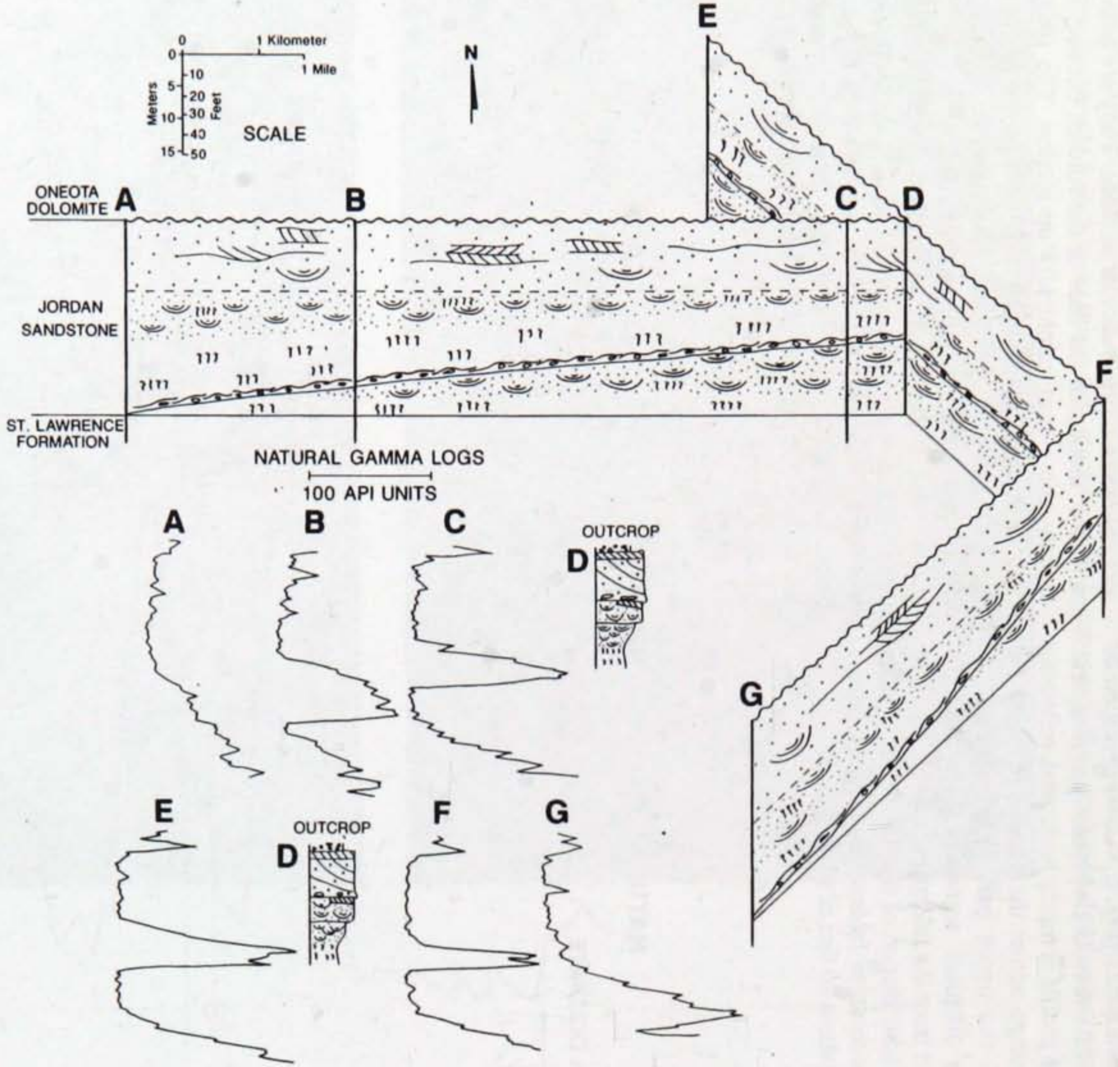

Figure 7. Fence diagram of the Jordan Sandstone in the Minneapolis-St. Paul area based on correlated gamma logs, showing the shape and stratigraphic arrangement of the feldspathic facies (shaded). See Figure 1 for location.

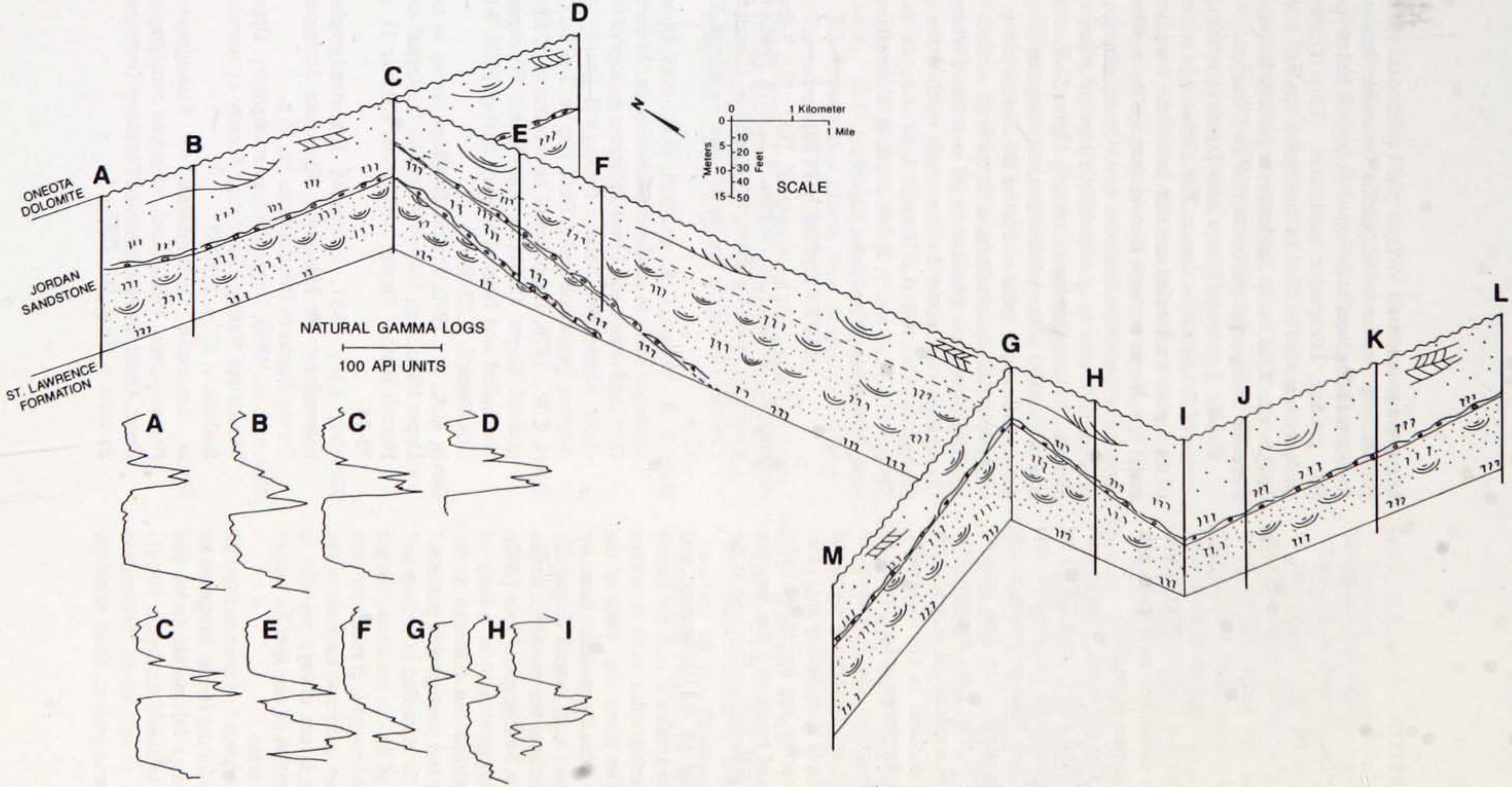

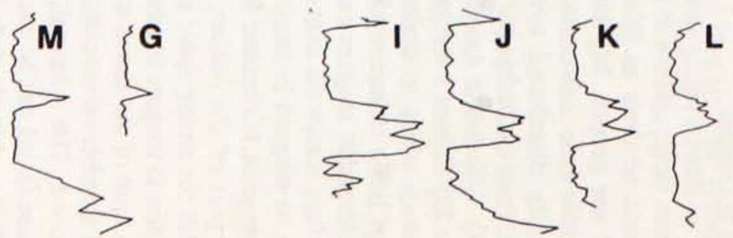

Figure 8. Fence diagram of the Jordan Sandstone in southeastern Minnesota based on correlated gamma logs, showing the shape and stratigraphic arrangement of the feldspathic facies (shaded). See Figure 1 for location.

DISCUSSION

The distinction between the quartzose and feldspathic facies is the only practical lithic division of the Jordan Sandstone. Such a division is readily recognizable in outcrop, as well as by subsurface geophysical methods. This distinction is in general how some workers have applied the Norwalk-Van Oser nomenclature, but it is very different from the formal lithic descriptions of these units by Stauffer (1925) and Stauffer and others (1939), which are indistinguishable by most subsurface techniques, and are extremely difficult to differentiate in the field.

Porter (1978) suggested that the terms Waukon and Sunset Point as defined by Odom and Ostrom (1978) be abandoned. I agree with that assessment. The two terms are adequately defined in terms of their lithic properties, in that they refer to units of feldspathic, very fine grained sandstone that are markedly distinct from the quartzose sandstone in which they are intercalated. However, these members are lithologically identical to the feldspathic facies at the base of the Jordan Sandstone and to tongues of this facies that occur throughout the formation in southeastern Minnesota. Therefore the terms Waukon and Sunset Point should be suppressed because they imply that the tongues bearing these names are stratigraphically discrete units confined to local areas, and that they are lithically different from the feldspathic sandstone at the base of the Jordan.

The stratigraphic setting of the feldspathic and quartzose facies relative to one another is such that formal definition of them as lithostratigraphic units is neither useful nor proper. My studies show that units of the feldspathic facies intercalated within the quartzose facies are regionally distributed tongues that extend diagonally upward from the feldspathic facies at the base of the Jordan (Fig. 4). The North American Stratigraphic Code (1983; Article 22) defines a lithostratigraphic unit as "a body of . . . strata which is distinguished and delimited on the basis of lithic characteristics and stratigraphic position." The feldspathic tongues can be identified in outcrop and subsurface across the extent of the Jordan Sandstone but cannot be mapped in detail. Although it is relatively easy to distinguish feldspathic from quartzose intervals in the upper part of the Jordan, it is not always possible to establish the stratigraphic position of any specific tongue in relation to tongues in other areas.

In light of the above arguments I recommend that all formal member nomenclature for the Jordan Sandstone be abandoned. The informal terms feldspathic facies and quartzose facies can be used to divide the Jordan into (1) very fine grained, mostly structureless, feldspathic sandstone; and (2) fine- to coarse-grained, cross-stratified, quartzose sandstone. Where the quartzose facies gradationally overlies the feldspathic, the contact between them should be placed at the top of the highest bed of very fine grained, feldspathic sandstone. This informal nomenclature can be used to distinguish the two lithic components of the Jordan Sandstone, and it does not imply a specific stratigraphic position within the formation.

Finally, I propose here a new principal reference section of the Jordan Sandstone. The original type section of the Jordan consisted of less than half of the formation, and it is no longer exposed. I recommend that the excellent exposure of the Jordan Sandstone near Homer, Minnesota, in Winona County be considered the principal reference section. The formation is continuously exposed and easily accessible at this outcrop. In addition, the feldspathic facies occurs both as the basal interval of the Jordan, and as a tongue within the quartzose facies higher in the section.

This exposure is a roadcut on the east side of Winona County Road 15, about 2 miles south of the town of Homer in the NE1/4NW1/4NE1/4 sec. 16 and SE1/4SW1/4SE1/4 sec. 9, T. 106 N., R. 6 W. (measured section 14 on Figs. 1 and 2 and Appendix).

REFERENCES CITED

Anderson R., McKay R.M., Witzke, B.J., 1979, Field trip guidebook to the Cambrian stratigraphy of Allamakee County: Geological Society of Iowa Guidebook 32, 12 p.

Berg, R. R., Nelson, C.A., and Bell, W.C., 1956, Upper Cambrian rocks in southeast Minnesota, *in* Schwartz, G.M., and others, eds, Lower Paleozoic geology of the upper Mississippi Valley: Geological Society of America Guidebook Series, Field Trip no. 2, p. 1-23.

Byers, C.W., 1978, Depositional environments of fine-grained Upper Cambrian lithofacies: Wisconsin Geological and Natural History Survey Field Trip Guidebook 3, p. 52-66.

Davis, R.A., Jr., 1970, Prairie du Chien Group in the Upper Mississippi Valley: Wisconsin Geological and Natural History Survey Information Circular 11, p. 35-44.

Mossler, J.H., 1987, Paleozoic lithostratigraphic nomenclature for Minnesota: Minnesota Geological Survey Report of Investigations 36, 36 p.

Nelson, C.A., 1956, Upper Croixan stratigraphy, Upper Mississippi Valley: Geological Society of America Bulletin, v. 67, p. 165-183.

North American Commission on Stratigraphic Nomenclature, 1983, North American Stratigraphic Code: American Association of Petroleum Geologists Bulletin, v. 67, p. 841-875.

Odom, I.E., 1978, Mineralogy of Cambrian sandstones, Upper Mississippi Valley: Wisconsin Geological and Natural History Survey Field Trip Guidebook 3, p. 46-51.

Odom I. E., and Ostrom M.E., 1978, Lithostratigraphy, petrology, and sedimentology of the Jordan Formation near Madison, Wisconsin: Geological and Natural History Survey Field Trip Guidebook 3, p. 23-45.

Ostrom, M.E., 1987, St. Lawrence and Jordan Formations (Upper Cambrian) south of Arcadia, Wisconsin, *in* Biggs, D.L., ed., North Central section of the Geological Society of America, Centennial Field Guide, v. 3, p. 191-194.

Owen, D.D., 1852, Report of a geological survey of Wisconsin, Iowa and Minnesota: Philadelphia, Lippincott, Grambo and Co., 638 p.

Porter, J., 1978, Stratigraphy and depositional environments of the Norwalk Member of the Jordan Formation (Upper Cambrian), southwestern Wisconsin: Unpublished M.S. thesis, University of Wisconsin, Madison, 160 p.

Raasch, G.O., 1951, Revision of Croixan Dikelocephalidae: Illinois State Academy of Science Transactions, v. 44, p.137-151.

Runkel, A.C., 1992, Deposition of the Upper Cambrian Jordan Sandstone, Upper Mississippi Valley region: Geological Society of America Abstracts with Programs, v. 24, p. A350.

Smith, G.L., Byers, C.W., and Dott, R.H., Jr., 1993, Sequence stratigraphy of the lower Ordovician Prairie du Chien Group on the Wisconsin Arch and in the Michigan basin: American Association of Petroleum Geologists Bulletin, v. 77, p. 49-67.

Stauffer, C.R, 1925, The Jordan Sandstone: Journal of Geology, v. 33, p. 699-713.

Stauffer, C.R., Schwartz, G.M., and Thiel, G.A., 1939, The St. Croixan classification of Minnesota: Geological Society of America Bulletin, v. 50, p. 1227-1243.

Thomas, D.A., 1991, Lithostratigraphy, petrology, diagenesis and environments of deposition of the Upper Cambrian Jordan Sandstone: Unpublished M.S. thesis, University of Minnesota, Duluth.

Ulrich, E.O., 1924, Notes on new names in the table of formations and on physical evidence of breaks between Paleozoic systems in Wisconsin: Wisconsin Academy of Science, Arts and Letters Transactions, v. 21, p. 71-107.

Winchell, N.H., 1874, Second annual report for the year 1873: Minnesota Geological and Natural History Survey: Published in the Regents Report for 1873, p. 73-219.

Witzke B.J., and McKay, R.M., 1987, Cambrian and Ordovician stratigraphy in the Lansing area, northeastern Iowa, *in* Biggs, D.L., ed., North Central section of the Geological Society of America, Centennial Field Guide, v. 3, p. 81-87.

APPENDIX 1. MEASURED SECTIONS

1-Along west bank of St. Croix River about 2 miles south of Osceola, Wisconsin, Chisago County. SW1/4 NE1/4 NE1/4 sec. 32, T. 33 N., R. 19 W.

2-East side of Minnesota Highway 95, 1.4 miles north of junction with Minnesota Highway 96, Washington County. NW1/4 SW 1/4 NW1/4 sec. 14, T. 30 N., R. 20 W.

3-In city of Stillwater at NW corner of intersection of Minnesota Highway 95 and Elm Street, Washington County. NW1/4 NE1/4 NE1/4 sec. 28, T. 30 N., R. 20 W.

4-About 1 mile south of city of Afton on east side of Douglass Road, Washington County. NW1/4 NE1/4 NE1/4 sec. 27, T. 28 N., R. 20 W.

5-About 50 m east of Lock and Dam #2 on Mississippi River, Washington County. NE1/4 SE1/4 SE1/4 sec. 1, T. 26 N., R. 21 W.

6-Along north side of Minnesota Highway 58, 1 mile northeast of town of Hay Creek, Goodhue County. SW1/4 SW1/4 SE1/4 sec. 18, T. 112 N., R. 14 W.

7-Along north side of County Road 30, 2 miles west of U.S. Highway 61, Wabasha County. SE1/4 SE1/4 SW1/4 sec. 36, T. 111 N., R. 11 W.

8-Along north side of Minnesota Highway 60 about 4.5 miles west from U.S. Highway 61, Wabasha County. NE1/4 NW1/4 SE1/4 sec. 12, T. 110 N., R. 11 W.

9-Along north side of Minnesota Highway 60 about 1 mile west from U.S. Highway 61. Wabasha County. SE1/4 NE1/4 SE1/4 sec. 5, T. 110 N., R. 10 W.

10-Along north side of County Road 26 about 3/4 mile west of the town of Weaver, Wabasha County. SE1/4 SW1/4 NW1/4 sec. 30, T. 109 N., R. 9 W.

11-Along east side of County Road 116, 0.7 mile north of County Road 30 near Whitewater State Park, Winona County. NE1/4 NE1/4 NE1/4 sec. 16, T. 108 N., R. 10 W.

12- Along north side of U.S. Highway 14 about 1/4 mile east of the town of The Arches, Winona County. SW1/4 NE1/4 NW1/4 sec. 8, T. 106 N., R. 8 W.

13-Along north side of U.S. Highway 14 about 1.5 miles west of U.S. Highway 61, Winona County. NW1/4 SE1/4 SW1/4 sec. 30, T. 107 N., R. 7 W.

14-Along east side of County Road 15 about 2 miles south of the town of Homer, Winona County. NE1/4 NW1/4 NE1/4 sec. 16 and SE1/4 SW1/4 SE1/4 sec. 9, T. 106 N., R. 6 W.

15-Along west side of Minnesota Highway 43 about 2.2 miles north of the town of Rushford, Fillmore County. NW1/4 SE1/4 NE1/4 sec. 2, T. 104 N., R. 8 W.

16-Along north side of County Road 14, half a mile west of Minnesota Highway 26, Houston County. NW1/4 NW1/4 SW1/4 sec. 14, T. 101 N., R. 4 W.

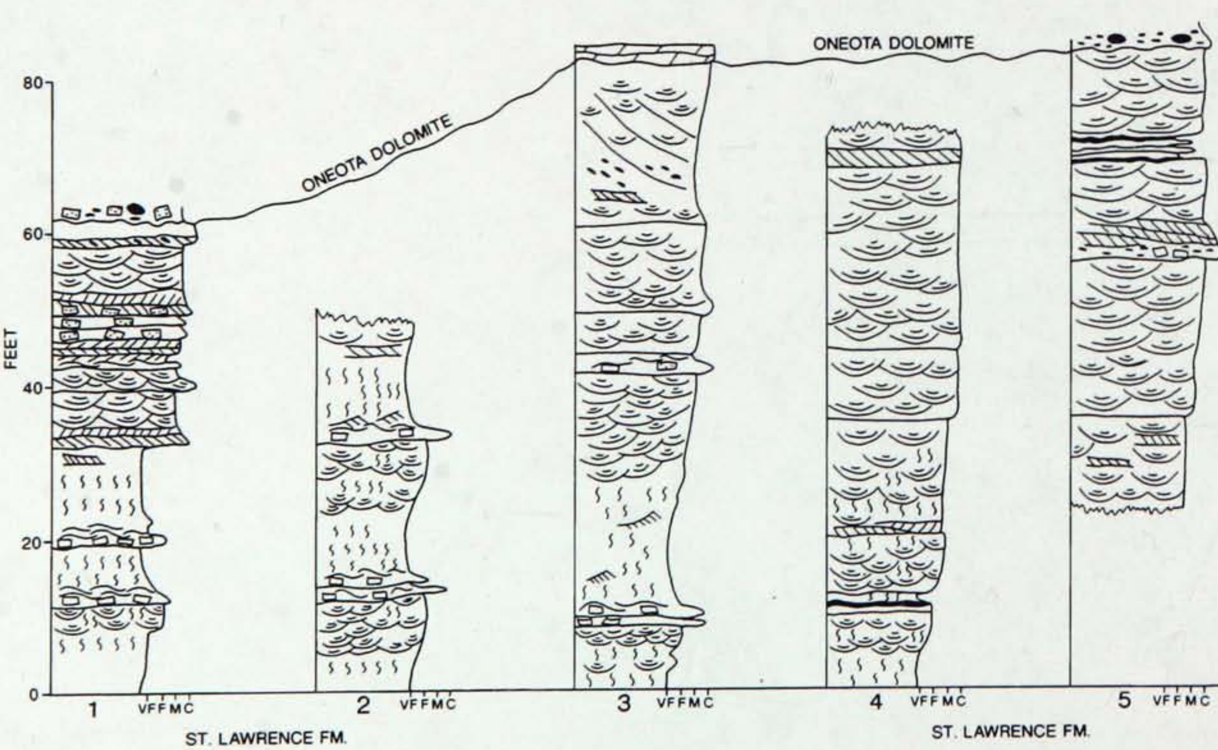

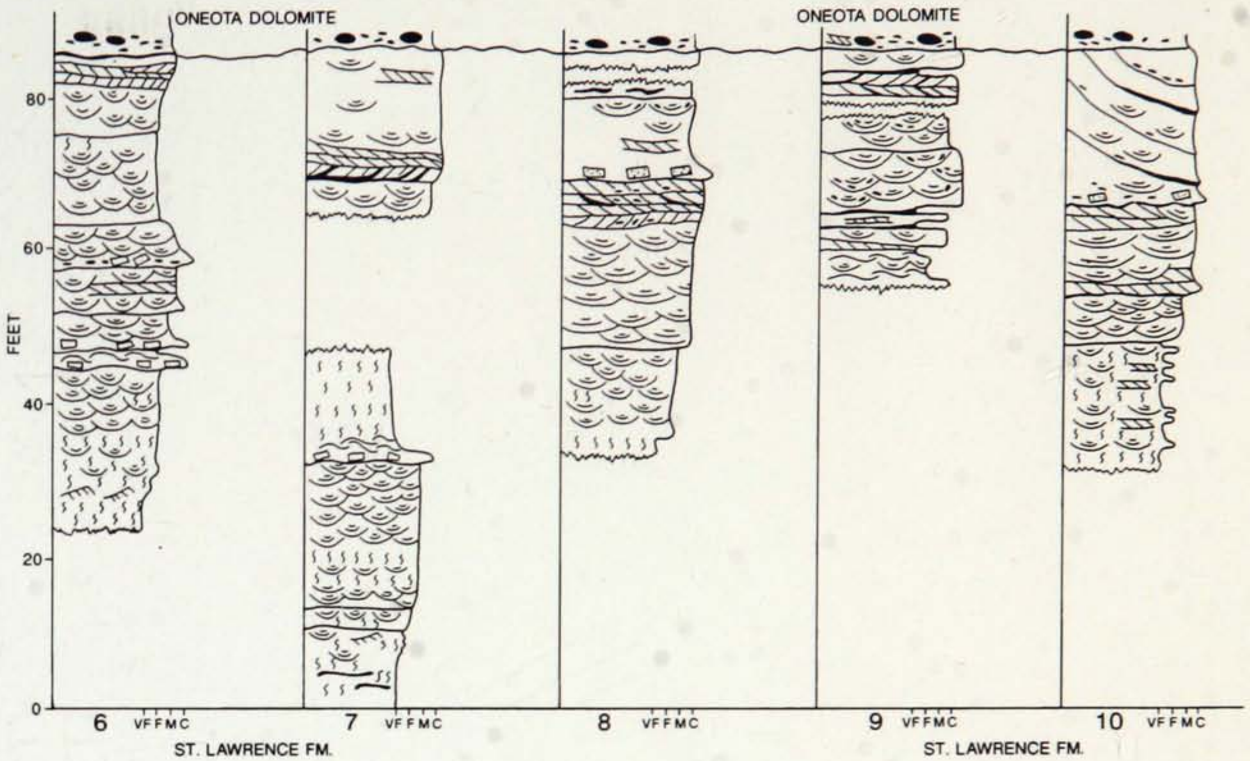
ONEOTA DOLOMITE
ONEOTA DOLOMITE
FEET
80
60
40
20
0
6 VF F M C
7 VF F M C
8 VF F M C
9 VF F M C
10 VF F M C
ST. LAWRENCE FM.
ST. LAWRENCE FM.

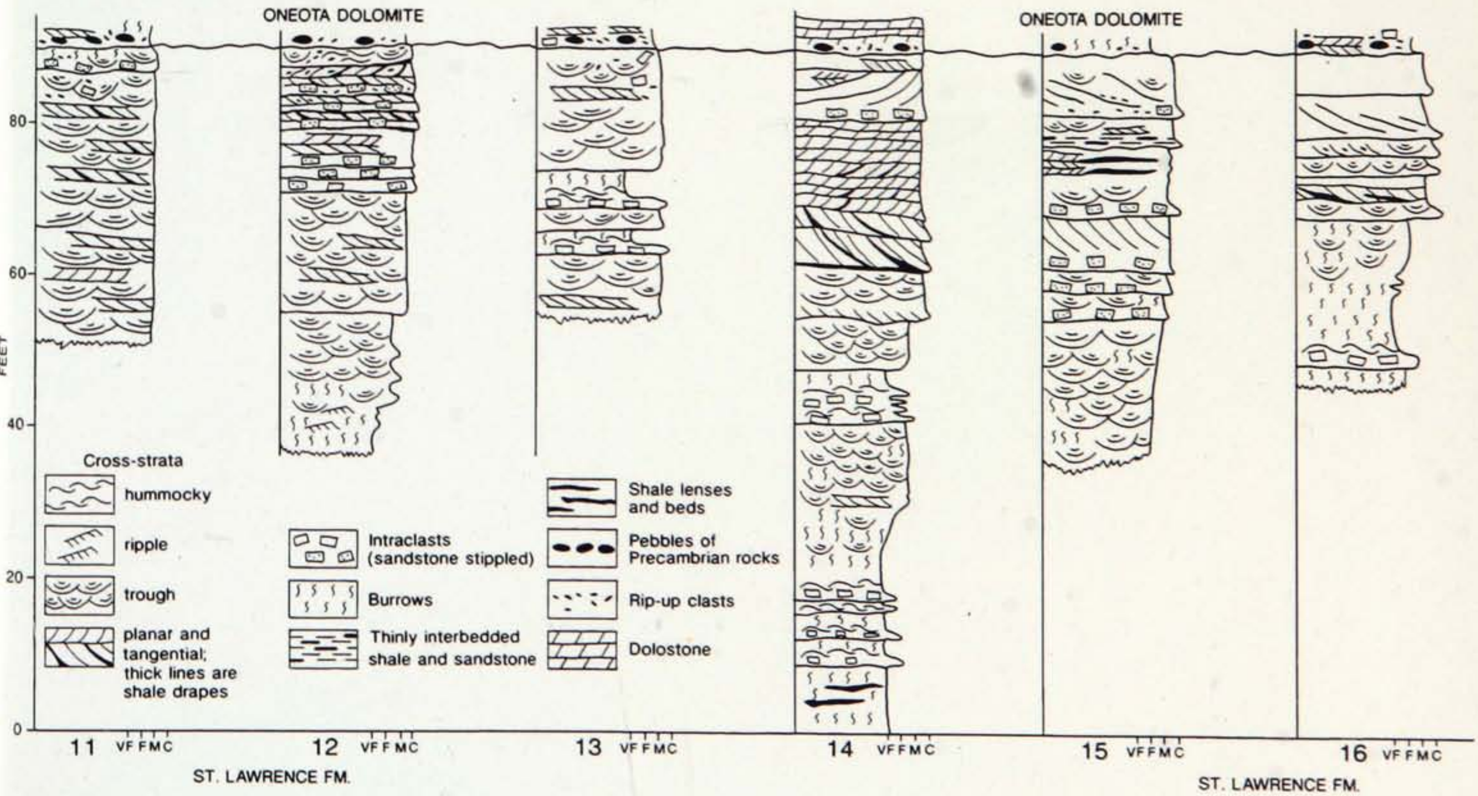
ONEOTA DOLOMITE
ONEOTA DOLOMITE
FEET
80
60
40
20
0
Cross-strata
hummocky
ripple
trough
planar and tangential; thick lines are shale drapes
Intraclasts (sandstone stippled)
Burrows
Thinly interbedded shale and sandstone
Shale lenses and beds
Pebbles of Precambrian rocks
Rip-up clasts
Dolostone
11 VF F M C
12 VF F M C
13 VF F M C
14 VF F M C
15 VF F M C
16 VF F M C
ST. LAWRENCE FM.
ST. LAWRENCE FM.